UNIVERSITA' DEGLI STUDI DEL PIEMONTE ORIENTALE

DiSIT-Dipartimento di Scienze e Innovazione Tecnologica

Dottorato di ricerca in Scienze Ambientali (Acque interne e agroecosistemi)

XXVIII Ciclo

Modulation of Ca^{2+} signaling by polyphenols in malignant mesothelioma cells

Tutor:

Prof. Bruno Burlando

Prof. Mauro Patrone

Ph.D. Student:

Dott.ssa Stefania Ribulla

Coordinator:

Prof. Giorgio Malacarne

Table of contentents

Abbreviations and Acronyms

AA: Ascorbic Acid

Akt: also known as Protein Kinase B (PKB)

AND therapy: Active Nutrients/Drug therapy

BCA: Bicinchoninic Acid

$[Ca^{2+}]_i$: Cytosolic Ca^{2+} concentration

CAD: Collision activated dissociation gas

Calcein-AM: Calcein-acetoxymethylester

CT: Computerized tomography

CTLA-4: Cytotoxic T lymphocyte antigen-4

DM-4: Drug maytansinoids

DMEM: Dulbecco's Modified Eagle's Medium

DMSO: DiMethyl SulfOxide

DNA: deoxyribonucleic acid

EDTA: EthyleneDiamineTetraacetic Acid

EGCG: EpiGalloCathechin-3-Gallate

EGF: Epidermal Growth Factor

EGFR: Epidermal Growth Factor Receptor

EPP: Pneumonectomy

ERK: Extracellular signal–regulated kinase

FBS: Foetal Bovine Serum

FDG: fludeoxyglucose F 18

Fura-2AM: Fura-2-acetoxymethyl ester

H&E stain: Hematoxylin & eosin stain

HGF: Hepatocyte growth factor

HMGB1: High-mobility group box 1

HT: Hydroxythyrosol

IARC: International Agency for Research on Cancer

IC_{50}: half maximal Inhibitory Concentration

ICD: International Classification of Disease

IGF: Insulin-like growth factor

IL-4-6-8: Interleukin 4-6-8

INF: Interferon

IPV: inactivated poliovirus vaccine

LC/MS: Liquid chromatography–mass spectrometry

MAP kinase or MAPK: Mitogen-Activated Protein Kinase

MM: Malignant Mesothelioma

MPM: Malignant Pleural Mesothelioma

MPF: megakaryocyte potentiating factor

MRI: Magnetic resonance imaging

MTT: 3-(4,5-Dimethylthiazol-2-yl)-2,5-Diphenyltetrazolium Bromide

NF-kβ: Nuclear Factor k beta

OL: Oleuropein

PBS: Phosphate Buffered Saline

P/D: pleurectomy/decortication

PDGF: Platelet Derived Growth Factor

PD-L1: Programmed death ligand 1

PDT: Photodynamic Therapy

PET: Positron emission tomography

PMSF: Phenyl-methylsulfonyl fluoride

Rb: retinoblastoma

ReNaM: National Mesothelioma Register

Res: Resveratrol

ROS: Reactive Oxygen Species

siRNA: Small interfering RNA

SMRP: Soluble mesothelin related protein

SV-40: Simian Virus 40

TGF-β: Transforming growth factor beta

TIS: Turbo ion spray

TLC: Thin Layer Chromatography

TNF-α: Tumor Necrosis Factor-α

TNM: Tumor node metastasis

TP53: Tumor protein p53

VATS: Video assisted thoracoscopic surgery

VEGF: Vascular Endothelial Growth Factor

WHO: World Health Organization

Introduction

DISEASE DEFINITIONS

Malignant Mesotheliomas (MM) are, by definition, tumors that arise from mesothelial cells of any body cavity: pleura, peritoneum, pericardial sac, and tunica vaginalis testis. Malignant pleural mesothelioma (MPM) is the most common of these, accounting for approximately 90% of disease, and pathologically the best defined one (1). (Fig.1).

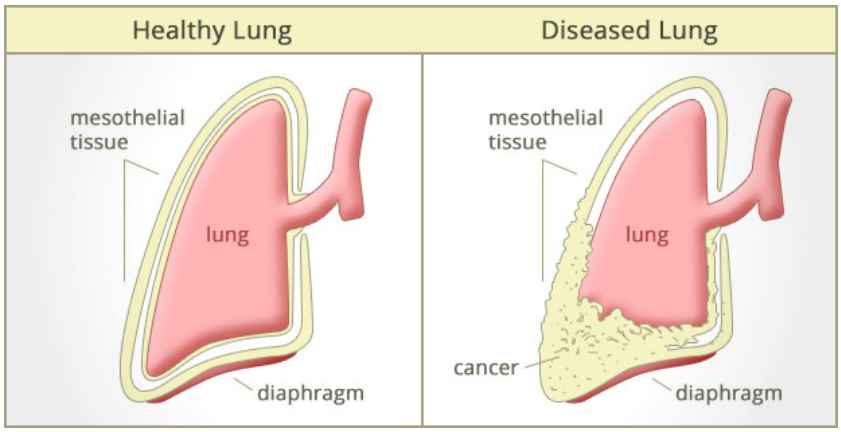

Figure 1. Normal and diseased pleura

The risk of MPM is attributable to asbestos exposure, and has been reported to range between 86% and 95% in most recent epidemiological studies (2-4).

The estimated rate of non-asbestos-related MPM varies widely among studies and is allegedly influenced by the different methods of assessing exposure (5).

HISTORICAL OUTLINE

There is clear evidence of asbestos use among various cultures since ancient times (6). The word asbestos is derived from a Greek term meaning inextinguishable or unquenchable, a reference to its fire-resistant properties (1).

Heat resistant and insulating properties made asbestos a valuable commodity, particularly as the industrial revolution began. In the USA, mining and subsequent use of asbestos increased steadily during the first half of the 20th century, escalated rapidly following World War II, and peaked in 1973, after which it precipitously declined.

Asbestos was widely used for the insulation of water and combustion pipes, as material for house construction and shipbuilding, as car brakes and gaskets, or in the manufacture of toys, jewellery, and cigarette filters. At the peak of asbestos use in industrial activities, about 3000 asbestos-containing products were registered (7).

The first report of a pleural tumor occurred in 1767 by Joseph Lieutand, the founder of pathologic anatomy in France, who in a study of 3000 autopsies found two cases of “pleural tumors”. Thereafter, mesothelioma was characterised as a specific disease by Klemperer and Rabin in 1931 (8). It took almost a further 30 years for mesothelioma to become widely accepted as a separate cancer entity. The definitive epidemiological study linking mesothelioma to asbestos came from South Africa, and was published in 1960 by J.C. Wagner, C.A. Sleggs and P. Marchand. These authors showed that mesothelioma was very prevalent in people living or working in crocidolite asbestos mine areas (9). Subsequently, several studies from the USA, Europe, Australia and Japan verified asbestos inhalation as the etiological cause of mesothelioma (10-12).

DISEASE ETIOLOGY

Asbestos

The association of mesothelioma with asbestos exposure is well established, with an etiological fraction above 80% (13).

This tumor was once rare, but its incidence has been increasing in several countries because of widespread exposure to asbestos in the past, and it is predicted that it will increase in the next decades, especially in developing countries where asbestos has not yet been banned for use (14).

Asbestos refers to a group of crystalline-hydrated silicate minerals and is classified into two main families, the serpentines and the amphiboles (Tab. 1). The serpentines consist of chrysotile, consisting of short, curly fibres. This mineral is called “white asbestos”, due to its color, and accounts for 95% of marketed asbestos (15). The amphiboles, with straight, longer fibres, include crocidolite or “blue asbestos”, amosite, tremolite, actinolite and anthophyllite (16) (Fig. 2).

Mixtures of chrysotile and amphiboles were used to produce an array of roofing, insulation and fire-proofing materials.

Evidence exists that all types of asbestos fibres induce pulmonary toxicity in a dose-dependent manner. Moreover, all fibre types possess carcinogenic potential; however, exposure to amphibole fibres, rather than to chrysotile, is more likely to cause mesothelioma (17). The association between amphibole asbestos exposure and MPM development is well known. In particular, crocidolite is considered the most carcinogenic type of asbestos. Erionite, an asbestos-like mineral, also causes MPM.

Evidence suggesting a link between asbestos exposure and MPM insurgence has been deemed sufficient by the World Health Organisation (WHO) to conclude that all types of asbestos cause cancer in humans (18).

The median latency between asbestos exposure and disease onset is 44.6 years, and it tends to increase over time in a linear fashion. Therefore, despite asbestos banning, incidence rates in Europe are still rising, with a peak expected around 2020 or beyond (19).

There is some evidence that disease latency has an inverse relationship with the duration or degree of asbestos exposure (20).

Although short or low-level asbestos exposures have been linked to the development of mesothelioma, the risk of disease demonstrates dose dependence (21). However, it has been shown that other etiologic factors have a role in MPM pathogenesis.

Name	Composition	Source	Morphology
Chrysotile	$Mg_6Si_4O_{10}(OH)_8$	U.S. and Canada	Curly, pliable
Crocidolite	$Na_2(Fe^{3+})_2(Fe^{2+})_3Si_8O_{22}(OH)_2$	South Africa Western Australia	Rodlike, durable
Amosite	$(Fe, Mg)_7Si_8O_{22}(OH)_2$	South Africa	Rodlike, durable
Anthophyllite	$(Mg, Fe)_7Si_8O_{22}(OH)_2$	Finland	Rodlike, durable
Tremolite	$Ca_2Mg_5Si_8O_{22}(OH)_2$	Exists in some deposits of Canadian chrysotile	Rodlike, durable
Actinolite	$Ca_2(Mg, Fe)_5Si_8O_{22}(OH)_2$	Not mined	Rodlike, durable

Table 1. Composition and characteristics of asbestos fibers. Chrysotile is a hydrated magnesium silicate. The amphiboles are a group of hydrated silicates with a wide range of cation substitutions within the silicate backbone of the crystal structure (22).

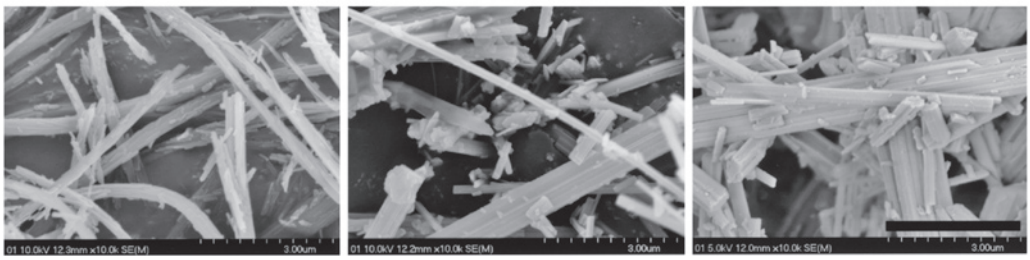

Figure 2. Scanning electron micrographs contrast curved fibers of chrysotile asbestos (left) with straight fibers of crocidolite (center) and amosite (right; bar=3 mm). Typically, chrysotile fibers exhibit a curved, curly, or wavy morphology, which is most apparent in fiber bundles exceeding 10 mm in length. In addition, the ends of chrysotile fiber bundles often exhibit a splayed appearance because of the separation of individual fibrillar units. This curly morphology influences the interceptive deposition of chrysotile fibers, which in turn, affects the depth of penetration into the lower respiratory tract. The diameters of individual fibers vary considerably with substantial overlap among members of the amphibole group. However, crocidolite generally has the finest fiber diameters (22).

SV40

The DNA virus, Simian Virus 40 (SV40), has been suggested as a causal co-factor of MPM insurgence (1). The most likely route of SV40 transmission from monkey to human was through SV40-contaminated polio vaccines that were produced between 1955 and 1978 (23). The first inactivated poliovirus vaccine (IPV) and live oral poliovirus vaccine were prepared in primary cell cultures derived from rhesus monkey kidneys. Studies of these vaccines led to the discovery of the DNA virus SV40 in 1959, a virus endemic in rhesus monkeys (24).

SV40 contributes to the transformation of human cells by perturbing several intracellular pathways, including p53 and retinoblastoma (Rb) tumour suppressor pathway disabling (25).

The strong and consistent relationship between experimental SV40 infection and cancer development in rodents motivated the investigation of its carcinogenic potential in humans. The interpretation of the repeated finding of SV40 in human tumors is still controversial and its role in overall human mesothelioma incidence remains unclear (26). However, recent studies showed that animals infected or transfected with SV40 were extremely susceptible to asbestos carcinogenesis, and these techniques are currently used as an *in vivo* model to study SV40 as a co-carcinogen for MPM development (27).

Genetics

Observation of high MPM rates in the Cappadocian villages of Turkey has identified other potential etiological factors. Genetic susceptibility to MPM was observed in the Cappadocian villages of Tuzkoy, Karain, and ‘‘Old’’ Sarihidir. Although mineralogical studies showed that all the buildings of these villages contained similar amounts of erionite, MPM was prevalent in certain families but not in others. Pedigree studies of the three MPM villages showed that the tendency to develop MPM seemed to be inherited in an autosomal dominant pattern. Genetically predisposed family members born and raised outside the MPM villages did not seem to develop MPM, supporting the observation that the combination of genetics and erionite exposure (gene and environment) was responsible for causing MPM in these villages (28).

Radiation

Long-term effects of ionizing radiations have been etiologically linked to MPM, although in a much smaller group of individuals compared to those exposed to asbestos. Several case reports have documented MPM in patients who had received therapeutic radiation to the

thorax or abdomen (29). The average interval between exposure to radiations and MM diagnosis was 21 years (30). Animal studies using rats also suggest the role of radiation as a causative factor of MPM.

It is also well documented that MPM is over-represented in testicular cancer and Hodgkin's lymphoma survivors who have been treated with external radiotherapy (31,32). However, due to improved knowledge on secondary cancer formation and the introduction of alternative treatments, ionizing radiations are rarely used at present.

EPIDEMIOLOGY

MPM incidence is variable within and between countries because of differences in asbestos use (33). MPM was extremely rare until the second half of the 20th century. Since then, the incidence of MPM has increased significantly, in association with widespread use of asbestos. Currently, there are about 2000 to 3000 cases per year in the United States (34) and an additional 5000 deaths in Western Europe (35).

Overall, except Australia and USA, incidence of MPM is expected to peak between 2015 and 2033 (36). (Tab. 2).

Country	Incidence at peak (new cases per million per year)	Peak year(s)	Predicted deaths per year at peak	Study
Australia	40	2010	1000	Leigh 2002 (e8)
United Kingdom	38	2016	2040	Tan 2010 (e9)
Germany	20	2015–2020	1600	Pesch 2010 (e10) Peto 1999 (e11)
France	20	2020–2040	1300	Banaei 2000 (e12)
USA	15	2010	2800	Larson 2007 (e13)
Japan	15	2025–2033	1200	Azuma 2009 (e14)
Spain	11	2016	520	Pitarque 2008 (e15)
Netherlands	10	2028	900	Segura 2003 (e16)

Table 2 Predicted peak incidence years and incidence at peak for mesothelioma in various countries (37).

The WHO estimates that at least 125 million people globally are occupationally exposed to asbestos. Based on the International Agency for Research on Cancer (IARC), a total of 120,544 new cases of MM were reported during the period 1988-2002, with 58% of these cases from North America, 33% from Europe, 5% from Oceania, and 3% from Asia (38).

However, the planetary occurrence of MM is likely to be underestimated, owing to unreported cases in mortality registries of developing countries (39), inaccurate death certification (40,41), and undifferentiated International Classification of Diseases (ICD) codes for pleural malignancy until 1994 (42). The latency period, i.e. the interval between first exposure and the development of MPM, ranges between about 25-71 years (43).

Moreover, analysis of MPM trends in different countries revealed a significant annual increase in Japan (3.5%) and a decrease in the United States (0.84%) (44) suggesting that disease burden is slowly shifting toward countries that have used asbestos more recently. The delayed peak in Japan can be correlated to the historical delay in heavy asbestos usage (45).

MPM is a less common disease in women (with a male to female ratio of 3.8:1) (38). Approximately 80% of patients who develop MPM are men (46).

The disease can occur in any age group but is more common in 6th decade and only about 2% to 5% of cases are reported in the first two decades of life (47). The median age at the diagnosis of MPM is 72–74 years (48,49).

Given the role of asbestos in the etiology of MPM, three waves of disease occurrence have been described (50). The first affected miners and millers employed in the extraction of raw asbestos and in the manufacture of asbestos products. A second wave of disease became evident in workers who used asbestos products in industry, such as carpenters, plumbers, defence personnel, shipbuilders, and insulation installers. The third wave of disease included people with unknown, short-term, or low-level exposure to asbestos. Examples of these kinds of exposures, frequently non-occupational ones, include domestic (relatives of asbestos workers), air pollution from nearby asbestos industry, and exposure to asbestos in place (buildings containing asbestos) (51).

MPM IN ITALY

In a period going from the 1950's to total national banning in 1992, Italy was an important producer and user of asbestos and asbestos-containing materials. Up to the end of the 1980's Italy was the second largest asbestos producer in Europe, after the Soviet Union, and the largest in the European Community.

In particular, asbestos production reached a peak in the 1976–1980 period, but remained steadily over 100,000 tons/year until 1987. These temporal patterns made the peak in asbestos consumption to occur later on in Italy with respect to other European countries and the United States (52). Therefore, considering the long latency of MPM (generally around 35–40 years from first exposure), a high number of cases is still expected in Italy in the next few decades (53).

Because of its previous high utilization, the wide spectrum of industries involved and the number of workers and non-workers exposed, Italy is among those countries that are most prone to adopt measures for preventing asbestos related diseases. In addition, Italy has a specific system for mesothelioma epidemiological surveillance: the National Mesothelioma Register (ReNaM), active since 2002 and operating through a regional structure. The registry currently holds data about cases of malignant mesothelioma between 1993 and 2008, concerning subjects resident in Italy. Data from cases diagnosed between 2009–2013 are currently under acquisition (54).

In the period 1993-2008, 15,322 incident cases of all-site MM were recorded. Most MM cases (93%) occurred in the pleural site. Standardised incidence rates for pleural mesothelioma in 2008 were 3.84 per 100,000 for men and 1.45 for women, respectively. Among the 15,845 mesothelioma cases, exposure to asbestos fibres was assessed for 12,065 individuals (76.1%), identifying 530 (4.4%) with familial exposure (they lived with an occupationally exposed cohabitant), 514 (4.3%) with environmental exposure to asbestos (they lived near sources of asbestos pollution and were never occupationally exposed) and 188 (1.6%) exposed through hobby-related or other leisure activities. (Tab. 2). Clusters of cases due to environmental exposure are mainly related to the presence of asbestos-cement industry plants (Casale Monferrato, Broni, Bari), to shipbuilding and repair activities (Monfalcone, Trieste, La Spezia, Genova) and soil contamination (Biancavilla, Sicily) (55). (Fig. 3). The mean age at diagnosis was 69.3 years with no significant difference by gender (70.3 for women and 68.9 for men). Less than 10% of cases occurred in subjects younger than 55 years.

		Men		Women	
		Number of cases	%	Number of cases	%
Age class	0-54	1,046	9.6	450	10.3
	55-64	2,646	24.1	856	19.7
	65-74	4,015	36.6	1,404	32.2
	75+	3,257	29.7	1,648	37.8
Period of diagnosis	1993-1996	1,042	9.5	382	8.8
	1997-2000	2,271	20.7	884	20.3
	2001-2004	3,706	33.8	1,503	34.5
	2005-2008	3,945	36.0	1,589	36.4
Area	Northwest	5,158	47.1	2,423	55.6
	Northeast	2,586	23.6	901	20.7
	Centre	1,450	13.2	454	10.4
	South & Islands	1,770	16.1	580	13.3
Diagnostic certainty	Definite	8,708	79.4	3,234	74.2
	Probable	1,142	10.4	574	13.2
	Possible	1,114	10.2	550	12.6
Site of lesion	Pleura	10,312	94.0	3,941	90.4
	Peritoneum	579	5.3	403	9.3
	Pericardium	26	0.2	14	0.3
	Testis	47	0.4	-	-
Exposure ascertainment	Direct interview	4,585	41.8	1,401	32.2
	Indirect interview	4,139	37.8	1,727	39.6
	No interview	2,240	20.4	1,230	28.2
Type of exposure	Occupational, definite	4,987	45.5	526	12.1
	Occupational, probable	890	8.1	112	2.6
	Occupational, possible	1,291	11.8	402	9.2
	Familial	76	0.7	446	10.2
	Environmental	214	1.9	294	6.7
	Other non-occupational	80	0.7	108	2.5
	Unlikely	193	1.8	223	5.1
	Unknown	993	9.1	1,017	23.3
	Undefined	2,240	20.4	1,230	28.2
Total		10,964		4,358	

Italy, 1993–2008 (N = 15,322).

Table 2. Incident cases of malignant mesothelioma recorded by the Italian national mesothelioma registry (ReNaM) selected for cluster analysis. (54).

Figure 3. Crude incidence rates of malignant mesothelioma (MM) cases by Italian municipalities. Italian National Mesothelioma Register (ReNaM). Italy, men and women, 1993–2008. Diagnosis of MPM definite, probable or possible, all site of lesion (56).

MOLECULAR PATHOGENESIS OF MPM

MPM develops insidiously in patients who are usually diagnosed at advanced stages, because radiological diagnostic tools are not effective for early detection, while early serum biomarkers have not been established yet. The anatomical location and characteristics of the body cavities where MPM initially develops also cause malignant cells to easily spread and invade tissues.

Pathologically MPM is subdivided into three major subtypes, viz. epithelioid, sarcomatoid, and biphasic, the latter showing both epithelioid and sarcomatoid components (57).

MPM subtypes differ in their morphology, biological/clinical phenotypes, aggressiveness and response to treatment (58).

The epithelioid MPM consists of cuboidal or polygonal cells with abundant cytoplasm and uniform round nuclei forming a tubular and papillary pattern. The sarcomatoid MPM consists of sheets or fascicles of spindle cells of variable cellularity and pleomorphism. According to the World Health Organization, biphasic MPM must contain at least 10% epithelial and at least 10% sarcomatoid patterns (59). Epithelioid is the most common sub-type among MPM patients, being associated with a relatively better prognosis (60). (Fig. 4).

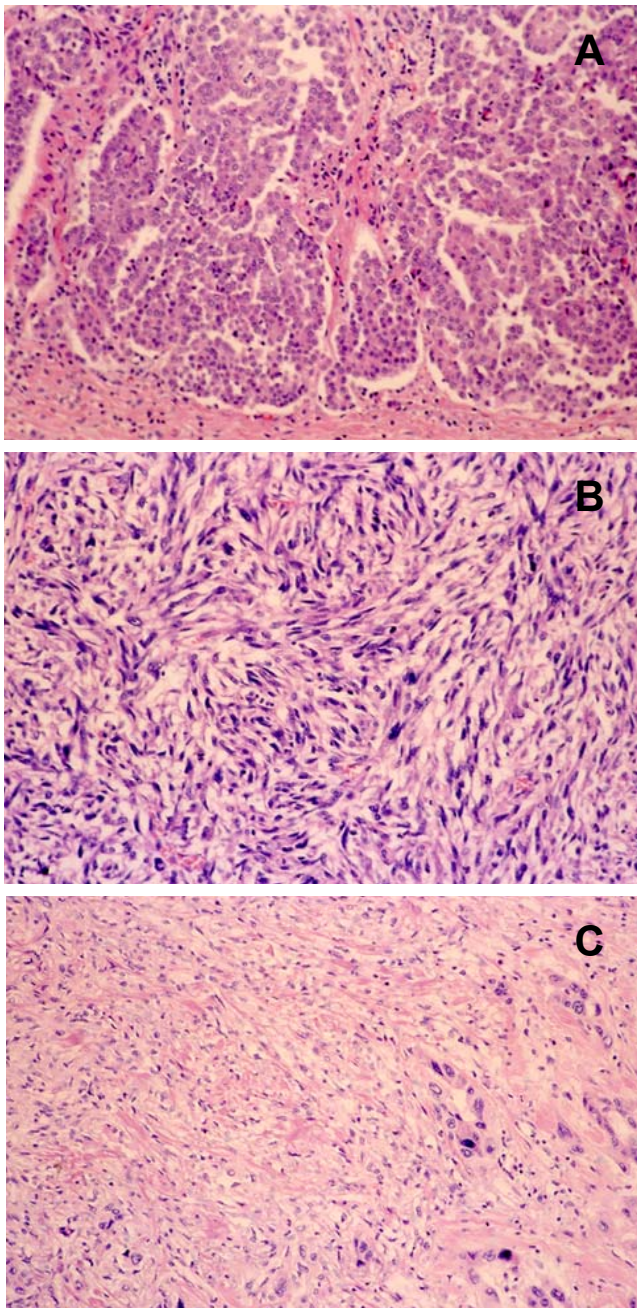

Figure 4. Histologic types of MPM. Microphotograph (H&E stain) of epithelioid mesothelioma (A), sarcomatoid mesothelioma (B) and biphasic mesothelioma (C) (61).

The exact mechanisms of mesothelioma pathogenesis are unknown. However, several recent MM reviews report comprehensive lists of genetic, epigenetic and signaling alterations (62).
A main mechanism is thought to be triggered by asbestos fiber penetration within the lung tissue. When long and thin asbestos fibers are inhaled deeply into the lung and penetrate the pleural space, they start to interact with mesothelial cells and inflammatory cells. (Fig. 5). This is thought to trigger prolonged cycles of damage/repair in lung tissue, accompanied by prolonged local inflammation, allegedly leading to MPM carcinogenesis (63).

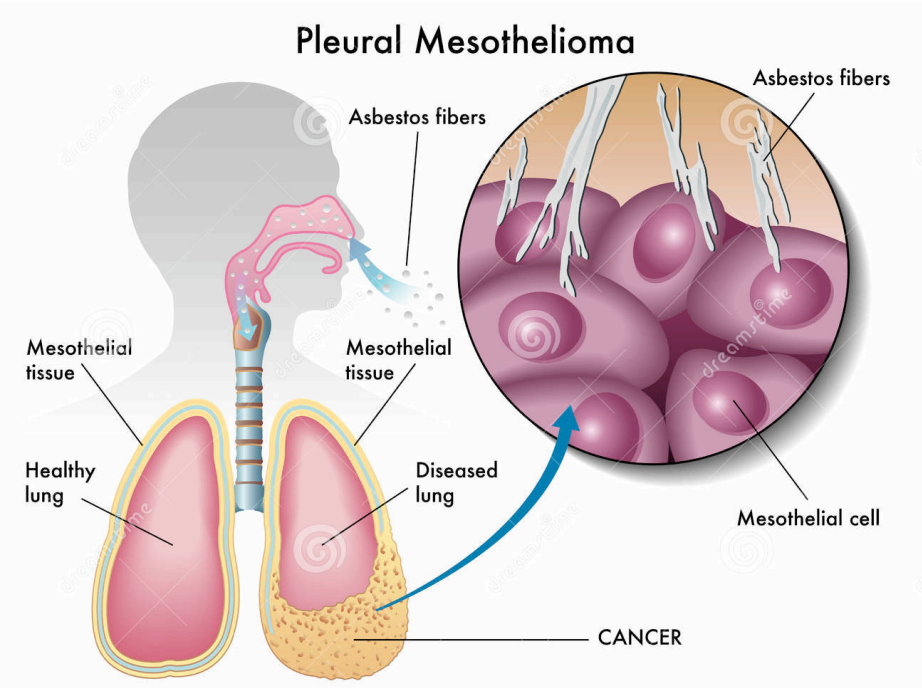

Figure 5. Development of malignant pleural mesothelioma (MPM) in response to asbestos exposure

Alternative routes of fiber translocation to the parietal pleura include lymphatic and haematogenous dissemination (17). The exact way in which asbestos fibers cause these changes is uncertain, but researchers believe such changes are responsible for cancer development. It also remains unclear why the initial affected site of MPM development by asbestos exposure is the parietal instead of the visceral pleura. Compared with other cell types, human mesothelial cells are very susceptible to asbestos cytotoxicity, which raises a paradoxical issue of how asbestos causes MPM if human mesothelial cells exposed to

asbestos die (64). It is however known that several features of asbestos fibers contribute to their carcinogenicity, including chemical composition, fibers length and form, and their biopersistence (65). It has been also shown that asbestos has pleiotropic effects on cell signaling pathways (66, 67). (Fig. 6). First, reactive oxygen species generated by asbestos fibers lead to DNA damage and strand breaks (68-70). Second, macrophages that phagocyte asbestos fibers are unable to digest them, resulting in further production of reactive oxygen species (70). These events activate MAP-kinase signaling pathways through the epithelial growth factor (EGF) receptor, which is frequently highly expressed in mesothelioma together with downstream transcription factors.

The long latency period of the disease (up to 40 years) suggest that multiple genetic alterations are important in the conversion from normal to malignant mesothelial cell. Comprehensive karyotypic analysis has revealed that malignant mesotheliomas display multiple clonal chromosomal abnormalities (more than 10 of them in most cases). This can be explained by considering that asbestos fibers engulfed by mesothelial cells can physically interfere with the mitotic process of the cell cycle, thereby damaging the mitotic spindle. This may result in chromosomal structural abnormalities and aneuploidy of mesothelial cells (71).

The loss of one copy of chromosome 22 is the most typical single chromosomal change in patients with mesothelioma. Specific deletions of chromosomal sites involve the short arm (p) of chromosomes 1, 3 and 9, as well as the long arm (q) of chromosome 6. Other non-random cytogenetic alterations have been detected on other chromosomes (72). Mutations of the p53 gene (TP53) are occasionally observed in MPM (73). Loss and/or inactivation of tumor suppressor genes like TP52 may play a role in the development and progression of MPM.

Asbestos fibers can absorb chemicals to their surface, with the consequent accumulation of hazardous molecules (including carcinogens). Fibers can also bind cellular proteins, possibly leading to detrimental deficiency for normal mesothelial cells (74). Finally, asbestos-exposed mesothelial cells and macrophages release a variety of cytokines and growth factors, including inflammation and tumor promotion agents like transforming growth factor beta (TGF-β), which might have a role in stimulating tumor growth; platelet-derived growth factor (PDGF), which may act as a regulatory factor in MM cell proliferation, insulin-like growth factor (IGF), which promotes tumor proliferation and cell migration (75); interleukins such as IL-6 and IL-8, which may promote tumor growth and the development of new capillaries (76); vascular endothelial growth factor (VEGF), which also promotes tumor angiogenesis (77), and hepatocyte growth factor (HGF), which stimulates mesothelioma cell migration and invasiveness (78).

Tumor necrosis factor-α (TNF-α) has been shown to activate nuclear factor-κB (NF-κβ), which leads to mesothelial cell survival and inhibits asbestos-induced cytotoxicity (79, 80). High-mobility group box 1 (HMGB1) protein is also released from mesothelial cells, which are exposed by asbestos and then undergo necrotic cell death, promoting an inflammatory response (81).

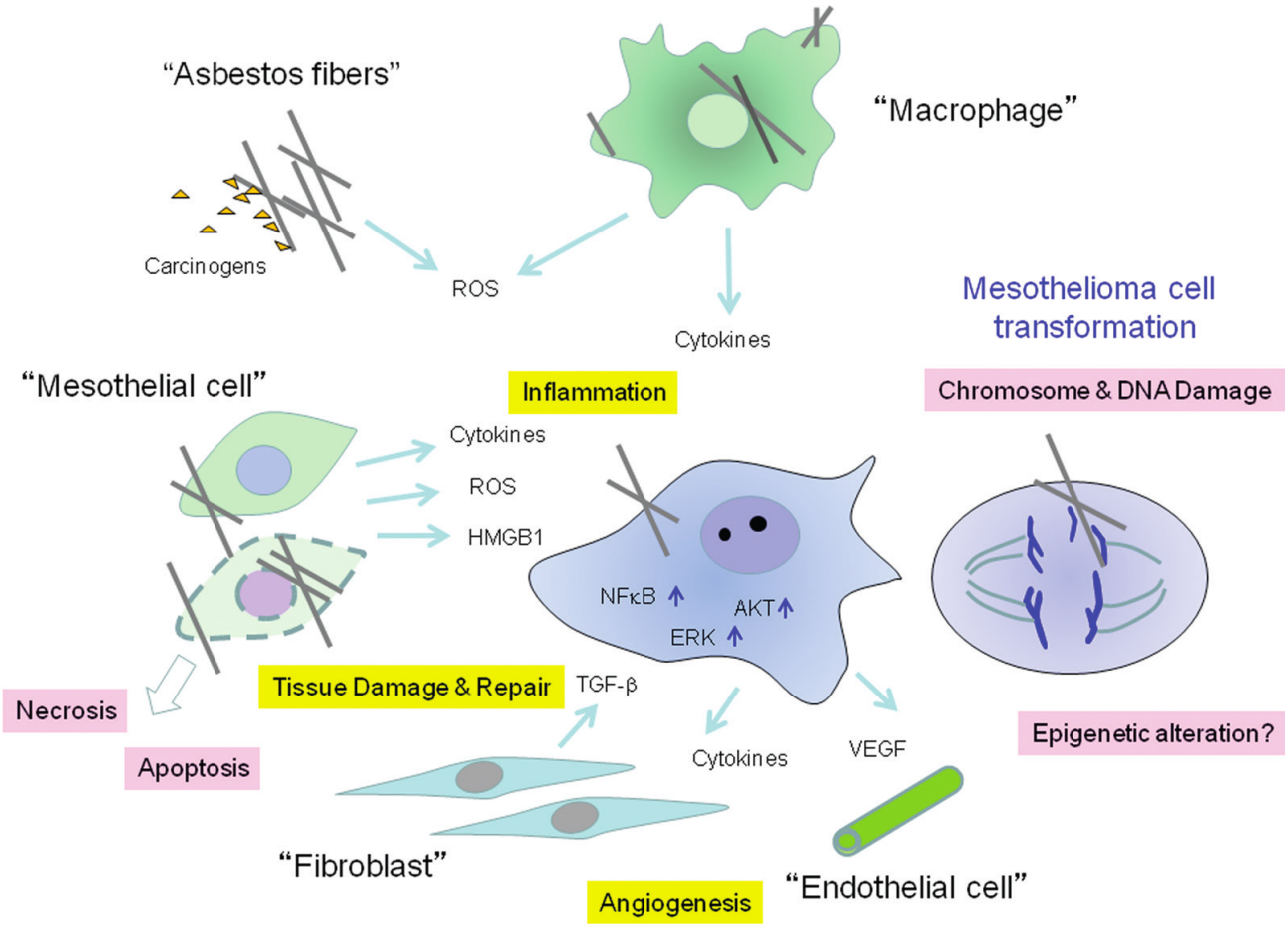

Figure 6. Possible mechanisms of asbestos-induced carcinogenesis. HMGB1, high-mobility group box 1 protein; ROS, reactive oxygen species; TGF-β, transforming growth factor-β; VEGF, vascular endothelial growth factor (74).

CLINICAL FEATURES AND DIAGNOSIS

Clinical MPM symptoms are usually atypical and nonspecific. The most common one is dyspnea (90% of cases) that is typically caused by pleural effusion. Commonest initial symptoms are pain (35%) caused by irritation of intercostal nerves or by infiltration into the chest wall, distension of abdomen (31%), and less frequently night sweats. Patients also commonly develop cachexia, anorexia or ascites (77%) (47). Weight loss is a late sign of disease, along with generalized malaise and failure to thrive (82). Rarely, patients present with fever of unknown origin, intestinal obstruction or acute abdominal surgical emergency. Symptomatic metastases are unusual. In addition, the majority of patients report late due to very elusive and atypical symptoms, leading to diagnostic delays of up to six months (83). Considering the elusive nature of the disease, the diagnosis of MPM should be considered in any patient with a unilateral pleural effusion or thickening, especially if chest pain is present. Whenever MPM is suspected, a detailed occupational history should be taken and the patient should be referred to an experienced center for pulmonary medicine.

An important help to clinicians in this phase can be provided by imaging diagnostic tools, which also play an important role in staging, treatment planning (especially in terms of resectability), response assessment, and follow up of MPM patients. Initially, non-invasive tests such as ultrasonography, computerized tomography (CT), and magnetic resonance imaging (MRI) can be used to obtain further support for the suspected diagnosis and assess the extent of disease. CT is useful to judge the extent of tumor and to detect lymphonode metastases. MRI is the best way to determine whether the tumor has invaded the diaphragm or the chest wall. Positron emission tomography (PET) is also coming into wide use; its main advantage is a greater sensitivity for the detection of distant metastases (84). The integration of PET functional data coupled to radio-pharmaceutical FDG, with anatomical data from CT (PET/CT) could be useful in the diagnosis and preoperative staging of patients. (85).

In order to render an accurate diagnosis, a biopsy sample must provide adequate diagnosable tissue. For the diagnosis of MPM, a biopsy sample typically is obtained form open procedures such as thoroscopy. Biomarkers would be helpful in managing three clinical aspects of MPM: early diagnosis, prognosis, and outcome prediction. Researchers have actively sought MPM biomarkers for more than 20 years. However, at present, there are no biomarkers in clinical use for MPM. In fact, MPM remains a rare disease and the small number of patients and the difficult accessibility to a uniform tumor population renders the search for biomarker frustrating. For early diagnosis, optimal serum biomarker for mesothelioma would predict mesothelioma development in asbestos-exposed subjects, differentiate mesothelioma from

benign pleural disease or metastatic cancer, could be useful for pathologic subtypes, and correlate with disease extent in order to monitor treatment response and predict prognosis. (86). The biomarkers osteopontin (87), soluble mesothelin-related protein (SMRP) (88), and megakaryocyte potentiating factor (MPF) are currently most promising for diagnosis, but each of them has limitations (89, 90).

CURRENTLY ESTABLISHED THERAPY

Treatment options depend on multiple factors, including patient age, performance status, tumor histology, and disease stage at presentation.

The staging system proposed by the International Mesothelioma Interest Group was accepted by the International Union Against Cancer and the American Joint Commission on Cancer (Tab. 3 and 4). This system describes the extent of tumor according to the tumor-node-metastasis (TNM) classification, i.e. local extent of the primary tumor (T descriptor), presence and location of lymphnodes (N descriptor), and presence of distant metastatic disease (M descriptor) (91).

T—primary tumor
T1a tumor limited to ipsilateral parietal pleural, including mediastinal and diaphragmatic pleura
No involvement of visceral pleura
T1b tumor involving ipsilateral parietal pleura, including mediastinal and diaphragmatic pleura
Scattered foci of tumor also involving visceral pleura
T2 tumor involving each ipsilateral pleural surface with at least 1 of the following features:
- involvement of diaphragmatic muscle
- confluent visceral pleural tumor (including fissures) or extension of tumor from visceral pleura into underlying pulmonary parenchyma

T3 locally advanced but potentially resectable tumor
Tumor involving all of ipsilateral pleural surfaces with at least 1 of the following:
- involvement of endothoracic fascia
- extension into mediastinal fat
- solitary, completely resectable focus of tumor extending into soft tissues of chest wall
- nontransmural involvement of pericardium

T4 locally advanced technically unresectable tumor
Tumor involving all of ipsilateral pleural surfaces with at least 1 of the following:
- Diffuse-extension or multifocal masses of tumor in chest wall, with or without associated rib destruction
- direct transdiaphragmatic extension of tumor to peritoneum
- direct extension of tumor to contralateral pleura
- direct extension of tumor to 1 or more mediastinal organs
- direct extension of tumor into spine
- tumor extending through to internal surface of pericardium with or without pericardial effusion, or tumor involving myocardium

N—lymph nodes
NX regional lymph nodes not assessable
N0 no regional lymph node metastases
N1 metastases in ipsilateral bronchopulmonary or hilar lymph nodes
N2 metastases in subcarinal or ipsilateral mediastinal lymph nodes, including ipsilateral internal mammary nodes
N3 metastases in contralateral mediastinal, contralateral internal mammary, and ipsilateral or contralateral supraclavicular lymph nodes

M—metastases
MX distant metastases not assessable
M0 no distant metastases
M1 distant metastases present

Table 3. Staging Evaluation: TNM International Staging System for Diffuse MPM (92).

Stage	Description
1a	T1aN0M0
1b	T1bN0M0
II	T2N0M0
III	Any T3M0
	Any N1M0
	Any N2M0
IV	Any T4
	Any N3
	Any M1

Table 4. Classification of Stage by TNM Description (92).

The relatively low incidence of MPM poses a challenge to the evaluation of the effectiveness of treatment options because of difficulties in the accrual of patients in clinical trials, particularly large, randomized prospective trials. Given this limitation, the failure of single-modality therapy, i.e. chemotherapy, radiation therapy, or surgery alone, has led to the increasing use of multimodality regimens, by combining these treatment options (93).

Surgery

The role of surgery in MPM treatment is still uncertain. In general, patients with stage I disease can be considered candidates for radical surgery. The three most common surgical procedures are debulking surgery (also known as cytoreductive surgery or pleurectomy/decortication (P/D)), extra pleural pneumonectomy (EPP), and surgical pleurodesis via video assisted thoracoscopic surgery (VATS). P/D is a lung-sparing operation in which the pleura is mobilized off the chest wall, mediastinum, diaphragm, and pericardium, and stripped from the surface of the lung. Pleurectomy has not been shown to prolong survival but can reduce the recurrence of pleural effusion better than talc pleurodesis (94). In contrast, EPP is the radical *en bloc* resection of the lung, visceral and parietal pleura, ipsilateral diaphragm, and adjacent pericardium (95). It is a rather complex operation, which should be performed by skilled surgeons and in selected centres. VATS is a type of thoracic surgery performed using a small video camera that is introduced into the patient's chest via a scope. It is a minimally invasive surgical technique used to diagnose and treat problems in the chest. Operations that were traditionally carried out with thoracotomy or sternotomy and are currently performed with VATS include: biopsy for diagnosis of pulmonary, pleural or

mediastinal pathology, decortication, pleurodesis for recurrent pleural effusions or spontaneous pneumothorax, surgical stapler-assisted wedge resection of lung masses, and resection of mediastinal (96). The goal of surgery is gross total resection of the tumor. As mesotheliomas tend to grow diffusely, they are usually not totally resectable; some residual tumor tissue (often microscopic) is generally left behind. Adjuvant chemotherapy is therefore frequently administered in order to achieve full elimination of remaining tumor cells (97).

Chemotherapy

The use of chemotherapy in malignant mesothelioma aims to lengthen survival, improve quality of life and provide symptomatic relief. At present, there is no single drug or combination therapy that could be considered as a standard treatment for mesothelioma.

Chemotherapy is the mainstay of therapy because of the fact that most MPM patients present with advanced disease. In a meta-analysis of studies published between 1965 and 2001, cisplatin was found to be the most active single drug, while its use in combination chemotherapy has been associated with higher response rates, but not with longer survival (98). Several new cytotoxic agents with definite activity in mesothelioma have recently been evaluated, including gemcitabine, imatinib, and the antifolates pemetrexed and raltitrexed. The pemetrexed/cisplatin combination significantly improved response rates, time to progression, overall survival and quality of life compared to cisplatin alone (99).

Radiotherapy

The role of radiation therapy in MPM is as controversial as the role of surgery. Radiotherapy can be used to control local MPM growth and occasionally causes regression of disease, but there is no evidence that radiotherapy alone affects survival (100). Patients with mesothelioma are given prophylactic radiotherapy at puncture sites and after surgical interventions to prevent local recurrence and to relieve pain in palliative care. Radical radiotherapy of the entire tumor is not currently feasible, because these tumors tend to grow in a complex geometrical configuration, and the resulting high radiation load of treatment would be likely to cause collateral damage to heart and lungs (101).

Multimodal approaches

Specialized mesothelioma centers employ multi-modality approaches, including surgical resection, chemotherapy, and radiation, with survival in excess of 20 months depending on stage (102).

In a clinical trial, neo-adjuvant chemotherapy combined with pleuropneumectomy and followed by radiotherapy has led to a survival rate 3-year longer, on average, then those obtained with unimodal treatments (76 %) (103). In another study, multimodal approach has prolonged the median survival time up to 22 months for stage I disease (104).

NOVEL THERAPIES

Many novel strategies are being attempted to improve survival for patients with MPM. Several classes of targeted therapies have emerged from preclinical work and are being evaluated. These treatments focus on the following broad mechanisms:

- Tyrosine kinase inhibitors
- Antibody conjugated toxins
- Immune checkpoint inhibitors
- Gene therapy
- Tumor vaccines

Tyrosine kinase inhibitors

Molecular studies of mesothelioma specimens have shown marked overexpression of protein targets such as epidermal growth factor receptor (EGFR) and vascular endothelial growth factor (VEGF) (105).

The inhibition of EGFR-dependent signaling pathway in mesothelioma cell lines leads to decreased cell survival (106); based on these findings, several clinical trials have been conducted but, disappointingly, these studies did not show improved survival.

Higher levels of VEGF may be reflective of more-advanced disease and have been associated with shorter survival. *In vitro* studies have demonstrated that increased mesothelioma cell proliferation occurs upon treatment with VEGF and that significant inhibition of cell growth can be achieved by blocking this pathway (107). It is therefore thought that interference with this pathway could potentially lead to successful therapy. Numerous clinical trials have evaluated the effect of VEGF inhibitors alone and in combination with other drugs, but also the results of these trials have been disappointing.

Therapy targeting cell-surface receptors

Mesothelin is a 40-kDa, glycosylphosphatidylinositol-anchored cell-surface glycoprotein present on normal mesothelial cells and overexpressed on the surface of mesothelioma. Mesothelin overexpression, occurring more prominently on epithelioid tumors, may serve to alter cell adhesion and/or invasion. Preclinical studies in nude mice suggested that MORAb-009 (amatuximab), a monoclonal antibody with high affinity for human mesothelin combined with chemotherapy (gemcitabine or paclitaxel) was more effective than either chemotherapy alone (108). BAY 94-9343 (anetuman ravtansine) is a human antimesothelin antibody

coupled via a reducible disulfide bond to DM4, a microtubule-targeting toxophore that shows highly selective cytotoxicity against cells with high mesothelin expression. Preclinical studies have shown a dose-dependent and receptor-dependent, 94% reduction of tumor growth with BAY 94-9343 compared to 70% reduction with cisplatin and pemetrexed (109).

SS1P is an immunotoxin consisting of an antimesothelin antibody variable fragment linked to a cytotoxic fragment of *Pseudomonas* exotoxin A. Phase I trial including 16 mesothelioma patients has shown that SS1P was well tolerated up to 25 μg/kg/day × 10 days, with modest clinical activity and minor responses, and that two mesothelioma patients had symptomatic improvement (110).

High levels of interleukin-4 (IL-4) receptor expression have been shown on fresh human mesothelioma specimens and correlated with a worse outcome. In a human mesothelioma xenograph, nude mouse model, intratumoral injection of the recombinant toxin IL-4 (38–37)-PE38KDEL significantly reduced tumor volumes in a dose-dependent manner compared to the control and IL-4-treated mice (111).

Immune checkpoint inhibitors

Cytotoxic T lymphocyte antigen-4 (CTLA-4) is vital for maintaining host immune tolerance to established tumors. A Phase II trial evaluating anti-CTLA-4 antibody (tremelimumab) in 29 patients with chemotherapy-resistant advanced mesothelioma (28 pleural and 1 peritoneal) has been recently reported (112). Objective clinical responses have been observed in only 2 of 29 patients (6,9%) and disease stabilization has been noted in 9 patients (31%).

Programmed death receptor is found on the surface of T-cells and its stimulation leads to T-cell deactivation, thus allowing escape from the immune system surveillance in the presence of otherwise antigenic substrate. Activation of this receptor occurs by a programmed death ligand 1 (PD-L1), which is present in the tumor microenvironment and on the surface of tumor cells. The effect of PD-L1 blockade on different subpopulations of T-cells has produced opposing effects on tumor progression, suggesting that tumor-derived immune suppression is mediated by specific subsets of T-cells (113). Several trials are currently evaluating the inhibition of this pathway using different agents (lambrolizumab and nivolumab) in cancers other than MPM.

Gene therapy

Multiple genetic abnormalities have been identified in MPM, and a variety of genetic manipulation strategies have been employed in preclinical studies.

Suicide gene therapy utilizes engineered viruses that deliver transgenes encoding enzymes that metabolize pro-drugs into toxic metabolites capable of killing tumor cells. In a clinical trial conducted with intrapleural *Adenovirus herpes simplex* thymidine kinase/ganciclovir, a few patients have experienced prolonged survival, suggesting the induction of antitumor immunity in addition to acute viral-mediated cytotoxicity (114).

Another gene therapy strategy involves the administration of viral vectors encoding specific cytokine genes that may exert a direct cytotoxic effect on tumor cells or alter immunologic responses to the tumor. For instance, several clinical trials have evaluated adenoviral-mediated interferon (INF) (α and β) therapy (115).

Immunotherapy and vaccines

The rationale for immunotherapy in mesothelioma stems from the observation that patients whose tumor demonstrated lymphocytic infiltrate had a better prognosis. This kind of therapy has focused on both passive immunity, where effectors such as cytokines are used to activate the host immune system, and active immunity, where the lymphocytes of a patient are exposed to cancer-specific antigens (116). Several ongoing studies using immunotherapy in MPM have shown some early promise. Preclinical *in vitro* and *in vivo* data support the use of dendritic cell vaccines as a valuable strategy in mesothelioma (117).

Direct physical cytotoxic therapies

Photodynamic therapy (PDT) is a type of cancer treatment based on the premise that unicellular organisms, if first treated with certain photosensitive drugs, will die when exposed to light at a particular frequency. PDT destroys cancerous cells by using this fixed frequency light to activate photosensitizing drugs which have accumulated in body tissues. In a Phase I–II experience, the median disease-free progression has been set to 15 months, obtaining an overall survival of over 40 months (118).

Experimental data suggest that heating chemotherapeutic agents increases their entry into tumor cells. Data come from Phase I–II studies have evaluated the systemic toxicity of intrapleural drug (most commonly cisplatin) administration in highly selected patients. However, evidence supporting the use of hyperthermia is quite limited (119). A Phase I–II trial of intraoperative hyperthermic (41°C) iodine–povidone lavage following surgery (either P/D or EPP) has been recently reported (120). Although this treatment has been well tolerated

and the surgical outcomes have been acceptable, convincing evidence of its efficacy is still lacking.

Cryotherapy has been used for decades in the treatment of cancer (121). This kind of treatment may improve the immune response through enhanced natural killer cell activity, T-cell responses and systemic IFN production. A recent study reports the use of percutaneous cryoablation in 24 mesothelioma patients for control of limited recurrent local disease following P/D. The treatment was well tolerated, and was associated with a median survival of 11.4 months following first therapy (36.1 months following surgery) (122).

CANCER CHEMOPREVENTION USING NATURAL PRODUCTS

Pharmacological activities associated with natural products have been recognized since the beginning of mankind. Despite the vast interest in diet as a mode to prevent and cure cancer, it was not until the late 20th century that the mechanism of action of diet-derived chemoprevention began to unravel. The beneficial effects of fruits and vegetables have been attributed, among others, to the high content of bioactive compounds that are non-nutrient constituents commonly present in food (123).

Natural products are important sources of anti-cancer lead molecules. Many successful anti-cancer drugs are natural products or their analogues. Natural products have been used for the treatment of various cancers and are becoming an important research area for drug discovery. These products, especially phytochemicals, have been extensively studied and have exhibited anti-carcinogenic activities by interfering with the initiation, development and progression of cancer through the modulation of various mechanisms, including cell proliferation, differentiation, apoptosis, angiogenesis, and metastasis (Fig. 7). This concept is gaining attention because it is a cost-effective alternative to cancer treatment.

Drug toxicity continues to be a subject of great concern. Chemoprevention, by definition, is a means of cancer control by which the occurrence of the disease can be entirely prevented, slowed down, or reversed by the administration of one or more naturally occurring and/or synthetic agents. Chemoprevention began in the 1920s with Isaac Berenblum (124) and, after a period of relative dormancy, re-entered the cancer research mainstream in the 1970s through the work of Michael D. Sporn (125).

In recent years, natural dietary agents have drawn a great deal of attention from both researchers and the general public, because of their potential ability to suppress ongoing cancer and reduce the risk of cancer development. A major group of these products is represented by antioxidants, while other compounds include reactive chemicals endowed with cytoprotective properties. These natural products are found in vegetables, fruits, plant extracts, and herbs. Most of non-nutrient antioxidants in food are phenolic or polyphenolic compounds, such as isoflavones in soybeans, catechins in tea, phenolic esters in coffee, phenolic acids in red wine, quercetin in onions, and rosmarinic acid in rosemary (126).

Multiple epidemiological and animal studies have made it clear that the consumption of food rich in fruits and vegetables decreases the occurrence of cancers (127).

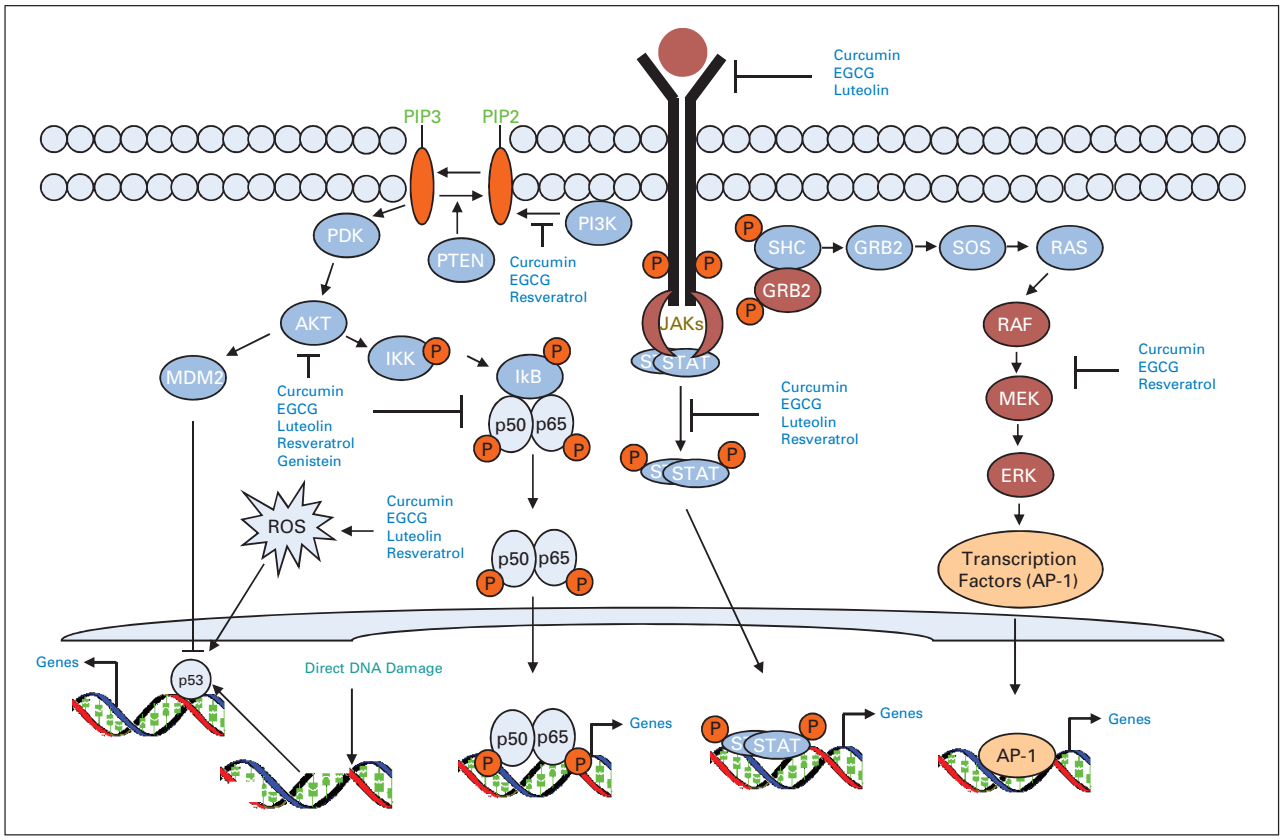

Figure 7. Molecular targets of natural chemopreventive agents. The cell signaling pathways activated by natural dietary agents are numerous and different for different agents. Multiple growth factor receptors (epidermal growth factor receptor, insulin-like growth factor 1 receptor, fibroblast growth factor, platelet-derived growth factor receptor) are activated at the cell surface in tumorigenesis. Activation of these receptors activates several downstream signaling pathways. Among these pathways, the Ras-MAPK (such as ERK and JNK) pathways, the JAK-STAT pathways, the PI3K-AKT pathways and the NF-κB pathways are important and are the targets of natural chemopreventive agents. Some natural agents inhibit the receptors at the cell surface either by dephosphorylating them or by inducing their degradation, which ultimately modulate the downstream signaling pathways important for proliferation, angiogenesis, and apoptosis. Inhibition of AKT and ERK signaling by natural agents is quite common, although in many cases this inhibition is the result of growth factor receptor inhibition. Inhibition of NF-κB signaling pathway by interfering with multiple targets of signaling is another common target of natural agents. Many natural compounds generate reactive oxygen species (ROS), which activate p53 family members and induce cell cycle arrest and apoptosis. EGCG, epigallocatechin-3-gallate; ERK, extracellular signal–regulated kinase (127).

NATURAL PRODUCTS AS TREATMENT IN MPM

Conventional therapies for MPM cause serious side effects and, at best, merely extend the patient's lifespan by a few years. There is thus the need to utilize alternative concepts or approaches to the prevention and treatment of cancer.

Natural products, especially those from terrestrial plants and microbes, have long been a traditional source of drug molecules. Modern pharmaceutical discovery programmes owe much to natural products. Indeed, pharmacologically active compounds from plants and microbes represent an important pipeline for new investigational drugs.

Previous research has revealed that some natural compounds act on MPM cells.

Specifically, ascorbate (AA) and the green tea polyphenol epigallocathechin-3-gallate (EGCG) are selectively cytotoxic to MPM cells with respect to normal mesothelial cells. AA promotes the formation of H_2O_2 in the cell medium, and its toxicity is suppressed by extracellular catalase. The data indicate that AA-induced extracellular H_2O_2 production induces a strong oxidative stress in MPM cells because of their high rate of superoxide production. This explains the selective toxicity of AA to MPM cells (128).

EGCG exerts an MPM antitumor effect, as shown by its selective *in vitro* cytotoxicity on MPM cells through a mechanism of action based on extracellular H_2O_2 production, Ca^{2+} homeostasis loss, and intracellular ROS increase. EGCG induces H_2O_2 release at the outside of cells that acts by inducing T-channel opening at the plasma membrane. Ca^{2+} leakage into the cytosol causes $[Ca^{2+}]i$ rise and triggers ROS production. Ca^{2+} and ROS cooperate in inducing either apoptosis or necrosis, depending on damage (129).

In an *in vitro* screening of various AA/drug combinations, AA and EGCG showed synergistic effects against MPM cells with the standard antitumor drug gemcitabine. A triple combined treatment based on EGCG, AA and gemcitabine (AND therapy for Active Nutrients/Drug) reduces mesothelioma growth and metastatization, suggesting its possible use in the clinical treatment of this problematic cancer. (130).

Aims

Polyphenols are an important group of phytochemicals that has gained increased research attention since it was found that they could affect cancer cell growth. Initial evidence came from epidemiologic studies suggesting that a diet that includes regular consumption of fruits and vegetables (rich in polyphenols) significantly reduces the risk of cancer. (131).

In the following works I have studied the effects of different types of polyphenols (oleuropein (OL), hydroxytyrosol (HT) and resveratrol (Res)) on malignant mesothelioma cancer cells.

Oleuropein and its metabolite hydroxytyrosol are phenolic compound found in olive leaf and fruit. Hydroxytyrosol is a simple phenol and oleuropein is a secoiridoid (Fig. 8).

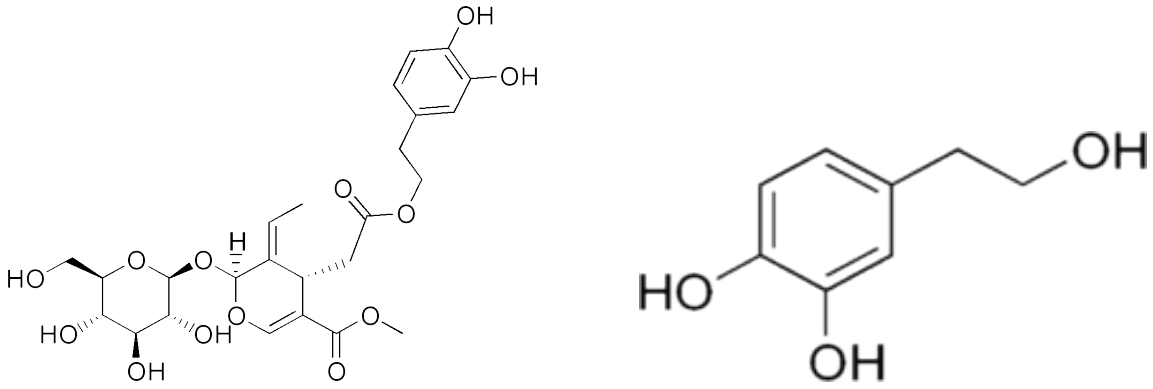

Figure 8. Structures of oleuropein and hydroxythyrosl

Hydrolysis of oleuropein, which occurs during olive oil storage, results in the formation of hydroxytyrosol (132).

OL and HT represent the molecules of major interest for their biological and pharmacological properties, and, with no doubt, are among the most investigated antioxidant natural compounds (133). OL has several pharmacological properties, including antioxidant (134), anti-inflammatory (135), anti-atherogenic (136), anti-cancer (137), antimicrobial (138), and antiviral effects (139). In addition, it has been shown to exhibit anti-ischemic and hypolipidemic activities (140). For these reasons, oleuropein is commercially available as food supplement in Mediterranean countries.

Resveratrol (trans-3,5,4'-trihydroxystilbene) is a phytoalexin found in many plant species, including various human food such as grapes, peanuts, and berries; it is produced in plants in response to mechanical injury, fungal infection, and u.v. radiation (Fig. 9).

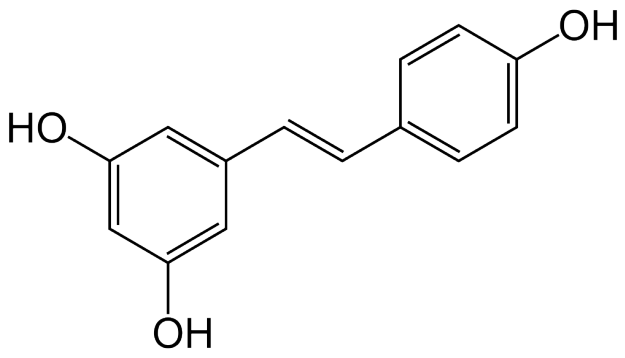

Figure 9. Structure of resveratrol

Resveratrol has attracted increasing attention since 1992, when it was associated with the cardioprotective effects of red wine consumption, a phenomenon commonly known as the "French Paradox" (141). Thereafter, a wide range of favorable properties has been attributed to resveratrol in many illnesses, including cardiovascular diseases (142), ischemic injuries (143), diabetes (144), inflammation (145), neurodegenerative diseases (146), and cancer (147, 148).

Resveratrol can affect the processes underlying all three stages of carcinogenesis, viz. tumor initiation, promotion, and progression. It has been found to exert strong anti-proliferative properties on many cultured cancer cell lines, being able to arrest cell cycle and induce apoptosis, and suppress angiogenesis and metastatization (149 - 151).

Resveratrol is a potent regulator of genomic and non-genomic processes, including the regulation of membrane potential, DNA transcription, enzyme activity, secretion, apoptosis, mitochondrial activity, and intracellular ion homeostasis, including the regulation of cytosolic Ca^{2+} (152).

Polyphenol anticancer effects have been attributed not only to their ability of acting as antioxidants but also to their ability to interact with basic cellular mechanisms. Such interactions include interference with membrane and intracellular receptors, interaction with the basic enzymes involved in tumor promotion and metastasis, interaction with oncogenes

and oncoproteins, and, finally, modulation of intracellular calcium (Ca^{2+}) signaling and homeostasis. (153).

Intracellular calcium (Ca^{2+}) is an essential signal transduction element involved in several physiological functions, such as cell growth and proliferation, cell cycle control and gene expressions (154). Although changes in Ca^{2+} homeostasis may not be a necessity for malignant initiation, modified Ca^{2+} signaling in cancer cells is thought to contribute to important events during tumor progression, including proliferation, migration, invasion, and metastasis (155).

This study has been devoted to explore the effects of the above polyphenols, i.e. resveratrol, hydroxytyrosol and oleuropein, on MPM cells in terms of Ca^{2+} mobilization. Mechanisms of action have also been pursued for these effects, in order to individuate possible therapeutic targets to be addressed for a Ca^{2+}-mediated, antiproliferative use of these polyphenols, possibly in combination with conventional antitumor drugs.

References

1. Robinson B.M. *Malignant pleural mesothelioma: an epidemiological perspective*. Annals of cardiothoracic surgery. 2012; 1:4.
2. Rushton L, Hutchings S.J, Fortunato L, Young C, Evans G.S, Brown T, et al. *Occupational cancer burden in Great Britain.* Br J Cancer. 2012;107(Suppl 1):S3–7.
3. Rake C, Gilham C, Hatch J, Darnton A, Hodgson J, Peto J. *Occupational, domestic and environmental mesothelioma risks in the British population: a case–control study*. Br J Cancer. 2009;100:1175–83.
4. Lacourt A, Gramond C, Rolland P, Ducamp S, Audignon S, Astoul P, et al. *Occupational and non-occupational attributable risk of asbestos exposure for malignant pleural mesothelioma*. Thorax. 2014;69:532–9.
5. Burdorf A, Heederik D. *Applying quality criteria to exposure in asbestos epidemiology increases the estimated risk.* Ann Occup Hyg. 2011;55:565–8.
6. Rapp G.R. *Archaeomineralogy.* Berlin, Springer, 2009.
7. National Toxicology Program. NTP 11th report on carcinogens. Rep Carcinog 2004; 11: A1–A32.
8. Ribak J, Lilis R, Suzuki Y, et al. *Malignant mesothelioma in a cohort of asbestos insulation workers: clinical presentation, diagnosis, and causes of death*. Br J Ind Med 2008; 45: 182–187.
9. Wagner J.C, Sleggs C.A, Marchand P. *Diffuse pleural mesothelioma and asbestos exposure in the North Western Cape Province*. Br J Ind Med 1960; 17: 260–271.
10. Armstrong BK, Musk AW, Baker JE, et al. *Epidemiology of malignant mesothelioma in Western Australia.* Med JAust 1984; 141: 86–88.
11. Gennaro V, Ceppi M, Boffetta P, et al. *Pleural mesothelioma and asbestos exposure among Italian oil refinery workers*. Scand J Work Environ Health 1994; 20: 213–215.
12. Morinaga K, Kishimoto T, Sakatani M, et al. *Asbestos-related lung cancer and mesothelioma in Japan.* Ind Health 2001; 39: 65–74.
13. McDonald J.C, McDonald A.D. *The epidemiology of mesothelioma in historical context.* Eur Respir J 1996;9:1932-42.
14. Zucalia P.A., Giaccone G. *Biology and management of malignant pleural mesothelioma. Europeam Journal of Cancer*. 2006; 42 :2706 –2714.
15. Virta R.L. *Worldwide asbestos supply and consumption trends from 1900 to 2000* (Open-file report): U.S. Dept. of the Interior, U.S. Geological Survey;2003:59.

16. International Agency for Research on Cancer. Asbestos (Chrysotile, Amosite, Crocidolite, Tremolite, Actinolite, and Anthophyllite). IARC Monographs. Arsenic, Metals, Fibres and Dusts. Lyon, International Agency for Research on Cancer, 2009; 147–167.
17. Cugell D.W. and Kamp D.W. *Asbestos and the pleura: a review.* Chest. 2004;125: 1103-1117.
18. World Health Organisation (WHO). Elimination of asbestos-related diseases. Geneva: WHO, 2006.
19. Peto J., Decarli A., La Vecchia C., et al. *The European mesothelioma epidemic*. Br J Cancer 1999; 79:666-72.
20. Hilliard A.K, Lovett J.K, McGavin C.R. *The rise and fall in incidence of malignant mesothelioma from a British Naval Dockyard, 1979-1999*. Occup Med (Lond) 2003;53:209-12.
21. Hansen J, de Klerk N.H, Eccles J.L, et al. *Malignant mesothelioma after environmental exposure to blue asbestos.* Int J Cancer 1993;54:578-81.
22. Toyokuni S. *Mechanisms of asbestos-induced carcinogenesis*. Nagoya J. Med. Sci.2009; 71:1-10.
23. Cutrone R, Lednicky J, Dunn G, et al. *Some oral poliovirus vaccines were contaminated with infectious SV40 after 1961.* Cancer Res 2005;6:10273–9.
24. Hilleman M.R. *Discovery of simian virus 40 (SV40) and its relationship to poliomyelitis virus vaccines.* Dev Biol Stand 1998; 94: 183–190.
25. Bocchetta M, Eliasz S, De Marco M.A, et al.: *The SV4 large T antigen-p53 complexes bind and activate the insulin-like growth factor-I promoter stimulating cell growth*. Cancer Res 2008, 68: 1022–1029.
26. Gazdar, A.F. and Carbone, M. *Molecular pathogenesis of malignant mesothelioma and its relationship to simian virus 40*. Clinical Lung Cancer, 2003; 5:177-181.
27. Røe O.D. and Stella G.M. *Malignant pleural mesothelioma: history, controversy and future of a manmade epidemic*. Eur Respir Rev. 2015; 24: 115–131.
28. Carbone M, Emri S, Dogan A.U, et al. *A mesothelioma epidemic in Cappadocia: scientific developments and unexpected social outcomes*. Nat Rev Cancer 2007, 7: 147–154.
29. Cavazza A, Travis L.B, Travis W.D, et al. *Post-irradiation malignant mesothelioma*. Cancer 1996;77(7):1379–1385.

30. Jasani B, Gibbs A. *Mesothelioma Not Associated With Asbestos Exposure*. Archives of Pathology & Laboratory Medicine. 2012, Vol. 136, No. 3, pp. 262-267.
31. Goodman J.E, Nascarella M.A, Valberg P.A. *Ionizing radiation: a risk factor for mesothelioma.* Cancer Causes Control 2009; 20: 1237–1254.
32. Hodgson D.C, Gilbert E.S, Dores G.M, et al. *Long-term solid cancer risk among 5-year survivors of Hodgkin's lymphoma.* J Clin Oncol 2007; 25: 1489–1497.
33. Stayner L, Welch L.S, Lemen R. *The worldwide pandemic of asbestos-related disease*. Annu Rev Public Health 2013;34:205–16.
34. Grondin S.C, Sugarbaker D.J. *Malignant mesothelioma of the pleural space*. Oncology (Williston Park) 1999, 13:919–926.
35. Ismail-Khan R, Robinson L.A, Williams C.C Jr., Garrett C.R, Bepler G, Simon G.R. *Malignant pleural mesothelioma: a comprehensive review*. Cancer Control. 2006; 13(4):255–263.
36. Craighead J.E. *Epidemiology of mesothelioma and historical background*. Rec Res Cancer Res 2011;189:13–25.
37. Neumann V, Löseke S, Nowak D, Herth F.J, Tannapfel A. *Malignant Pleural Mesothelioma Incidence, Etiology, Diagnosis, Treatment, and Occupational Health*. Dtsch Arztebl Int. 2013 May; 110(18): 319–326.
38. Soeberg M.J, Takahashi K, Movahed M, et al. *Global patterns in the incidence of malignant mesothelioma, 1988-2002, using data published by the international Agency for Research on Cancer (IARC).* J Thorac Oncol 2013; 8(P2.14-007).
39. Park E.K, Takahashi K, Hoshuyama T, et al. *Global magnitude of reported and unreported mesothelioma.* Environ Health Perspect 2011;119:514–8.
40. Robinson B. *Malignant pleural mesothelioma: an epidemiologic prospective.* Ann Cardiothorac Surg 2012;1:491–6.
41. Okello C, Treasure T, Nicholson A.G, et al. *Certified causes of death in patients with mesothelioma in South East England*. BMC Cancer 2009;9:28.
42. Camidge D.R, Stockton D.L, Bain M. *Factors affecting the mesothelioma detection rate within national and international epidemiological studies: insights from Scottish linked cancer registry-mortality data*. Br J Cancer 2006;95:649-52.
43. Bianchi C, Bianchi T, Tommasi M. *Long latency periods in asbestos-related mesothelioma of the pleura.* Eur J Oncol. 2007; 12(3):189–195.

44. Delgermaa V, Takahasi K, Park E.K, et al. *Global mesothelioma deaths reported to the World Health Organization between 1994 and 2008.* Bull World Health Organ 2011;89:716–24.
45. Murayama T, Takahashi K, Natori Y, et al. *Estimation of future mortality from pleural malignant mesothelioma in Japan based on an age-cohort model.* Am J Ind Med 2006;49:1-7.
46. Pass H.I, Vogelzang N.T, Hahn S.M et al. *Benign and malignant mesothelioma.* In: DeVita VT, Hellman S, Rosenberg S.A. Cancer: principles and practice of oncology. 8th ed. Philadelphia: Lippincott, Williams & Wilkins; 2008:1835–62.
47. Ahmed I, Tipu S.A, Ishtiaq S. *Malignant mesothelioma.* Pak J Med Sci 2013;29(6):1433-1438.
48. National Cancer Institute. SEER cancer statistics review, 1975–2008.
49. National Institute for Occupational Safety and Health, Centers for Disease Control and Prevention. The work-related lung disease surveillance report, 2002.
50. Huncharek M. *Changing risk groups for malignant mesothelioma.* Cancer 1992;69:2704-11.
51. Hillerdal G. *Mesothelioma: cases associated with non-occupational and low dose exposures.* Occup Environ Med 1999; 56:505–513.
52. Marinaccio A, Binazzi A, Marzio D.D, Scarselli A, Verardo M, Mirabelli D, et al. *Pleural malignant mesothelioma epidemic: incidence, modalities of asbestos exposure and occupations involved from the Italian National Register*. Int J Cancer. 2012;130:2146–54.
53. Marinaccio A, Montanaro F, Mastrantonio M, Uccelli R, Altavista P, Nesti M, et al. *Predictions of mortality from pleural mesothelioma in Italy: a model based on asbestos consumption figures supports results from age-period-cohort models*. Int J Cancer. 2005;115:142–7.
54. Corfiati et al. *Epidemiological patterns of asbestos exposure and spatial clusters of incident cases of malignant mesothelioma from the Italian national registry*. BMC Cancer. 2015;15:286.
55. Marinaccio A et al. *Malignant mesothelioma due to non-occupational asbestos exposure from the Italian national surveillance system (ReNaM): epidemiology and public health issues*. Occup Environ Med. 2015.
56. National Mesothelioma Registry (ReNaM) – 4th Report. INAIL, 2012.

57. Husain, A.N. et al. *Guidelines for pathologic diagnosis of malignant mesothelioma: a consensus statement from the International Mesothelioma Interest Group*. Arch. Pathol. Lab. Med. 2009:133, 1317–1331.
58. Beasley M.B., *et al. The 2004 World Health Organization classification of lung tumors.* Semin. Roentgenol. 2005;40:90–97.
59. Chirieac L.R.C.J. *Pathologic evaluation of malignant pleural mesothelioma*. Semin Thorac Cardiovasc Surg. 2009;21:121-124.
60. Pinto C, Novello S, Torri V, et al. *Second Italian consensus conference on malignant pleural mesothelioma: state of the art and recommendations*. Cancer Treat Rev 2013;39:328-39.
61. Inai K. *Pathology of mesothelioma*. Environ Health Prev Med. 2008;13:60–64.
62. Jean D. et al. *Molecular changes in mesothelioma with an impact on prognosis and treatment.* Arch. Pathol. Lab. Med. 2012;136, 277–293.
63. Sekido Y. *Molecular pathogenesis of malignant mesothelioma*. Carcinogenesis. 2013; 34(7): 1413–1419.
64. Liu W. et al. *Phagocytosis of crocidolite asbestos induces oxidative stress, DNA damage, and apoptosis in mesothelial cells*. Am. J. Respir. Cell Mol. Biol. 2000;23, 371–378.
65. Godleski J.J. *Role of asbestos in etiology of malignant pleural mesothelioma*. Thoracic Surgery Clinics. 2004;14, 479-487.
66. Heintz,N.H. et al. *Asbestos, lung cancers, and mesotheliomas: from molecular approaches to targeting tumor survival pathways*. Am. J. Respir.Cell Mol. Biol. 2010; 42, 133–139.
67. Yang H, Testa J:R and Carbone M. *Mesothelioma Epidemiology, Carcinogenesis and Pathogenesis.* Curr Treat Options Oncol. 2008; 9(2-3): 147–157.
68. Kamp D.W, Graceffa P, Pryor W.A, Weitzman S.A. *The role of free radicals in asbestos-induced diseases.* Free Radic Biol Med. 1992; 12: 293–315.
69. Xu A, Zhou H, Yu D.Z, et al. *Mechanisms of the genotoxicity of crocidolite asbestos in mammalian cells: implication from mutation patterns induced by reactive oxygen species.* Environ Health Perspect. 2002;110:1003–1008.
70. Shukla A, Gulumian M, Hei T.K, et al. *Multiple roles of oxidants in the pathogenesis of asbestos-induced diseases.* Free Radic Biol Med. 2003;34:1117–1129.
71. Wang N, Jaurand M, Magne L, Kheuang L, Pinchon M, Bignon J. *The interactions between asbestos fibers and metaphase chromosomes of rat pleural mesothelial cells*

in culture: a scanning and transmission electron microscopic study. Am J Pathol. 1987; 126: 343.

72. Apostolou S, Balsara B.R, and Testa J.R. *Cytogenetics of Malignant Mesothelioma. Malignant Mesothelioma.* 2005, pp 101-111.
73. Altomare D.A, Vaslet C.A, Skele K.L, et al. *A mouse model recapitulating molecular features of human mesothelioma.* Cancer Res 2005, 65:8090–8095.
74. Yoshitaka Sekido *Molecular pathogenesis of malignant mesothelioma*. Carcinogenesis. 2013;34(7):1413–1419.
75. Liu Z, Klominek J. *Chemotaxis and chemokinesis of malignant mesothelioma cells to multiple growth factors.* Anticancer Res 2004;24:1625–1630.
76. Galffy G, Mohammed K.A, Dowling P.A, et al. *Interleukin 8: an autocrine growth factor for malignant mesothelioma.* Cancer Res. 1999;59:367–371.
77. Strizzi L, Catalano A, Vianale G, et al. *Vascular endothelial growth factor is an autocrine growth factor in human malignant mesothelioma*. J Pathol 2001;193:468–475.
78. Cacciotti P, Libener R, Betta P, et al. *SV40 replication in human mesothelial cells induces HGF/Met receptor activation: a model for viral-related carcinogenesis of human malignant mesothelioma.* Proc Natl Acad Sci USA. 2001;98:12032–12037.
79. Yang H, Bocchetta M, Kroczynska B, et al. *TNF-alpha inhibits asbestos-induced cytotoxicity via a NF-kappaB-dependent pathway, a possible mechanism for asbestos-induced oncogenesis.* Proc Natl Acad Sci U S A. 2006;103:10397–10402.
80. Janssen Y.M, Driscoll K.E, Howard B, Quinlan T.R, Treadwell M, Barchowsky A, Mossman B.T. *Asbestos causes translocation of p65 protein and increases NF-kappa B DNA binding activity in rat lung epithelial and pleural mesothelial cells.* Am J Pathol 1997;151: 389–401.
81. Yang,H. et al. *Programmed necrosis induced by asbestos in human mesothelial cells causes high-mobility group box 1 protein release and resultant inflammation*. Proc. Natl Acad. Sci. USA. 2010;107:12611–12616.
82. Raja S, Murthy S.C and Mason D.P. *Malignant Pleural Mesothelioma*. Curr Oncol Rep. 201;13:259–264.
83. Champbell N, Kindler H: *Update on malignant pleural mesothelioma.* Semin Respir Crit Care Med. 2011; 32: 102–10.
84. Opiz I. *Management of malignant pleural mesothelioma-The European experience*. Journal of Thoracic Disease. 2014;6(2).

85. Plathow C, Staab A, Schmaehl A, et al: *Computed tomography, positron emission tomography, positron emission tomography/computed tomography, and magnetic resonance imag ing for staging of limited pleural mesothelioma: Initial results*. Invest Radiol. 2008;43:737-744.
86. Zucali P.A. et al. *Advances in the biology of malignant pleural mesothelioma*. Cancer Treatment Reviews. 2011; 37:543–558.
87. Pass H.I, Lott D, Lonardo F, et al. *Asbestos exposure, pleural mesothelioma, and serum osteopontin levels*. N Engl J Med. 2008; 53: 1564–1573.
88. Robinson B.W, Creaney J, Lake R, et al. *Mesothelin-family proteins and diagnosis of mesothelioma*. Lancet. 2003; 362: 1612–1616.
89. Scherpereel A, Lee Y.C.G. *Biomarkers for mesothelioma.* Curr Opin Pulm Med. 2007;13:339–343.
90. Creaney J, Yeoman D, Demelker Y, et al. *Comparison of osteopontin, megakaryocyte potentiating factor, and mesothelin proteins as markers in the serum of patients with malignant mesothelioma*. J Thorac Oncol. 2008;3:851–7.
91. Rusch V.W: *A proposed new international TNM staging system for malignant pleural mesothelioma. From the International Mesothelioma Interest Group*. Chest. 1995; 108:1122-1128.
92. Mylene T. et al. *Malignant Pleural Mesothelioma: Role of CT, MRI, and PET/CT in Staging Evaluation and Treatment Considerations*. Seminars in Roentgenology. 2013. 48: 323–334.
93. Boutin C, Schlesser M, Frenay C, et al: *Malignant pleural mesothelioma*. Eur Respir J. 1998;12:972-981.
94. Maziak D.E, Gagliardi A, Haynes A.E, Mackay J.A, Evans W.K. *Cancer Care Ontario program in evidence-based care lung cancer disease site group. Surgical management of malignant pleural mesothelioma: a systematic review and evidence summary*. Lung Cancer. 2005;48:157–69.
95. Flores R.M, Pass H.I, Seshan V.E, et al: *Extrapleural pneumonectomy versus pleurectomy/decortication in the surgical management of malignant pleuralmesothelioma:* Results in 663 patients. J Thorac Cardiovasc Surg. 2008; 135:620-626.
96. Waller D.A, Morritt G.N, Forty J. *Video-assisted thoracoscopic pleurectomy in the management of malignant pleural effusion*. Chest 1995;107:1454-6.

97. Rice D. *Surgical therapy of mesothelioma.* Recent Results Cancer Res 2011;189:97-125.

98. Berghmans T, Paesmans M, Lalami Y, et al. *Activity of chemotherapy and immunotherapy on malignant mesothelioma: a systematic review of the literature with meta-analysis.* Lung Cancer. 2002;38:111–21.

99. Vogelzang N.J, Rusthoven J.J, Symanowski J, et al. *Phase III study of pemetrexed in combination with cisplatin versus cisplatin alone in patients with malignant pleural mesothelioma.* J Clin Oncol. 2003;21:2636–44.

100. Ceresoli G.L, Gridelli C, Santoro A: *Multidisciplinary treatment of malignant pleural mesothelioma.* Oncologist. 2007, 12:850-863.

101. Dhalluin X, Scherpereel A: *Chemotherapy and Radiotherapy for mesothelioma*. Rec Res Cancer Res 2011; 189: 127–47.

102. Flores R.M, Zakowsky M, Venkatraman E, et al. *Prognostic factors in the treatment of malignant pleural mesothelioma at a large tertiary referral center*. J Thorac Oncol. 2007;2(10):957–965.

103. Sienel W, Kirschbaum A, Passlick. *Multimodal therapy for malignant pleural mesothelioma including extrapleural pneumonectomy.* Zentralbl Chir 2008;133:231-7.

104. Sugarbaker D, Garcia J, Richards W: *Extrapleural pneumonectomy in the multimodality therapy of malignant pleural mesothelioma*. Results in 120 consecutive patients. Ann Surg 1996; 224: 288–94.

105. Kotsakis A, Georgoulias V. *Targeting epidermal growth factor receptor in the treatment of non-small-cell lung cancer.* Expert Opin Pharmacother. 2010;11(14):2363–89.

106. Jänne P.A, Taffaro M.L, Salgia R, Johnson B.E. *Inhibition of epidermal growth factor receptor signaling in malignant pleural mesothelioma*. *Cancer Res*. 2002; 62(18):5242–5247.

107. Masood R, Kundra A, Zhu S, et al. *Malignant mesothelioma growth inhibition by agents that target the VEGF and VEGF-C autocrine loops*. Int J Cancer. 2003;104(5):603–610.

108. Hassan R, Ebel W, Routhier E.L, et al. *Preclinical evaluation of MORAb-009, a chimeric antibody targeting tumor-associated mesothelin*. Cancer Immun. 2007;7:20.

109. Golfier S, Kopitz C, Kahnert A, et al. Anetumab ravtansine: a novel mesothelin-targeting antibody-drug conjugate cures tumors with heterogeneous target expression favored by bystander effect. *Mol Cancer Ther*. 2014;13(6):1537–1548.

110. Kreitman R.J. Hassan R, Fitzgerald D.J, Pastan I. *Phase I trial of continuous infusion anti-mesothelin recombinant immunotoxin SS1P.* Clin Cancer Res. 2009;15(16):5274–5279.

111. Beseth B.D, Cameron R.B, Leland P, et al. *Interleukin-4 receptor cytotoxin as therapy for human malignant pleural mesothelioma xenografts.* Ann Thorac Surg. 2004;78(2):436–443.

112. Calabrò L, Morra A, Fonsatti E, et al. *Tremelimumab for patients with chemotherapy-resistant advanced malignant mesothelioma: an open-label, single-arm, phase 2 trial.* Lancet Oncol. 2013;14(11):1104-1111.

113. Currie A.J, Prosser A, McDonnell A, et al. *Dual control of antitumor CD8 T cells through the programmed death-1/programmed death-ligand 1 pathway and immunosuppressive CD4 T cells: regulation and counterregulation*. J Immunol. 2009;183(12):7898–7908.

114. Sterman D.H, Recio A, Vachani A, et al. *Long-term follow-up of patients with malignant pleural mesothelioma receiving high-dose adenovirus herpes simplex thymidine kinase/ganciclovir suicide gene therapy*. Clin Cancer Res. 2005;11(20):7444–7453.

115. Sterman D.H, Haas A, Moon E, et al. *A trial of intrapleural adenoviral-mediated interferon-α2b gene transfer for malignant pleural mesothelioma*. Am J Respir Crit Care Med. 2011;184(12):1395–1399.

116. Gregoire M. *What's the place of immunotherapy in malignant mesothelioma treatments?* Cell Adhes Migrat. 2010;4(1):153–61.

117. Hegmans J.P, Hemmes A, Aerts J.G, Hoogsteden H.C, Lambrecht B.N. *Immunotherapy of murine malignant mesothelioma using tumor lysate-pulsed dendritic cells.* Am J Respir Crit Care Med. 2005;171(10):1168–1177.

118. Friedberg J.S, Culligan M.J, Mick R, et al. *Radical pleurectomy and intra operative photodynamic therapy for malignant pleural mesothelioma*. Ann Thorac Surg. 2012;93(5):1658-1665.

119. Mujoomdar A.A, Sugarbaker D.J. *Hyperthermic chemoperfusion for the treatment of malignant pleural mesothelioma.* Semin Thorac Cardiovasc Surg. 2008;20(4):298–304.

120. Lang-Lazdunski L, Bille A, Belcher E, et al. *Pleurectomy/decortication, hyperthermic pleural lavage with povidone-iodine followed by adjuvant chemotherapy*

in patients with malignant pleural mesothelioma. J Thorac Oncol. 2011;6(10):1746–1752.

121. Zemlyak A, Moore W.H, Bilfinger T.V. *Comparison of survival after sublobar resections and ablative therapies for stage I non-small cell lung cancer*. J Am Coll Surg. 2010;211(1):68–72.

122. Abtin F, Suh R, Sandberg J, Rorie A, Cameron RB. *Role of percutaneous cryoablation in management of recurrent mesothelioma following lung sparing pleurectomy and decortications.* Society of Interventional Radiology 38th Annual Scientific Meeting; 2013; New Orleans, LA. J Vasc Interv Radiol. 2013;24(4):S139.

123. Rafter, J.J., *Scientific basis of biomarkers and benefits of functional foods for reduction of disease risk: cancer*. Br J Nutr, 2002;88(2)2:S219-24.

124. Berenblum I. *The modifying influence of dichloroethyl sulphide on the induction of tumors in mice by tar*. J Pathol Bacteriol. 1929;32:425–434.

125. Sporn M.B, Dunlop N.M, Newton D.L. *Prevention of chemical carcinogenesis by vitamin A and its synthetic analogs (retinoids*) Fed Proc. 1976;35:1332–1338.

126. Reddy L, Odhav B, Bhoola K.D. *Natural products for cancer prevention: A global perspective.* Pharmacol Ther. 2003;99:1–13.

127. Ruhul A.R.M, Kucuk O, Khuri F.R, and Shin D.M. *Perspectives for Cancer Prevention With Natural Compounds*. J Clin Oncol. 2009;27:2712-2725.

128. Ranzato E, Biffo S, Burlando B. *Selective ascorbate toxicity in malignant mesothelioma: a redox Trojan mechanism*. Am J Respir Cell Mol Biol. 2011;44:108–117.

129. Ranzato E, Martinotti S, Magnelli V, Murer B, Biffo S, et al. *Epigallocatechin-3-gallate induces mesothelioma cell death via H2O2-dependent T-type Ca2+ channel opening.* J Cell Mol Med. 2012;16:2667–2678.

130. Martinotti S, Ranzato E, Burlando B. *In vitro screening of synergistic ascorbate-drug combinations for the treatment of malignant mesothelioma*. Toxicology in Vitro. 2011; 25(8): 1568–1574.

131. Greenwell M. and Rahman P.K.S.M. *Medicinal Plants: Their Use in Anticancer Treatment*. J Pharm Sci Res. 2015; 6(10): 4103–4112.

132. Waterman E, and Lockwood B. *Active Components and Clinical Applications of Olive Oil.* Alternative Medicine Review. 2007;12:4.

133. Omar S.H. *Oleuropein in olive and its pharmacological effects*. Sci Pharm 2010; 78:133–154.

134. Visioli F, Poli A, Galli C. *Antioxidant and other biological activities of phenols from olives and olive oil.* Med Res Rev. 2002; 22: 65–75.

135. Visioli F, Bellosta S, Galli C. *Oleuropein, the bitter principles of olives, enhances nitric oxide production by mouse macrophages*. Life Sci. 1998; 62: 541–546.

136. Ahmadvand H. et al. *Hypoglycemic, hypolipidemic and antiatherogenic effects of oleuropein in alloxan-induced Type 1 diabetic rats*. Asian Pac J Trop Dis 2014; 4(1): S421-S425.

137. Han J, Talorete T.P.N, Yamada P, Isoda H. *Anti-proliferative and apoptotic effects of oleuropein and hydroxytyrosol on human breast cancer MCF-7 cells*. Cytotechnology. 2009;59:45–53.

138. Fleming H.P, Walter W.M, Etchells J.L. *Antimicrobial properties of oleuropein and products of its hydrolysis from green olives*. Appl. Microbiol. 1973;26:777–782.

139. Micol V, Caturla N, Pérez-Fons L, Más V, Pérez L, Estepa A. *The olive leaf extract exhibits antiviral activity against viral haemorrhagic septicaemia rhabdovirus (VHSV)* Antivir. Res. 2005;66:129–136.

140. Andreadou I, Iliodromitis E.K, Mikros E, Const antinou M, Agalias A, Magiatis P, Skaltsounis AL, Kamber E, Tsantili-Kakoulidou A, Kremastinos D.T. *The olive constituent oleuropein exhibits anti-ischemic, antioxidative, and hypolipidemic effects in anesthetized rabbits*. J Nutr. 2006; 136: 2213–2219.

141. Renaud S., de Lorgeril M. *Wine, alcohol, platelets, and the French paradox for coronary heart disease.* Lancet 1992; 339:1523-6.

142. Bradamante, S., Barenghi, L. and Villa, A. *Cardiovascular protective effects of resveratrol.* Cardiovasc. Drug Rev. 2004;22, 169–188.

143. Petrovski G., Gurusamy N., Das D.K. *Resveratrol in cardiovascular health and disease.* Ann N Y Acad Sci, 1215. 2011;22–33.

144. Su H.C, Hung L.M, and Chen J.K. *Resveratrol, a red wine antioxidant, possesses an insulin-like effect in streptozotocin-induced diabetic rats*. Am. J. Physiol. Endocrinol. Metab. 2006;290:E1339–E1346.

145. Martinez J., Moreno J. *Effect of resveratrol, a natural polyphenolic compound, on reactive oxygen species and prostaglandin production*. Biochem Pharmacol 2000; 59:865–870.

146. Anekonda, T.S. *Resveratrol – a boon for treating Alzheimer's disease?* Brain

Res. Rev. 2006; 52, 316–326.

147. Frazzi R. and Tigano M. *The Multiple Mechanisms of Cell Death Triggered by Resveratrol in Lymphoma and Leukemia.* Int. J. Mol. Sci. 2014, 15, 4977-4993.

148. Kundu J.K, Surh Y.J. *Cancer chemopreventive and therapeutic potential of resveratrol: mechanistic perspectives*, Cancer Lett. 269. 2008; 243e261.

149. Polycarpou E, Meira L.B, Carrington S, Tyrrell E, Modjtahedi H. and Carew M.A. *Resveratrol 3-O-D-glucuronide and resveratrol 4'-O-D-glucuronide inhibit colon cancer cell growth: Evidence for a role of A3 adenosine receptors, cyclin D1 depletion, and G1 cell cycle arrest*. Mol. Nutr. Food Res. 2013;00,1–10.

150. Wang T.T, Schoene N.W, Kim Y.S, et al. *Differential effects of resveratrol and its naturally occurring methylether analogs on cell cycle and apoptosis in human androgen- responsive LNCaP cancer cells.* Mol Nutr Food Res. 2010; 54:335–344.

151. Trapp V., Parmakhtiar B., Papazian V., Willmott L., Fruehauf J.P. *Anti-angiogenic effects of resveratrol mediated by decreased VEGF and increased TSP1 expression in melanoma-endothelial cell co-culture.* Angiogenesis. 2010; 13:305–315.

152. Sareen D, Darjatmoko S.R, Albert D.M. and Polans A.S. *Mitochondria, Calcium, and Calpain are Key Mediators of Resveratrol-Induced Apoptosis in Breast Cancer.* Mol Pharmacol. 2007; 72:1466–1475.

153. M. Kampa, A.P. Nifli, G. Notas, E. Castanas. *Polyphenols and cancer cell growth.* Biochem Pharmacol. 2007;159:79 –113.

154. Berridge M.J, Bootman M.D, Roderick H.L. *Calcium signalling: dynamics, homeostasis and remodelling.* Nat Rev Mol Cell Biol. 2003;20:517–529.

155. Monteith G.R, Davis F.M, Roberts-Thomson S.J. *Calcium channels and pumps in cancer: changes and consequences.* J Biol Chem. 2012;20:31666–31673.

Oleuropein-enriched olive leaf extract affects calcium dynamics and impairs viability of malignant mesothelioma cells.

Published on Evidence-Based Complementary and Alternative Medicine

2015

Hindawi Publishing Corporation
Evidence-Based Complementary and Alternative Medicine
Volume 2015, Article ID 908493, 9 pages
http://dx.doi.org/10.1155/2015/908493

Research Article

Oleuropein-Enriched Olive Leaf Extract Affects Calcium Dynamics and Impairs Viability of Malignant Mesothelioma Cells

Carla Marchetti,[1] Marco Clericuzio,[2] Barbara Borghesi,[3] Laura Cornara,[3] Stefania Ribulla,[2] Fabio Gosetti,[2] Emilio Marengo,[2] and Bruno Burlando[1,2]

[1]*Istituto di Biofisica, Consiglio Nazionale delle Ricerche, Via De Marini 6, 16149 Genova, Italy*
[2]*Dipartimento di Scienze e Innovazione Tecnologica (DISIT), Università del Piemonte Orientale, Viale Teresa Michel 11, 15121 Alessandria, Italy*
[3]*Dipartimento di Scienze della Terra dell'Ambiente e della Vita (DISTAV), Università degli Studi di Genova, Corso Europa 26, 16132 Genova, Italy*

Correspondence should be addressed to Bruno Burlando; bruno.burlando@uniupo.it

Received 14 September 2015; Revised 3 November 2015; Accepted 11 November 2015

Academic Editor: I-Min Liu

Malignant mesothelioma is a poor prognosis cancer in urgent need of alternative therapies. Oleuropein, the major phenolic of olive tree (*Olea europaea* L.), is believed to have therapeutic potentials for various diseases, including tumors. We obtained an oleuropein-enriched fraction, consisting of 60% w/w oleuropein, from olive leaves, and assessed its effects on intracellular Ca^{2+} and cell viability in mesothelioma cells. Effects of the oleuropein-enriched fraction on Ca^{2+} dynamics and cell viability were studied in the REN mesothelioma cell line, using fura-2 microspectrofluorimetry and MTT assay, respectively. Fura-2-loaded cells, transiently exposed to the oleuropein-enriched fraction, showed dose-dependent transient elevations of cytosolic Ca^{2+} concentration ($[Ca^{2+}]_i$). Application of standard oleuropein and hydroxytyrosol, and of the inhibitor of low-voltage T-type Ca^{2+} channels NNC-55-0396, suggested that the effect is mainly due to oleuropein acting through its hydroxytyrosol moiety on T-type Ca^{2+} channels. The oleuropein-enriched fraction and standard oleuropein displayed a significant antiproliferative effect, as measured on REN cells by MTT cell viability assay, with IC_{50} of 22 μg/mL oleuropein. Data suggest that our oleuropein-enriched fraction from olive leaf extract could have pharmacological application in malignant mesothelioma anticancer therapy, possibly by targeting T-type Ca^{2+} channels and thereby dysregulating intracellular Ca^{2+} dynamics.

1. Introduction

Malignant mesothelioma is a poor prognosis cancer with worldwide increasing insurgence, arising from the pleura and other mesothelial tissue and showing close association with asbestos exposure. An effective therapeutic approach for the disease is currently lacking, while alternative treatments are urgently needed [1]. Among alternative remedies for cancer treatment, there is a growing interest in the anticancer action of natural substances, some of which are present in large amounts in byproducts from agrofood chains.

Olive (*Olea europaea* L.) is a main temperate fruit crop, mostly destined to oil production [2]. Olive oil is reputed to be an important health promoting factor in the Mediterranean diet, especially because of its alleged prevention of cardiovascular problems, metabolic syndrome, cancer, alleviation of inflammatory and autoimmune conditions, and wound healing [3]. However, olive tree leaves have a several-century-long tradition in the folk medicines of the Mediterranean basin and are currently contemplated in the Pharmacopoeia Ph. Eur. 5 [4].

Leaves and other materials from olive tree pruning accumulate in yearly amounts as high as about 25 kg per tree [5]. This material is generally disposed by olive tree growers, representing an overhead cost of olive and oil production, while the possibility of using it as biomass for thermal energy

is under study [6]. Olive leaves are used in the form of herbal extracts, tea, and powder for nutritional supplement and cosmetics [4], but these products represent a minimal portion with respect to the huge amount of disposed materials.

The major leaf secondary metabolite is the secoiridoid oleuropein, a glycosylated ester of elenolic acid with hydroxytyrosol (2-(3,4-dihydroxyphenyl)ethanol). Oleuropein leaf content has been reported to vary about tenfold among different olive varieties, rating on average between 10 and 100 mg/g of dry matter [7, 8]. Many other biologically active phenolics are present in olive leaves, including hydroxytyrosol itself [9].

Oleuropein is deemed to have great potential as an antioxidant and food additive, but also as a possible therapeutic tool. A wide range of studies on oleuropein have been carried out using *in vitro* assays, animal models of disease, or human volunteers, in order to explore possible beneficial effects for human health [10]. The reported findings mainly include antioxidant and anti-inflammatory effects, hepatoprotection, neuroprotection, hypoglycemic and hypolipidemic activities, and cardiovascular protection [11, 12]. Antiproliferative activities on cancer cell lines, antitumor effects in animals, and antimicrobial and antiviral effects have also been shown [13].

Hydroxytyrosol in olive leaves, fruits, and extracts is believed to derive from oleuropein hydrolysis, both by specific enzymes and as an extraction artifact [9]. *In vitro* and *in vivo* studies suggest that this compound shares remarkable antioxidant and anti-inflammatory power with oleuropein, allegedly related to antiatherogenic, antithrombotic, cardioprotective, and anticancer effects [14, 15].

The value of olive leaf extract for possible use in health products and medical food has been previously assessed in terms of antioxidant and antimicrobial power [16]. However, the profitable reutilization of agrofood chain byproducts needs to overcome several problems, including the costs of transport and processing and the seasonal availability of these materials. In this study, we have developed a rapid method for obtaining olive leaf extract enriched in oleuropein, involving raw extraction, extract partitioning, and chromatographic separation. The material has been tested in pharmacologically relevant, intracellular Ca^{2+} mobilization assay and antiproliferative assay on mesothelioma cells. In these experiments, standard oleuropein has been used as control, while hydroxytyrosol has been also used in Ca^{2+} assays to provide insight into the Ca^{2+} mobilizing properties of the oleuropein molecule.

2. Materials and Methods

2.1. Plant Material. Branch specimens of *Olea europaea* L. cultivar "Taggiasca" [17] were obtained from olive groves located at Imperia, Italy, owned by the Pietro Isnardi S.r.l. food company. The material was taxonomically identified by one of us (LC), and a voucher specimen was deposited at DISTAV, University of Genova (cat.: GE-*Olea europaea* cultivar "Taggiasca"). Leaves were separated from twigs, air-dried for one week, minced to <1 mm using a grinder, and then subjected to extraction procedure.

2.2. Reagents and Solutions. HPLC grade methanol Chromasolv (>99.9%) and glacial acetic acid were purchased from Sigma-Aldrich (Milwaukee, USA). Ammonium acetate (99%) was acquired from Fluka (Buchs, Switzerland). Ultrapure water was produced by a Millipore Milli-Q system (Milford, USA). Analytical grade chemicals were purchased from Sigma-Aldrich, unless otherwise specified.

For LC/MS analysis, standard stock solutions of oleuropein and hydroxytyrosol (each at concentration of 100.0 mg L^{-1}) were prepared in methanol and diluted as required with a buffer solution of ammonium acetate 10.0 mM brought to pH 4.0 for acetic acid. For *in vitro* bioassays, stock solutions of oleuropein and hydroxytyrosol (each at 100 mM) were prepared in DMSO and diluted as indicated with cell medium or loading buffer for Ca^{2+} measurements. Stock solutions were preserved at −20°C in dark conditions and were stable for three months.

2.3. Olive Leaf Extraction Procedure. The minced leaves were extracted with a mixture of 2-propanol : water of 9 : 1. Aliquots of 10 g of leaves were extracted twice with 200 mL of solvent each time. The extraction was carried out at RT for about 1.5 h. The resulting solutions were mixed and the solvent was eliminated under vacuum, yielding an amount of 2.35 g of dried material. This raw extract was then partitioned between a mixture of methanol : water of 3 : 1 and a mixture of toluene : petroleum ether of 2 : 1 (100 mL each phase). The hydrocarbon phase became deep green, indicating that it contained all the chlorophyll of the raw extract. The aqueous methanol phase was dried under vacuum, yielding 1.8 g of subextract. This material was then again partitioned between water and 2-butanone (100 mL each phase), to remove sugars and other water-soluble compounds. The organic phase was dried out, obtaining a partitioned subextract that amounted to 1.03 g (43% recovery from the first raw extract, 10% from the plant material). A control TLC showed that in the former partition no oleuropein passed in the hydrocarbon phase, while in the latter only a tiny amount of it was lost in the water phase.

2.4. Chromatographic Separation. Liquid chromatography was performed by means of an MPLC system, consisting of an Alltech 426 HPLC pump equipped with a VWR LaPrep 3101 detector. Glass columns from Omnifit were used, home-packed with Fluka silica gel 100 RP-18 (15–35 μm) stationary phase. TLC was performed with Merck F_{254} glass plates (RP-18); the spots were detected using a UV lamp (254 and 366 nm) and additionally by spraying with sulfovanillin and heating at 100°C, obtaining an oleuropein coral pink spot on TLC.

The above subextract was loaded on a RP-18 preparative column and eluted with 80% water and 20% methanol. Fractioning was monitored through the UV detector ($\lambda = 250$ nm) and with TLC. Finally, an oleuropein-enriched fraction was collected and subjected to further study.

2.5. LC/MS Analysis

2.5.1. Apparatus. LC/MS analysis was performed on the above raw extract and subfractions by Nexera Liquid Chromatography Shimadzu (Kyoto, Japan) system equipped with a DGU-20A3R Degasser, two LC-30AD Pumps, a SIL-30AC Autosampler, a CTO-20AC column compartment, and a CMB-20A Lite system controller. The system was interfaced with a 3200 QTrap LC-MS/MS system (AB Sciex, Concord, Canada) by a Turbo V interface equipped with an ESI probe. The 3200 QTrap data were processed by Analyst 1.5.2 software (Toronto, Canada).

2.5.2. UHPLC-MS/MS Conditions. The stationary phase was a Kinetex C18 column (2.1 mm × 100 mm, 2.6 μm) (Phenomenex, Italy). The mobile phase was a mixture of ammonium acetate 10.0 mM in ultrapure water with the addition of 0.1% acetic acid (A), and aqueous ammonium acetate 10.0 mM/methanol 5/95 (v/v) with the addition of 0.1% acetic acid (B), eluting at flow-rate 0.400 mL min^{-1} in the following gradient conditions: 0.0–0.5 min 5% B, 0.6–8.0 min 65% B, 8.1–12.0 min 100% B, and 12.1–15.0 min 5% B. The injection volume was 5.0 μL. Oven temperature was set at 40°C.

The turbo ion spray (TIS) ionization was obtained using the Turbo V interface working in negative ion mode. The instrumental parameters were set as follows: curtain gas (N_2) at 30 psig, nebulizer gas GS1 and GS2 at 50 and 40 psig, respectively, desolvation temperature (TEM) at 550°C, collision activated dissociation gas (CAD) at 6 units of the arbitrary scale of the instrument, and ion spray voltage (IS) at −4500 V.

The 3200 QTrap was used in scheduled multiple reaction monitoring (sMRM) considering the transitions of each species at a prefixed retention time. Unit mass resolution was established and maintained in each mass-resolving quadrupole by keeping a full width at half maximum (FWHM) of about 0.7 u.

The analytes were previously subjected to MS/MS characterization study, to identify the fragmentation patterns taking place under increasing collisional energy. Characterization experiments were carried out for direct infusion of 1.0 mg L^{-1} standard solutions of each analyte connected through a T valve to the syringe pump (syringe flow-rate 20.0 μL min^{-1}; chromatographic pump flow-rate 200 μL min^{-1}). For each species, the most intense transition was used for the quantitative analysis and referred to as "quantifier" transition, while the second intense one (the "qualifier" transition) was employed in the identification step, as a confirmation. The "quantifier" and "qualifier" transitions and the instrumental potential values for each compound are reported in Table 1.

Calibration plots of five concentration levels (between LOQ value and 1000.0 μg L^{-1}), relating the peak area of the "quantifier" transition signal (y) versus standard concentration (x), were built for all the analytes. To avoid a possible influence of the experimental error on the execution order of analyses, the standard solutions were injected in randomized order. For all the analytes a linear regression fit was used with a weighting factor $1/x$ and for all the calibration plots a good linearity with regression coefficients (R^2) always greater than 0.9982 was obtained.

Detection limit values expressed as the concentration of the analyte that gives a signal equal to the average background (S_{blank}) plus 3 times the standard deviation of the blank (LOD = S_{blank} + 3s_{blank}) are 0.3 μg L^{-1} for hydroxytyrosol and 0.4 μg L^{-1} for oleuropein. The quantitation limits (LOQ), evaluated as LOQ = S_{blank} + 10s_{blank}, are 1.0 μg L^{-1} for hydroxytyrosol and 1.2 μg L^{-1} for oleuropein.

2.6. In Vitro Cell Culture.

In vitro experiments were carried out using the tumorigenic malignant mesothelioma REN cell line [1]. Cells were grown in DMEM, supplemented with 10% foetal bovine serum (FBS, Euroclone), at 37°C, in a 5% CO_2, fully humidified atmosphere.

2.7. Cell Viability Assay.

Cell viability was determined on REN cells by the MTT assay. Cells were settled in 96-well plates for 24 h, exposed to various agents for 48 h as specified, incubated with 100 μL/mL tetrazolium salt (MTT, 5 mg/mL in PBS) in cell culture medium without serum for 3 h at 37°C, and treated with a solution of 1 N HCl-isopropanol (1 : 24, v/v) followed by mixing to dissolve the dark-blue formazan crystals formed. After a few minutes at room temperature, the plates were read at 550 nm in a VMax microplate reader (Molecular Devices, Sunnyvale, CA).

2.8. Intracellular Ca^{2+} Measurements.

Cytosolic free Ca^{2+} concentration was measured in fura-2-loaded REN cells using a microspectrophotometry fluorescence-ratio setup equipped with a perfusion system, as previously described [18]. Cells were incubated in loading buffer containing 10 μM fura-2-AM at 37°C for 30 minutes, washed with buffer, and mounted on the stage of an inverted microscope (Axiovert Zeiss, Germany), where they were continually superfused with different solutions. Cells were illuminated by a xenon lamp through a wavelength selector monochromator; emission was observed through ×40 quartz objective and recorded by a photomultiplier. The ratio E_{340}/E_{380} was calculated every 40 msec to acquire a time-dependent internal Ca^{2+} sensitive signal.

At the end of each experiment, cells were incubated with 10 μM ionomycin in a Ca-free solution containing 2 mM EGTA for 20–40 min until the ratio reached a minimum value (R_{min}); then EGTA was washed out, normal external Ca^{2+} (1 mM) was restored, and the ratio readily reached a maximum value (R_{max}). Finally, $MnCl_2$ (5 mM) was added to the bath to quench the fura-2 fluorescence and determine the background (cell autofluorescence) values. The fluorescence emissions relative to each excitation wavelength (E_{340} and E_{380}, resp.) were corrected for this background signal before ratio $R = E_{340}/E_{380}$ determination. Internal Ca^{2+} was calculated according to the Grynkiewicz equation [19].

2.9. Statistics.

Statistics were obtained with the *R* package, version 3.0.1 (http://www.r-project.org/foundation/), using *t*-test with Bonferroni's correction for multiple comparisons.

Table 1: sMRM NI transitions (Q1 and Q3 masses) and mass spectrometry parameters. The two most sensitive transitions for each species were monitored.

Analytes	Q1 (m/z)	Q3 (m/z)	t_R (min)	DP (V)	EP (V)	CEP (V)	CE (V)	CXP (V)
Hydroxytyrosol	153	123/93	3.4	−34	−75	−17.32	−20/−31	−1.08/−1.35
Oleuropein	539	275/307	7.9	−40	−5	−31.61	−28/−29	−1.89/−2.12

t_R: retention time; DP: Declustering Potential; EP: Entrance Potential; CEP: Collision cell Entrance Potential; CE: Collision Energy; CXP: Collision cell eXit Potential.

Table 2: Percent content (w/w) of oleuropein and hydroxytyrosol in different olive leaf extracts.

	RE	SE	EF
Oleuropein	21.4 ± 0.3	43.2 ± 1.4	60.1 ± 0.3
Hydroxytyrosol	0.37 ± 0.04	0.91 ± 0.03	n.d.

Data are means ± s.d. of three independent measures. RE: raw extract; SE: subextract; EF: oleuropein-enriched fraction; n.d.: not detected.

Cytotoxicity was determined using a logistic dose-response curve as reported in Ranzato et al. [20]. Analysis of data from Ca^{2+} measurements and determination of EC_{50} values were done by Sigmaplot 8 (Systat Software Inc., San Jose, CA).

3. Results

Multistep processing of olive leaves consisted of the following: (1) extraction of dried, minced leaves in 2-propanol : water (9 : 1), to obtain a raw extract; (2) partitioning between methanol : water (3 : 1) and toluene : petroleum ether (2 : 1), followed by partitioning of the dried aqueous methanol phase between water and 2-butanone, to obtain a subextract; (3) liquid (column) chromatography separation of the dried organic phase, to obtain an oleuropein-enriched fraction (see Methods). Oleuropein and hydroxytyrosol quantification in the raw extract and fractions was achieved by LC-MS technique. Data showed a progressive enrichment in oleuropein, up to a value of 60% w/w in the final fraction obtained through chromatographic separation (Table 2).

In order to evaluate the pharmacological potentials of the oleuropein-enriched, leaf extract fraction, and of its major component oleuropein, we tested the ability of mobilizing cell Ca^{2+} in mesothelioma REN cells. Intracellular Ca^{2+} is a main regulator of cell growth, and therefore agents able to deregulate Ca^{2+} dynamics can be possibly used to hinder cell proliferation.

Fura-2-loaded cells were transiently exposed by perfusion to the oleuropein fraction. This treatment induced $[Ca^{2+}]_i$ rises followed by a prompt recovery of the baseline level upon washout (Figure 1(a)). Data indicate that the observed $[Ca^{2+}]_i$ spikes are not due to cell membrane injury but rather depend on the influx of Ca^{2+} through membrane Ca^{2+} channels. Moreover, the $[Ca^{2+}]_i$ transient elevations were dependent on the nominal concentration of oleuropein (10–30 μM) contained in the extract (Figure 1(b)).

To explore more in depth the mechanism of action, we also studied the Ca^{2+} mobilizing property of standard oleuropein. Similar to the oleuropein fraction, increasing doses of standard oleuropein, in the range 10–100 μM, induced dose-dependent $[Ca^{2+}]_i$ spikes (Figures 1(c) and 1(d)). Removal of Ca^{2+} from the external solution almost abolished the oleuropein effect (Figure 1(d)). In addition, the use of the T-type Ca^{2+} channel inhibitor NNC-55-0396 (Sigma, ≥98%, HPLC) [21] reversibly reduced the Ca^{2+} spike induced by the highest dose of 100 μM oleuropein (Figures 1(c) and 1(d)), suggesting at least a partial involvement of T-type Ca^{2+} channels.

We tried to provide some hint as to which oleuropein moiety could be active on cell Ca^{2+} mobilization. Hydroxytyrosol is known to induce modulatory effects on $[Ca^{2+}]_i$ [22]. We therefore used standard hydroxytyrosol on fura-2-loaded REN cells, observing the induction of dose-dependent $[Ca^{2+}]_i$ spikes that also in this case were inhibited by Ca^{2+}-free medium. Moreover, NNC-55-0396 also hindered the hydroxytyrosol-induced $[Ca^{2+}]_i$ spikes, with 80% inhibition at 10 μM hydroxytyrosol and 65% inhibition at 100 μM hydroxytyrosol (Figures 1(e) and 1(f)).

As for comparative quantification of the effect on $[Ca^{2+}]_i$, dose-response data allowed estimating an EC_{50} of 12 μM for hydroxytyrosol and of 53 μM for oleuropein, showing that hydroxytyrosol is more powerful than oleuropein in inducing Ca^{2+} spikes. No established drug is known to induce T-type Ca^{2+} channel opening. We therefore used the natural phenolic epigallocatechin-3-gallate (EGCG) as positive control, since we had previously shown that this compound induces Ca^{2+} rise in REN cells via T-type Ca^{2+} channels [23]. Presently, EGCG was found to induce dose-dependent $[Ca^{2+}]_i$ spikes with an estimated EC_{50} of 69 μM (Figures 1(e) and 1(f)).

The oleuropein-enriched fraction and standard oleuropein were separately used on REN cells at nominally equivalent oleuropein concentrations, in order to verify their antiproliferative activity. EGCG was used as positive control also in this case, since we had previously assessed its cytotoxicity on REN cells [24]. The cytotoxic effect of the oleuropein fraction (IC_{50} = 22 μg/mL expressed as oleuropein) was slightly, but not significantly, stronger than that of standard oleuropein (IC_{50} = 25 μg/mL). Both substances were slightly more cytotoxic than EGCG (IC_{50} = 33 μg/mL) (Figure 2).

4. Discussion

The oleuropein yield in our enriched fraction is very close to the highest concentrations present in commercially available olive leaf extract formulations [25], suggesting its possible direct use in medicinal preparations. Despite a vast array of

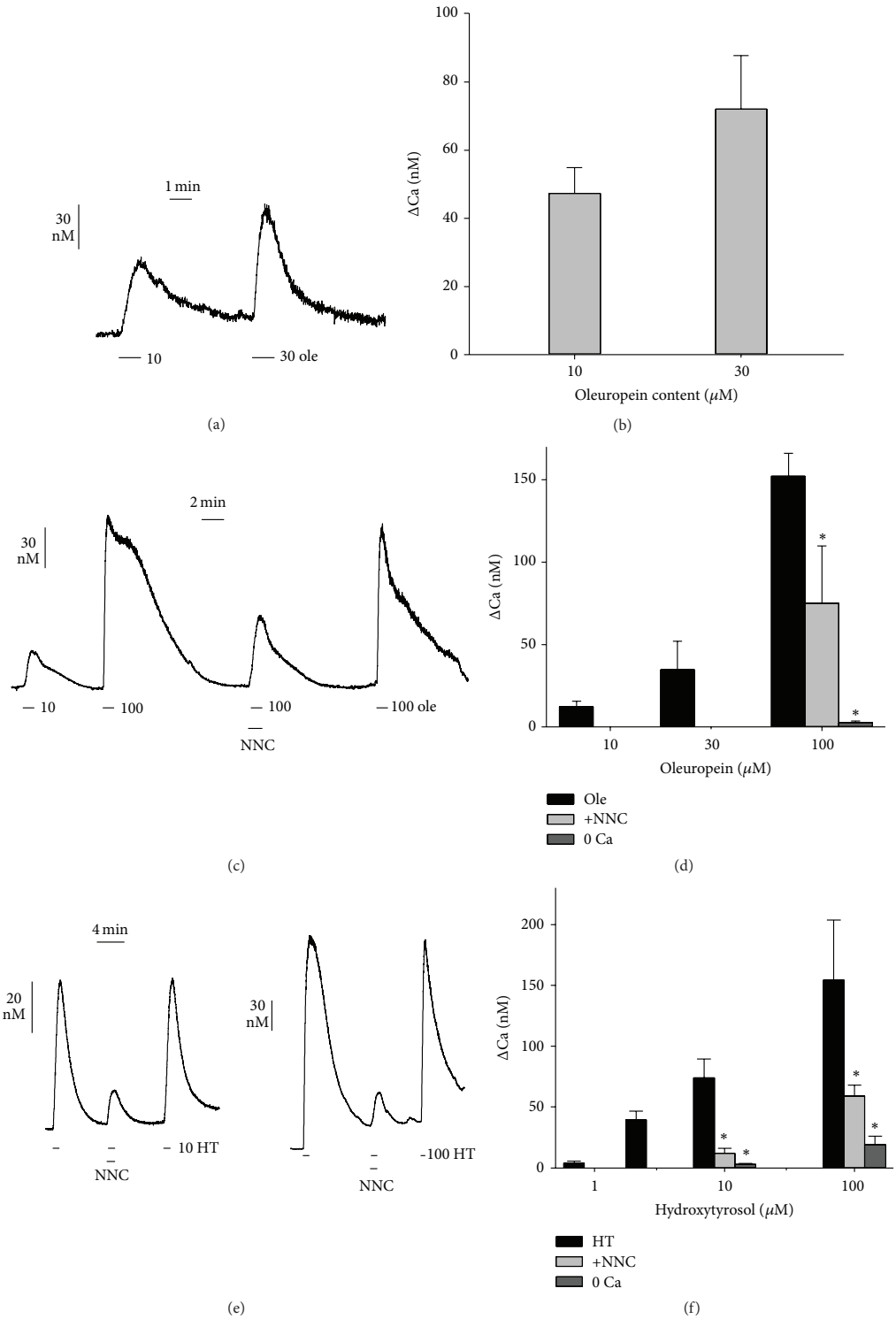

Figure 1: Continued.

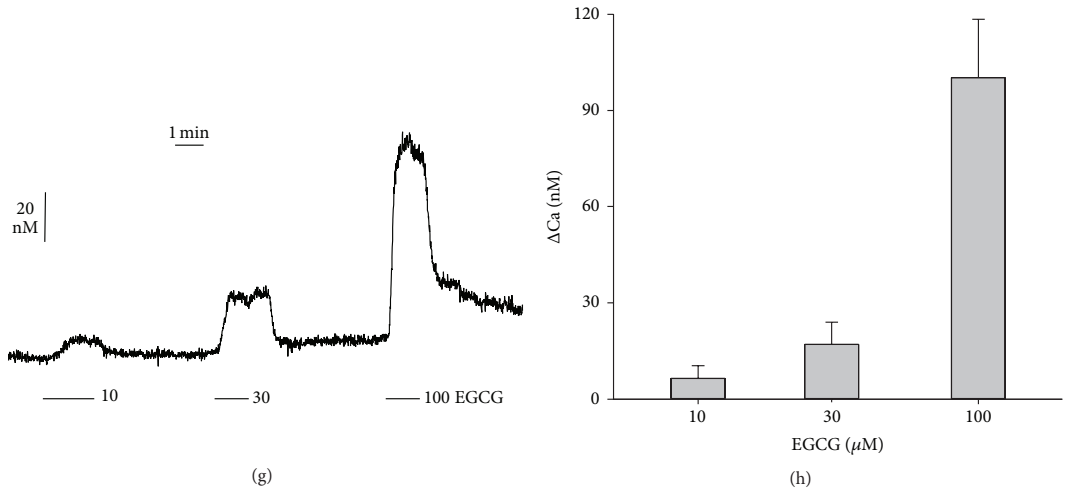

FIGURE 1: Time course of $[Ca^{2+}]_i$ level in mesothelioma REN cells loaded with fura-2 and alternatively exposed to the oleuropein-enriched fraction from olive leaf extract (a, b), to standard oleuropein (c, d) or to standard hydroxytyrosol (e, f). The oleuropein fraction and standard oleuropein have been used at nominal concentrations of oleuropein, expressed in μmoles/L. (a) Induction of $[Ca^{2+}]_i$ spikes in REN cells loaded with fura-2 by transient exposure to the oleuropein fraction (ole) at 10 and 30 μM oleuropein. (b) Quantification of dose-dependent induction of $[Ca^{2+}]_i$ spikes by the oleuropein fraction. Data are means ± s.e.m. ($n \geq 3$) of $\Delta[Ca^{2+}]_i$ (difference between peak value and basal level of $[Ca^{2+}]_i$). (c) Induction of $[Ca^{2+}]_i$ spikes in REN cells by transient exposure to standard oleuropein (ole) at 10 and 100 μM. The inhibitory effect of the T-type Ca^{2+} channel blocker NNC-55-0396 (5 μM) and recovery after washout are shown. (d) Quantification of dose-dependent induction of $[Ca^{2+}]_i$ spikes by standard oleuropein (EC_{50} = 53 μM), and inhibition by Ca^{2+}-free medium (0 Ca) or NNC-55-0396 measured at 100 μM oleuropein. Data as above; $* = p \leq 0.01$, t test. (e) Induction of $[Ca^{2+}]_i$ spikes by standard hydroxytyrosol (HT) at 10 and 100 μM, inhibitory effect of NNC-55-0396, and recovery after washout. (f) Quantification of dose-dependent effect of hydroxytyrosol (EC_{50} = 12 μM) and inhibition by Ca^{2+}-free medium (0 Ca) or NNC-55-0396 measured at 10 and 100 μM hydroxytyrosol. Data and statistics as above. (g, h) Induction of $[Ca^{2+}]_i$ spikes by EGCG and statistics of dose-dependent effect (EC_{50} = 69 μM). Data as above.

data on possible oleuropein cellular targets, our data about the effects on intracellular Ca^{2+} are new. The activity of oleuropein was slightly lower than that of the oleuropein-enriched fraction, possibly due to the occurrence in the fraction of other secoiridoid esters known to be present in olive leaves, such as demethyloleuropein, ligstroside, and oleuroside [26], allegedly coeluting with oleuropein in the HPLC separation.

We have previously found that low-voltage-activated T-type Ca^{2+} channels, specifically the isoform Cav3.2, mediate the Ca^{2+} rise induced in REN cells by the green tea polyphenol epigallocatechin-3-gallate [23]. We have also shown that Cav3.2 is responsible for Ca^{2+} spikes induced by epigallocatechin-3-gallate in MCF-7 breast cancer cells [20]. In the present study, an involvement of T-type Ca^{2+} channels is called into question also for the Ca^{2+} mobilizing effect of oleuropein by the use of Ca^{2+}-free medium, indicating a Ca^{2+} entry process, and of the specific T-type Ca^{2+} channel blocker NNC-55-0396.

The stronger activity of hydroxytyrosol with respect to oleuropein and the inhibitory effect of NNC-55-0396 suggest that the hydroxytyrosol moiety could be the active site mediating the oleuropein effect on T-type Ca^{2+} channels. The almost complete inhibition exerted by NNC-55-0396 on hydroxytyrosol at lower dose, compared with the partial inhibition at higher dose, seems to indicate that the effect of olive phenolics mostly involves a T-type Ca^{2+} channel-dependent mechanism at low doses (≤10 μM). At higher doses, these phenolics could instead act through a more complex mechanism, possibly including other Ca^{2+} mobilizing systems.

T-type Ca^{2+} channels have been linked to various kinds of epilepsy [27], while they are thought to play a role in tumor cell cycle progression and proliferation [28, 29]. Hence, much interest has been raised in their possible therapeutic targeting with more or less specific inhibitors [30, 31]. However, the blockage of these channels does not seem to be an exclusive strategy in antitumor therapy. Antiproliferative effects obtained with mibefradil and pimozide, two T-type Ca^{2+} channel inhibitors, have been partially ascribed to some unidentified mechanism [32]. Also, cell cycle progression needs a fine tuning of $[Ca^{2+}]_i$ oscillations, suggesting that intracellular Ca^{2+} dysregulation determining transient $[Ca^{2+}]_i$ rise may also interfere with tumor development, possibly leading to cell death [33]. Accordingly, pharmacological agents like olive phenolics, able to abnormally activate T-type Ca^{2+} channel activity, could be promising tools for the inhibition of cancerous cell growth.

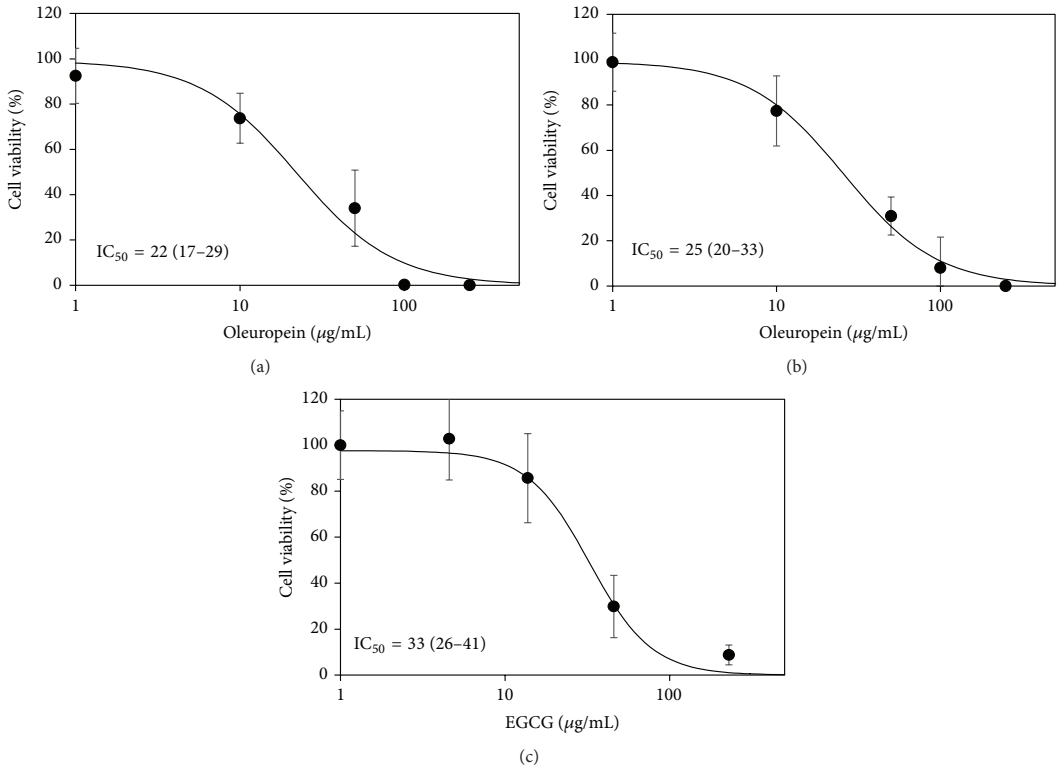

Figure 2: Dose-response data of cell viability obtained with the MTT assay after exposure of REN cells for 48 h to the oleuropein-enriched fraction (60% oleuropein) (a), standard oleuropein (b), and EGCG (c). The charts show means ± s.d. of percent MTT-formazan absorbance, logistic regression lines, and IC_{50} values expressed as μg/mL (95% CI). Concentrations are normalized as the logarithm of μg/mL.

In apparent contrast with the present data, it has been previously shown that an olive leaf extract exerts antagonistic effects on high-voltage-activated L-type Ca^{2+} channel, thereby inducing blood pressure lowering [34, 35]. A comparison between these previous reports and our study is difficult to make, owing to differences in both the extracts and the experimental models. However, such a complex of data advocates an intriguing scenario, entailing divergent effects of major olive phenolics on low-voltage and high-voltage Ca^{2+} channels.

More insight into the possibility of using the oleuropein fraction in antitumor treatment for mesothelioma is provided by our cytotoxicity tests, indicating that the antiproliferative activity of the oleuropein fraction essentially depends on its major constituent oleuropein. The United States National Cancer Institute plant screening program has established that a plant extract can be deemed to have a cytotoxic effect if IC_{50} for incubations of 48–72 h is 20 μg/mL or lower [36]. Our oleuropein-enriched fraction has an oleuropein content of 60% and a cytotoxicity IC_{50} of 22 (17–29) μg/mL in terms of oleuropein. We can then estimate IC_{50} of 36.7 (28.3–48.3) μg/mL for the oleuropein-enriched fraction as a whole. Hence, our oleuropein fraction is close to the cytotoxicity threshold established by NCI and could therefore be appropriate for the development of synergistic treatments allowing reducing the doses of highly toxic conventional drugs, as previously suggested for EGCG [1]. Such an approach could overcome critical drawbacks in the treatment of chemoresistant tumors like malignant mesothelioma [37].

There is no established standard dose of oleuropein for humans, but in acute toxicity studies, oleuropein and hydroxytyrosol have shown no lethality or adverse effects in mice up to doses of 1000 and 2000 mg/kg, respectively. In addition, studies conducted on humans with olive extract or its polyphenolics have shown no undesired effects [38, 39]. Pharmacokinetics of oral oleuropein and its metabolite hydroxytyrosol in human plasma indicates peaks of about 0.004 μg/mL (0.01 μM) for oleuropein, while its main metabolite hydroxytyrosol can reach values of about 0.15 μg/mL (1 μM) [40]. These values are close to the effective concentrations observed in our experiments for hydroxytyrosol, but intravenous delivery of oleuropein should allow reaching much higher blood peaks. Hence, pharmacokinetics data indicate that plasma concentrations compatible with dysregulating effects on tumor cell Ca^{2+} could be easily achieved upon clinical administrations of

oleuropein, followed by its conversion into the more effective metabolite hydroxytyrosol.

5. Conclusions

We have shown a method to obtain oleuropein-enriched olive leaf extract fractions that could be of industrial interest, because extraction is generally competitive with chemical synthesis for complex molecules like oleuropein. In addition, we have highlighted a novel mechanism of action for oleuropein and its metabolite hydroxytyrosol, consisting in a dysregulation of Ca^{2+} dynamics occurring via T-type Ca^{2+} channels. This kind of effect suggests a possible use of the oleuropein fraction from olive leaves in the treatment of mesothelioma.

Conflict of Interests

The authors declare no conflict of interests.

Acknowledgments

Bruno Burlando was supported by Fondazione Buzzi Unicem (Casale Monferrato, Italy), Grant no. FBU-P27. Laura Cornara was supported by a PO-CRO-FSE Project, Asse IV Capitale Umano, ob. Specifico I/6, 2007–2013 (Regione Liguria, Italy). Barbara Borghesi was recipient of a Research Fellowship from the PO-CRO-FSE Project. Stefania Ribulla was recipient of a Ph.D. scholarship from the Italian Ministry of University and Research (MIUR). The authors wish to thank the Pietro Isnardi S.r.l. food company (Imperia, Italy) for providing olive leaves.

References

[1] V. Volta, E. Ranzato, S. Martinotti et al., "Preclinical demonstration of synergistic Active Nutrients/Drug (AND) combination as a potential treatment for malignant pleural mesothelioma," *PLoS ONE*, vol. 8, no. 3, Article ID e58051, 2013.

[2] C. M. Diez, I. Trujillo, N. Martinez-Urdiroz et al., "Olive domestication and diversification in the Mediterranean basin," *The New Phytologist*, vol. 206, no. 1, pp. 436–447, 2015.

[3] C. Alarcón de la Lastra, M. D. Barranco, V. Motilva, and J. M. Herrerías, "Mediterranean diet and health: biological importance of olive oil," *Current Pharmaceutical Design*, vol. 7, no. 10, pp. 933–950, 2001.

[4] S. N. El and S. Karakaya, "Olive tree (*Olea europaea*) leaves: potential beneficial effects on human health," *Nutrition Reviews*, vol. 67, no. 11, pp. 632–638, 2009.

[5] M. Delgado-Pertíñez, A. Chesson, G. J. Provan, A. Garrido, and A. Gómez-Cabrera, "Effect of different drying systems for the conservation of olive leaves on their nutritive value for ruminants," *Animal Research*, vol. 47, no. 2, pp. 141–150, 1998.

[6] A. Garcia-Maraver, D. Salvachúa, M. J. Martínez, L. F. Diaz, and M. Zamorano, "Analysis of the relation between the cellulose, hemicellulose and lignin content and the thermal behavior of residual biomass from olive trees," *Waste Management*, vol. 33, no. 11, pp. 2245–2249, 2013.

[7] C. Savournin, B. Baghdikian, R. Elias, F. Dargouth-Kesraoui, K. Boukef, and G. Balansard, "Rapid high-performance liquid chromatography analysis for the quantitative determination of oleuropein in *Olea europaea* leaves," *Journal of Agricultural and Food Chemistry*, vol. 49, no. 2, pp. 618–621, 2001.

[8] M. Ansari, M. Kazemipour, and S. Fathi, "Development of a simple green extraction procedure and HPLC method for determination of oleuropein in olive leaf extract applied to a multi-source comparative study," *Journal of the Iranian Chemical Society*, vol. 8, no. 1, pp. 38–47, 2011.

[9] D. Ryan, M. Antolovich, P. Prenzler, K. Robards, and S. Lavee, "Biotransformations of phenolic compounds in *Olea europaea* L.," *Scientia Horticulturae*, vol. 92, no. 2, pp. 147–176, 2002.

[10] S. H. Omar, "Oleuropein in olive and its pharmacological effects," *Scientia Pharmaceutica*, vol. 78, no. 2, pp. 133–154, 2010.

[11] S. Bulotta, M. Celano, S. M. Lepore, T. Montalcini, A. Pujia, and D. Russo, "Beneficial effects of the olive oil phenolic components oleuropein and hydroxytyrosol: focus on protection against cardiovascular and metabolic diseases," *Journal of Translational Medicine*, vol. 12, article 219, 2014.

[12] F. Durlu-Özkaya and M. T. Özkaya, "Oleuropein using as an additive for feed and products used for humans," *Journal of Food Processing & Technology*, vol. 2, no. 3, article 113, 2011.

[13] B. Barbaro, G. Toietta, R. Maggio et al., "Effects of the olive-derived polyphenol oleuropein on human health," *International Journal of Molecular Sciences*, vol. 15, no. 10, pp. 18508–18524, 2014.

[14] S. Granados-Principal, J. L. Quiles, C. L. Ramirez-Tortosa, P. Sanchez-Rovira, and M. C. Ramirez-Tortosa, "Hydroxytyrosol: from laboratory investigations to future clinical trials," *Nutrition Reviews*, vol. 68, no. 4, pp. 191–206, 2010.

[15] R. Bernini, N. Merendino, A. Romani, and F. Velotti, "Naturally occurring hydroxytyrosol: synthesis and anticancer potential," *Current Medicinal Chemistry*, vol. 20, no. 5, pp. 655–670, 2013.

[16] O.-H. Lee and B.-Y. Lee, "Antioxidant and antimicrobial activities of individual and combined phenolics in *Olea europaea* leaf extract," *Bioresource Technology*, vol. 101, no. 10, pp. 3751–3754, 2010.

[17] T. Bracci, L. Sebastiani, M. Busconi, C. Fogher, A. Belaj, and I. Trujillo, "SSR markers reveal the uniqueness of olive cultivars from the Italian region of Liguria," *Scientia Horticulturae*, vol. 122, no. 2, pp. 209–215, 2009.

[18] M. Mazzolini, S. Traverso, and C. Marchetti, "Multiple pathways of Pb^{2+} permeation in rat cerebellar granule neurones," *Journal of Neurochemistry*, vol. 79, no. 2, pp. 407–416, 2001.

[19] G. Grynkiewicz, M. Poenie, and R. Y. Tsien, "A new generation of Ca^{2+} indicators with greatly improved fluorescence properties," *Journal of Biological Chemistry*, vol. 260, no. 6, pp. 3440–3450, 1985.

[20] E. Ranzato, V. Magnelli, S. Martinotti et al., "Epigallocatechin-3-gallate elicits Ca^{2+} spike in MCF-7 breast cancer cells: essential role of Cav3.2 channels," *Cell Calcium*, vol. 56, no. 4, pp. 285–295, 2014.

[21] M. Li, J. B. Hansen, L. Huang, B. M. Keyser, and J. T. Taylor, "Towards selective antagonists of T-type calcium channels: design, characterization and potential applications of NNC 55-0396," *Cardiovascular Drug Reviews*, vol. 23, no. 2, pp. 173–196, 2005.

[22] C. A. Palmerini, E. Carlini, C. Saccardi, M. Servili, G. Montedoro, and G. Arienti, "Activity of olive oil phenols on lymphomonocyte cytosolic calcium," *The Journal of Nutritional Biochemistry*, vol. 16, no. 2, pp. 109–113, 2005.

[23] E. Ranzato, S. Martinotti, V. Magnelli et al., "Epigallocatechin-3-gallate induces mesothelioma cell death via H_2O_2-dependent T-type Ca^{2+} channel opening," *Journal of Cellular and Molecular Medicine*, vol. 16, no. 11, pp. 2667–2678, 2012.

[24] S. Martinotti, E. Ranzato, and B. Burlando, "In vitro screening of synergistic ascorbate-drug combinations for the treatment of malignant mesothelioma," *Toxicology in Vitro*, vol. 25, no. 8, pp. 1568–1574, 2011.

[25] D. T. Kremastinos, "Olive and oleuropein," *Hellenic Journal of Cardiology*, vol. 49, no. 4, pp. 295–296, 2008.

[26] Y. Wang, S. Q. Wang, W. H. Cui, J. J. He, Z. F. Wang, and X. L. Yang, "Olive leaf extract inhibits lead poisoning-induced brain injury," *Neural Regeneration Research*, vol. 8, no. 22, pp. 2021–2029, 2013.

[27] E. Tringham, K. L. Powell, S. M. Cain et al., "T-type calcium channel blockers that attenuate thalamic burst firing and suppress absence seizures," *Science translational medicine*, vol. 4, no. 121, Article ID 121ra19, 2012.

[28] A. Panner, L. L. Cribbs, G. M. Zainelli, T. C. Origitano, S. Singh, and R. D. Wurster, "Variation of T-type calcium channel protein expression affects cell division of cultured tumor cells," *Cell Calcium*, vol. 37, no. 2, pp. 105–119, 2005.

[29] J. T. Taylor, X.-B. Zeng, J. E. Pottle et al., "Calcium signaling and T-type calcium channels in cancer cell cycling," *World Journal of Gastroenterology*, vol. 14, no. 32, pp. 4984–4991, 2008.

[30] W. Li, S.-L. Zhang, N. Wang, B.-B. Zhang, and M. Li, "Blockade of T-type Ca^{2+} channels inhibits human ovarian cancer cell proliferation," *Cancer Investigation*, vol. 29, no. 5, pp. 339–346, 2011.

[31] K. R. Loughlin, "Calcium channel blockers and prostate cancer," *Urologic Oncology*, vol. 32, no. 5, pp. 537–538, 2014.

[32] G. E. Bertolesi, C. Shi, L. Elbaum et al., "The Ca^{2+} channel antagonists mibefradil and pimozide inhibit cell growth via different cytotoxic mechanisms," *Molecular Pharmacology*, vol. 62, no. 2, pp. 210–219, 2002.

[33] G. R. Monteith, D. McAndrew, H. M. Faddy, and S. J. Roberts-Thomson, "Calcium and cancer: targeting Ca^{2+} transport," *Nature Reviews Cancer*, vol. 7, no. 7, pp. 519–530, 2007.

[34] A. Scheffler, H. W. Rauwald, B. Kampa, U. Mann, F. W. Mohr, and S. Dhein, "Olea europaea leaf extract exerts L-type Ca^{2+} channel antagonistic effects," *Journal of Ethnopharmacology*, vol. 120, no. 2, pp. 233–240, 2008.

[35] A. H. Gilani, A.-U. Khan, A. J. Shah, J. Connor, and Q. Jabeen, "Blood pressure lowering effect of olive is mediated through calcium channel blockade," *International Journal of Food Sciences and Nutrition*, vol. 56, no. 8, pp. 613–620, 2005.

[36] R. I. Geran, N. H. Greenberg, M. M. Macdonald, A. M. Shumacher, and B. J. Abbott, "Protocols for screening chemical agents and natural products against animal tumors and other biological systems," *Cancer Chemotherapy Reports Part 3*, vol. 3, pp. 1–103, 1972.

[37] M. Suganuma, A. Saha, and H. Fujiki, "New cancer treatment strategy using combination of green tea catechins and anti-cancer drugs," *Cancer Science*, vol. 102, no. 2, pp. 317–323, 2011.

[38] F. Visioli and C. Galli, "Phenolics from olive oil and its waste products. Biological activities in in vitro and in vivo studies," *World Review of Nutrition and Dietetics*, vol. 88, pp. 233–237, 2001.

[39] P. González, F. Florido, B. Sáenz de San Pedro, F. de la Torre, P. Rico, and S. Martín, "Immunotherapy with an extract of *Olea europaea* quantified in mass units: evaluation of the safety and efficacy after one year of treatment," *Journal of Investigational Allergology and Clinical Immunology*, vol. 12, no. 4, pp. 263–271, 2002.

[40] M. de Bock, E. B. Thorstensen, J. G. B. Derraik, H. V. Henderson, P. L. Hofman, and W. S. Cutfield, "Human absorption and metabolism of oleuropein and hydroxytyrosol ingested as olive (*Olea europaea* L.) leaf extract," *Molecular Nutrition and Food Research*, vol. 57, no. 11, pp. 2079–2085, 2013.

Resveratrol induces intracellular Ca^{2+} rise via T-type Ca^{2+} channels in a mesothelioma cell line.

Life Sciences (in press)

2016

Resveratrol induces intracellular Ca^{2+} rise via T-type Ca^{2+} channels in a mesothelioma cell line

Carla Marchetti[1,*] , Stefania Ribulla[2], Valeria Magnelli[2], Mauro Patrone[2], and Bruno Burlando[1,2].

[1] Istituto di Biofisica, Consiglio Nazionale delle Ricerche, via De Marini 6, 16149 Genova, Italy

[2]Dipartimento di Scienze e Innovazione Tecnologica (DISIT), Università del Piemonte Orientale, viale T. Michel 11, 15121 Alessandria, Italy

* Corresponding author

Address for correspondence:

Carla Marchetti

Istituto di Biofisica, Consiglio Nazionale delle Ricerche

via De Marini, 6

16149 Genova, Italy

phone: 39010-6475578

FAX: 39010-6475500

Email: marchetti@ge.ibf.cnr.it

Total words count : 6236 words

Abstract : 250 words

Introduction : 624 words

Discussion :1075words

Conclusion : 146 words

Figures : 4

Abstract

Aims: Intracellular calcium (Ca^{2+}) is known to play an important role in cancer development and growth. Resveratrol (Res) is a stilbene polyphenol occurring in several plant species and known for various possible beneficial effects, including its ability to inhibit proliferation and to induce apoptosis in cancer cells. This study was designed to determine whether Res affects Ca^{2+} signaling in cancer cells.

Main methods: We used the REN human mesothelioma cell line, as an *in vitro* cancer cell model, and the non-malignant human mesothelial MeT5A cell line, as normal cell model. Cytosolic Ca^{2+} concentration was measured by the fluorescent indicator Fura-2. Immunofluorescence, Western blot, and siRNA technique were employed to assess the involvement of T-type Ca^{2+} channels. Cell viability was determined by the calcein assay.

Key findings: REN cells transiently exposed to 1–10 μM Res showed increasing peaks of Ca^{2+} that were absent in Ca^{2+}-free medium and were reduced by non-selective (Ni^{2+}), and highly selective (NNC 55-0396) T-type Ca^{2+} channels antagonist, and by siRNA knockout of Cav3.2 T-type Ca^{2+} channel gene. Dose-dependent curve of Res-induced Ca^{2+} peaks showed a rightward shift in normal MeT-5A mesothelial cells (EC_{50}=4.9 μM) with respect to REN cells (EC_{50}=2.7 μM). Moreover, incubation with 3 and 10 μM Res for 7 days resulted in cell growth inhibition for REN, but not for MeT-5A cells.

Significance: Res induces Ca^{2+} influx, possibly mediated through T-type Ca^{2+} channels, with significant selectivity towards mesothelioma cells, suggesting a possible use as an adjuvant to chemotherapy drugs for mesothelioma clinical treatment.

Key words: Cytosolic Ca^{2+}, Fura-2, mesothelioma REN cells, mesothelial Met5A cells, Cav3.2 Ca^{2+} channels; cell growth inhibition.

Abbreviations: BSA=bovine serum albumin; $[Ca^{2+}]_i$=cytosolic Ca^{2+} concentration; EGCG=epigallocatechin-3-gallate; PBS=phosphate-buffered saline; Res=Resveratrol.

1. Introduction

Intracellular calcium (Ca^{2+}) is an essential signal transduction element involved in several physiological functions, such as cell growth, cell cycle control, and gene expression (Berridge et al., 2003). In cancer cells, modified Ca^{2+} signaling is thought to contribute to important events, including proliferation, migration, invasion, and metastasis, while an alteration of Ca^{2+} regulatory mechanisms could be detrimental for tumor growth (Monteith et al., 2012). Plasma membrane Ca^{2+}-permeable channels are a route of Ca^{2+} entry from the extracellular medium and sustain long-lasting intracellular Ca^{2+} elevations (Munaron et al., 2004). The possibility of arresting the proliferation of neoplastic cells by disturbing Ca^{2+} dynamics has led to a growing interest for Ca^{2+} channels as potential therapeutic targets (Monteith et al. 2007, Triggle 2007).

Low-threshold voltage-dependent, or T-type Ca^{2+} channels (namely Cav3.1, Cav3.2, and Cav3.3, which consist of α_{1G}, α_{1H} and α_{1I} subunits, respectively; (Zhang et al., 2013) are mainly present in excitable cells like nerve, muscle and endocrine cells, but are also abnormally expressed in various cancer cells, in which they are believed to promote cell proliferation via controlled increases of cytosolic Ca^{2+} (Taylor et al., 2008; Dziegielewska et al., 2014). These channels open at a membrane potential very close to, or even coincident with, the resting value (Perez-Reyes, 2003), thus they may drive a constant Ca^{2+} influx into the resting cell. Various studies indicate that antagonists of T-type Ca^{2+} channels may hinder the growth of certain cancer types (Li et al. 2011, Loughlin 2014). However, the need for a fine adjustment of cytosolic Ca^{2+} variations in cell proliferation suggests that activators of Ca^{2+} channels might also act as antagonists of cancer growth (Monteith et al. 2007).

Malignant pleural mesothelioma (MPM) is an aggressive, poor-prognosis tumor arising from the mesothelial lining cells of the pleura, commonly associated with asbestos exposure (Pass et al., 2004; Park et al., 2011). This cancer is in need of novel therapy, and among alternative remedies, there is a growing interest in the preventive action of active nutrients, like vitamins and polyphenols (Kampa et al., 2007) that may be used as tolerable drugs and exhibit synergistic effects with conventional chemotherapy (Volta et al. 2013). The inhibitory effect of polyphenols in tumorigenesis and tumor growth is apparently not due only to their antioxidant properties, but also to interferences with basic cellular functions such as apoptosis, cell cycle, angiogenesis, invasion, and metastasis (Kampa et al., 2007; Fantini et al., 2015).

Previous studies conducted in our laboratory have revealed a synergistic behavior of the drug gemcitabine in combination with ascorbate and the green tea polyphenol epigallocatechin-3-gallate (EGCG; Volta et al., 2013), while in another study we have reported intracellular Ca^{2+}

rise in mesothelioma cells treated with EGCG (Ranzato et al., 2012). Seeking other natural products that may be able to impair Ca^{2+} levels in mesothelioma cells, we used resveratrol (3,4′,5-trihydroxystilbene, Res), a stilbenoid produced by a wide variety of plants, such as grapes, peanuts, and mulberries, in response to stress, injury, ultraviolet irradiation, and fungal infection. This compound has shown a range of favorable properties in many illnesses, including cardiovascular diseases (Bradamante et al., 2004), ischemic injuries (Petrovski et al., 2011), diabetes (Su et al., 2006), inflammation (Martinez and Moreno, 2000), and neurodegenerative diseases (Anekonda, 2006). In particular, Res has been found to exert strong anti-proliferative properties on different cancer cell lines (Kundu and Surh, 2008; Frazzi and Tigano, 2014), being able to arrest cell cycle and induce apoptosis, as well as suppressing angiogenesis and metastasis (Trapp et al., 2010; Wang et al., 2010; Polycarpou et al., 2013). Being well tolerated by the human organism, and having multi-cellular targets, Res is an ideal candidate as a possible adjuvant of antitumor drugs. In this work we propose how it may explicate this role by dysregulating Ca^{2+} signaling.

2. Materials and Methods

2.1 Reagents

Culture media and reagents were purchased from Sigma-Aldrich (St. Louis, MO, USA), unless otherwise indicated.

2.2 Cell culture and viability assay

Experiments were carried out on the highly tumorigenic p53 mutant epithelial subtype REN cell line, a widely used *in vitro* human mesothelioma model, originally isolated and characterized by Dr Albelda SM (University of Pennsylvania, Philadelphia, PA, USA; Bertino et al., 2008; Ranzato et al., 2011). The non-malignant human mesothelial cell line, MeT5A, was used as a normal control (Ke et al., 1989). Cells were cultured in DMEM supplemented with 10% fetal bovine serum and 1% penicillin-streptomycin solution.

Cell viability and proliferation was determined by the calcein assay, carried out using the lipophilic calcein-acetoxymethylester (calcein-AM). Cells were settled in 96-well plates for 24 h and then subjected to the specified treatments. Thereafter, plates were washed with PBS, incubated for 30 min at 37 °C with a solution of 2.5 μM calcein-AM in PBS, and then read in a fluorescence plate reader (Infinite 200 Pro, Tecan, Wien) by using 485 nm excitation and 535 nm emission filters.

2.3 Intracellular calcium measurements

Cytosolic Ca^{2+} concentration ($[Ca^{2+}]_i$) was measured by loading cells with the fluorescent Ca^{2+} chelator Fura-2 (Mazzolini et al., 2001; Marchetti et al., 2014), using a microspectrophotometry fluorescence-ratio setup equipped with a perfusion system. Cells were plated on poly-L-lysine coated glass coverslips and incubated with 10 μm Fura-2-acetoxymethyl ester (Fura-2-AM, Molecular Probes™) in a physiological saline (see below), at 37 °C for 40 minutes. Then coverslips were washed and mounted on the stage of an inverted microscope (Axiovert Zeiss, Germany) where the cell monolayer was continually superfused by gravity flow (10 ml/min) and all modifiers were applied by bath solution exchange. Cells were illuminated by a xenon lamp through a wavelength selector monochromator; emission was observed through an X40 quartz objective and recorded by a photomultiplier. The ratio E340/E380 was calculated every 40 msec to acquire a time-dependent, $[Ca^{2+}]_i$-sensitive signal. The physiological standard bath solution contained (in mM) NaCl 140, KCl 5.4, $CaCl_2$ 1.0, $MgCl_2$ 1.0, 4-(2-hydroxyethyl)-1-piperazineethanesulfonic acid (HEPES) 10, and glucose 10. The pH was adjusted at 7.4 with NaOH. The Ca free solution had the same composition with 0 $CaCl_2$, 4 $MgCl_2$ and 2 ethylene glycol-bis(2-aminoethylether)-N,N,N',N'-tetraacetic acid (EGTA). $[Ca^{2+}]_i$ was calculated according to the function of Grynkiewicz et al., (1985). Parameters values were obtained at the end of each experiment by incubating the cells with 10μM ionomycin (Sigma-Aldrich) in Ca^{2+}-free and standard Ca^{2+} solutions, as described previously (Marchetti et al., 1995; Mazzolini et al., 2001). All data are presented as $[Ca^{2+}]_i$, unless otherwise stated.

2.4 Immunofluorescence

Cells were fixed for 10 min at room temperature with 3.7% (w/v) para-formaldehyde in PBS, and permeabilized for 2 min with 0.1% Triton-X100. Blocking reaction was performed with a buffer containing 2% BSA-PBS for 1 h, at 37 °C. Cells were then washed twice with PBS and incubated with primary antibody anti Cav3.2 (clone S55-10 dilution 1:200, Novus Biologicals, Littleton, CO), followed by proper secondary antibody conjugated to Alexa Fluor® (dilution 1:200, Termo Fisher Scientific Waltham, MA USA). Both incubations were performed at room temperature for 1 h. Then, cells were incubated with fluorescein isothiocyanate (FITC)-labeled phalloidin (5 μg/mL) for 15 min at room temperature. Cells were visualized in a Nikon confocal system (Nikon Europe B.V.), equipped with Andor Revolution XD spinning-disk (Andor Technology Ltd, Belfast), Agilent laserbox with 405, 488, 561 and 640 nm solid state laser, and Andor Ixon3 897 EMCCD camera.

2.5 RNA interference (siRNA)

RNA interference was obtained by transfecting cells with 5 μM siRNA oligonucleotides (T-type Ca^{2+} CP α1H siRNA (h): sc-42706, Santa Cruz Biotechnology, Dallas, TX) or with equimolar scramble siRNA, by using the N-ter Nanoparticle siRNA Transfection System (Sigma-Aldrich). Scramble siRNA was obtained using non-targeting siRNA (Control siRNA-A: sc-37007, Santa Cruz Biotechnology). Experiments were performed 48h after transfection.

2.6 Western blot

Cell cultures were transferred on ice, rinsed twice with PBS (without Ca^{2+} and Mg^{2+}) and lysed by incubation with 0.1 ml/well of RIPA buffer (150 mM NaCl, 1% NP-40, 0.5% sodium deoxycholate, 0.1% SDS, and 50 mM Tris, pH 8.0), supplemented with freshly added 0.5 mM PMSF (phenyl-methylsulfonyl fluoride), for 30 min at 4 °C. Lysates were scraped from the dish, collected by centrifugation for 10 min at 10,000 *g* at 4 °C, and then supernatants were aliquoted and stored at -80 °C. The protein concentration was determined by Bicinchoninic Acid (BCA) Protein Assay (G-Biosciences®, Geno Technology Inc, St. Louis, MO), using bovine serum albumin as a standard. Amounts of 25 μg of protein were loaded on gel, subjected to SDS-PAGE (10% gel), and transferred to a nitrocellulose membrane, using a Bio-Rad Mini Trans Blot electrophoretic transfer unit (Bio-Rad Laboratories, Hercules, CA). Membrane was blocked for nonspecific protein with 5% non-fat dry milk in PBS for 30 min, and then probed at room temperature for 1 hour with primary antibody against Cav3.2 (clone S55-10, dilution 1:5000, Novus Biologicals, Littleton, CO), or against β-actin as equal loading control. Membrane was then washed three times (10 min per wash) with PBS supplemented with 0.05% Tween-20, to remove unbound antibodies, and further incubated with proper secondary antibody conjugated with anti-mouse horseradish peroxidase (dilution 1:5000; Cell Signaling Technology®, Life Science, Danvers, MS). Membrane was developed using an Amersham ECL chemiluminescence kit (GE Healthcare, Little Chalfont, UK) according to the manufacturer's protocol, and digitized with Quantity One Image Software (ChemiDoc XRS, Bio-Rad).

2.7 Statistics

Data were analysed using Sigma Plot software (Systat Software Inc.). Data are shown as mean±sem, or mean±sd for proliferation assays. Statistical significance was evaluated by Student's t-test or Man-Whitney Rank Sum test, as indicated by the software. The difference between two conditions was considered significant if $p < 0.05$.

3. Results

3.1 Resveratrol fluorescence does not hinder Fura-2 measurements of $[Ca^{2+}]_i$ at pharmacological doses.

Resveratrol (Res) is a member of the stilbene family and, when stimulated by 340 nm light, emits fluorescence at 510 nm; thus its fluorophore spectral properties are remarkably similar to those of Fura2 and, in previous work, it has been claimed that Res is not compatible with a Fura2-based assay for measuring intracellular Ca^{2+} signaling (Kopp et al., 2013; Paudel et al., 2014). Therefore, we undertook a series of tests to verify if it is possible to use Fura2 to measure intracellular Ca^{2+} levels in the presence of Res. First, we measured the Res fluorescence emission at 510 nm, following 340 nm excitation, in free solution and the dose-response curve indicates that Res intrinsic fluorescence is negligible for concentration up to 10 μM (EC_{50} = 122 μM, Fig. 1A). Next, we examined the response to various concentrations of Res in Fura2-loaded cells with the microspectrophotometry system for Ca^{2+} measurements. In this case, cells were stimulated alternatively by 340 and 380 nm and emission was recorded again at 510 nm. When Res was added at a concentration of 100 and 400 μM, we recorded a steep increase in emitted fluorescence following 340 nm excitation, and a similar, smaller rise also with 380 nm excitation. This behavior indicates that the response was mainly due to Res intrinsic fluorescence, making it difficult to resolve the Fura2 Ca^{2+}-dependent signal (Fig. 1-B1). Yet, exposure of Fura2-loaded cells to 10 μM Res yielded fluorescence rise with 340 and fluorescence decrease with 380 nm excitation, indicating that in this case the fluorescent signal is almost completely due to Fura2 response to $[Ca^{2+}]_i$ rise (Fig. 1-B2). This concentration of Res (10 μM) caused a response that was qualitatively similar to that determined by treatment with thapsigargin, a well know Ca^{2+} mobilizer that blocks Ca^{2+}-ATPase and triggers release of Ca^{2+} from intracellular stores (fig. 1-B3). Hence, we concluded that as long as Res is used at concentrations ranging between 1 and 10 μM, the intrinsic Res fluorescence is negligible and measurements reflect the Ca^{2+}-dependent Fura2 response. Therefore, in subsequent experiments Res effects on $[Ca^{2+}]_i$ were investigated only in this concentration range.

3.2 Resveratrol caused a rise in $[Ca^{2+}]_i$ in MPM REN cells due to extracellular Ca^{2+} entry.

Fura-2-loaded REN cells were transiently exposed to 1-10 μM Res, showing dose-dependent peaks of $[Ca^{2+}]_i$ (Fig. 1C). When Ca^{2+} was removed from the external solution and EGTA

added, Res did not caused any effect (Fig. 1D), indicating that the observed $[Ca^{2+}]_i$ rise depends on the influx of external Ca^{2+}.

Previous findings on the same cells suggested the Ca^{2+} entry induced by Res can be linked to the activation of T-type Ca^{2+} channels and in particular the Cav3.2 isoform (Ranzato et al., 2012). Specific expression of Cav3.2 Ca^{2+} channels in REN cells was revealed by immunofluorescence coupled to confocal microscopy, suggesting a clustering of these channels in the plasma membrane (Fig. 2A). In addition, the Res-induced Ca^{2+} rise was significantly reduced by Ni^{2+} (30 μM), a low selective T-type Ca^{2+} channel blocker, as well as by the mibefradil analog NNC 55-0396 (5 μM) (Fig. 2B-D). The Ca^{2+} peak was reversibly affected by Ni^{2+} (30 μM), a low selective T-type Ca^{2+} channel blocker, as well as by the nonhydrolyzable analog of mibefradil NNC 55-0396 (5 μM) that has a higher selectivity for T-type channels (Huang et al., 2004; Okubo et al., 2011). To assure reversibility, this drug was applied very briefly and only together with Res (fig.2C).

3.3 Res-induced Ca^{2+} rise is mediated by the Cav3.2 T-type Ca^{2+} channel.

Further evidence for the involvement T-type Ca^{2+} channels, and specifically of the Cav3.2 channel protein, was obtained using siRNA knockdown targeting the human CACNA1H gene, which encodes for the α_{1H} subunit of the Cav3.2 T-type Ca^{2+} channel. Western blot analysis confirmed the expression of this channel in wildtype cells, or in cells subjected to scramble siRNA, while specific siRNA abolished the expression of the channel protein (Fig. 3A). Fura-2 measurements revealed that the Res induced $[Ca^{2+}]_i$ spike was significantly reduced following Cav3.2 knockdown, whereas $[Ca^{2+}]_i$ spike was retained in cells treated with scramble siRNA (Fig.3B,C).

3.4 Res is more effective on REN cells than on normal mesothelium MeT5A cells.

In order to evaluate the possible relevance of the Res effect on $[Ca^{2+}]_i$ for therapeutic purpose, a comparison between REN cells and the non-malignant human mesothelial cell line MeT5A was made. Dose-dependent curves of Res-induced $[Ca^{2+}]_i$ peaks showed a rightward shift for mesothelium (EC_{50} = 4.9 μM) with respect to mesothelioma (EC_{50} = 2.7 μM), indicating that tumor cells are more sensitive to the effect of Res on $[Ca^{2+}]_i$ (Fig. 4A,B).

Moreover, when REN cells were incubated for 7 days with 3 or 10 μM Res, proliferation was significantly inhibited, whereas Res was ineffective on proliferation of Met-5A cells, as illustrated by growth curves in Fig. 4C.

4. Discussion

Resveratrol has been reported to interact with Ca^{2+} regulatory mechanisms in different cells and potential clinical relevance of these effects has been suggested (McCalley et al., 2014). In this study, we describe an effect of Res that is largely dependent on extracellular Ca^{2+} and is likely to involve specific Ca^{2+} channels. The effect of Res on voltage-dependent Ca^{2+} channels (VDCC) was reported in vascular myocytes (Campos-Toimil et al., 2007) and insulinoma cells (Jakab et al., 2008) and these channels were proposed to be involved in the vasorelaxant effect of Res in rat mesenteric artery (Gojkovic-Bukarica et al., 2008). In vascular myocytes, stimulation of Ca^{2+} influx, allegedly mediated by other Ca^{2+}-permeable channels, was also reported (Campos-Toimil et al., 2007). In cancer cells, previous studies showed that Res is able to induce elevations of $[Ca^{2+}]_i$ that lead to compromised mitochondrial function and apoptosis (Ma et al., 2007; Sareen et al., 2007; Chang et al., 2013).

T-type Ca^{2+} channels have attracted attention as possible targets of anticancer treatments. These channels are abnormally expressed in various kinds of tumors and it has been hypothesized that their blockade may reduce cell proliferation and induce apoptosis (Taylor et al., 2008). Following this view, in a series of studies the arrest of tumor cell growth has been achieved by using T-type Ca^{2+} channels inhibitors with different degrees of specificity (Bertolesi et al., 2002; Taylor et al., 2008; Li et al., 2011; Loughlin, 2014). However, both proliferation and apoptosis are the result of an increase in intracellular Ca^{2+} (Lang and Stournaras, 2014). Proliferation is triggered by oscillating Ca^{2+} activity, while apoptosis by sustained Ca^{2+} entry caused by Ca^{2+} permeable cation channels (Berridge et al., 2003). The experiments presented in this study suggest that this kind of role may be played by T-type Ca^{2+} channels in cancer cells. Given that these channels can be constitutionally open at resting membrane potential, they may drive a sustained Ca^{2+} influx in cells exposed to Res. Due to this window current, T-type Ca^{2+} channels have been linked to the occurrence of apoptosis, and a recent study has demonstrated that in human embryonic kidney HEK293 cells the expression of recombinant Cav3.2 T-type Ca^{2+} channels triggers apoptosis via mitochondrial pathways (Uchino et al., 2013). In another model, PC12 cells, the opening of Cav3.2 channels was shown to contribute to cytotoxic Ca^{2+} overload in the cytosol and in mitochondria (Gouriou et al., 2013).

In the cancer cell model used in this study (malignant pleural mesothelioma REN cells), Res induced transient $[Ca^{2+}]_i$ elevations that appear to occur through T-type Ca^{2+} channels. The experiments concentrated on the Cav3.2 isoform (containing the α_{1H} subunit) because this

particular channel subtype has been shown to be highly expressed in REN cells, as well as in malignant pleural mesothelioma biopsies from patients, but not in normal mesothelium and in normal pleura. Moreover, in REN cells Cav3.2 siRNA has been previously found to reduce *in vitro* EGCG cytotoxicity (Ranzato et al., 2012). The immunofluorescence images presented here provide the first visual localization of these channels in this cell line. In addition, we identified the Cav3.2 T-type Ca^{2+} channel as the major responsible of Ca^{2+} entry in Res-induced peaks. This was done by pharmacological inhibition first using Ni^{2+}, which is considered a low specificity ionic blocker. However, high doses (mM range) of Ni^{2+} block all VDCC as well as other Ca^{2+}-permeable channels (Marchetti and Gavazzo, 2012), but in the 10 μM range, Cav3.2 is among the most sensitive to Ni^{2+} blocking (Lacinova et al., 2000), making the effect of this ion a significant preliminary test of Cav3.2 involvement. We also tested the mibefradil analog NNC 55-0396, a compound that displayed better specificity toward T-type Ca^{2+} channels with respect to L-type in HEK293 transfected with either α_{1G} (Cav3.1; Huang et al., 2004) or α_{1H} (Cav3.2) channel (Okubo et al., 2011). Finally, the role of Cav3.2 channel was confirmed by the ability of Cav3.2 siRNA to inhibit the effect of Res, in comparison with scramble siRNA (Fig.3).

Although these observations clearly suggest an important role of Cav3.2 channel in the action of Res on $[Ca^{2+}]_i$ in REN cells, the mechanism underlining this effect is still undetermined. In a previous study, it was shown that EGCG-induced H_2O_2 release stimulates the opening of Cav3.2 channels (Ranzato et al., 2012). In another system (MCF7 breast cancer cells) EGCG triggered the opening of T-type Ca^{2+} channels through K^+ channel inhibition and subsequent membrane depolarization (Ranzato et al., 2014). However, so far we have no indication that Res operates through these mechanisms in REN cells, while it is possible that it directly acts on T-type Ca^{2+} channels as a positive modulator, as observed with EGCG in HEK293 cells exogenously expressing Cav3.2 (Ranzato et al., 2014).

A significant relationship between the Res-induced $[Ca^{2+}]_i$ increase and mesothelioma cell proliferation was obtained by comparing the effect observed on REN cells with that on normal mesothelial counterparts. At a dose of 3 μM Res, i.e. close to its EC_{50} on $[Ca^{2+}]_i$ in REN cells, a sharp divergence was observed between the responses of cancer and normal cells. Also, in REN cells significantly higher alterations of $[Ca^{2+}]_i$ were accompanied by cell growth inhibition in 7 day treatment, whereas in mesothelial cells negligible alterations of $[Ca^{2+}]_i$ and cell growth were found.

We have used malignant mesothelioma REN cells as cancer model cells. Pleural mesothelioma are rare cancers, associated with asbestos exposure (Roe and Stella, 2015), and

with still rising incidence rates worldwide (Stayner et al., 2013). The prognosis of these tumors is very poor and the treatment options are far from satisfactory, with no single modality therapy proven effective, presumably because of the multiplicity of survival and chemoresistance pathways (Heintz et al., 2010). For this and other severe forms of cancer, it is important to explore the possibility of combining more tolerated compounds with conventional drugs and devise synergistic treatments with reduced side effects. Along with their preventive action, a number of dietary phytochemicals, like vitamins and polyphenols, exhibit synergistic effects with chemotherapy and radiotherapy (Kampa et al., 2007). Previous studies from our laboratory have revealed a synergistic behavior of the drug gemcitabine in combination with ascorbate and EGCG (Volta et al., 2013).

Our present findings demonstrate that Res-induced $[Ca^{2+}]_i$ dysregulation in mesothelioma cells, through stimulation of T-type Ca^{2+} channels, occurs at low pharmacological concentrations. These doses could be achieved in clinical treatments and are likely to induce limited side effects (Patel et al., 2010). Therefore, Res seems a good candidate for the development of low-toxicity, combined chemotherapies together with more cytotoxic conventional antitumor drugs.

5. Conclusion

We have shown a previously unreported effect of Res on $[Ca^{2+}]_i$, using malignant mesothelioma cells *in vitro* as a cancer model. The effect consists in the induction of $[Ca^{2+}]_i$ peaks involving the activity of Cav3.2 T-type Ca^{2+} channels. In contrast to present tendencies, our data suggest that it is possible to affect cancer cell growth by stimulating the activity of these channels, causing an influx of Ca^{2+} that may interfere with cell cycle progression, and be significant for apoptosis induction. The effect of Res appears to be dose-dependent within a pharmacologically achievable range, and these low concentrations are likely to induce limited side effects. Therefore, Res seems a candidate for the development of low-toxicity chemotherapies in combination with more cytotoxic conventional antitumor drugs. Accordingly, T-type Ca^{2+} channels are a possible new target in the therapy of mesothelioma, and possibly of other cancer types.

Acknowledgements

This work was supported by Fondazione Buzzi Unicem (Casale Monferrato, Italy), grant n. FBU-P27 to BB. SR was recipient of a PhD scholarship from the Italian Ministry of University and Research (MIUR). We thank Giacomo Cozzi, Cristiano Rumio, and the Nikon Imaging Center at the Fondazione Istituto Italiano di Tecnologia for help with light microscopy techniques.

Conflict of Interest statement

The authors declare that there are no conflicts of interest.

References

Anekonda, T. S. (2006). Resveratrol--a boon for treating Alzheimer's disease? Brain Res Rev 52:316-326.

Berridge, M. J., M. D. Bootman and H. L. Roderick (2003). Calcium signalling: dynamics, homeostasis and remodelling. Nat Rev Mol Cell Biol 4:517-529.

Bertino, P., F. Piccardi, C. Porta, R. Favoni, M. Cilli, L. Mutti and G. Gaudino (2008). Imatinib mesylate enhances therapeutic effects of gemcitabine in human malignant mesothelioma xenografts. Clin Cancer Res 14:541-548.

Bertolesi, G. E., C. Shi, L. Elbaum, C. Jollimore, G. Rozenberg, S. Barnes and M. E. Kelly (2002). The Ca(2+) channel antagonists mibefradil and pimozide inhibit cell growth via different cytotoxic mechanisms. Mol Pharmacol 62:210-219.

Bradamante, S., L. Barenghi and A. Villa (2004). Cardiovascular protective effects of resveratrol. Cardiovasc Drug Rev 22:169-188.

Campos-Toimil, M., J. Elies, E. Alvarez, I. Verde and F. Orallo (2007). Effects of trans- and cis-resveratrol on Ca2+ handling in A7r5 vascular myocytes. Eur J Pharmacol 577:91-99.

Chang, H. T., C. T. Chou, I. L. Chen, W. Z. Liang, D. H. Kuo, J. K. Huang, P. Shieh and C. R. Jan (2013). Mechanisms of resveratrol-induced changes in [Ca(2+)]i and cell viability in PC3 human prostate cancer cells. J Recept Signal Transduct Res 33:298-303.

Dziegielewska, B., L. S. Gray and J. Dziegielewski (2014). T-type calcium channels blockers as new tools in cancer therapies. Pflugers Arch 466:801-810.

Fantini, M., M. Benvenuto, L. Masuelli, G. V. Frajese, I. Tresoldi, A. Modesti and R. Bei (2015). In vitro and in vivo antitumoral effects of combinations of polyphenols, or polyphenols and anticancer drugs: perspectives on cancer treatment. Int J Mol Sci 16:9236-9282.

Frazzi, R. and M. Tigano (2014). The multiple mechanisms of cell death triggered by resveratrol in lymphoma and leukemia. Int J Mol Sci 15:4977-4993.

Gojkovic-Bukarica, L., A. Novakovic, V. Kanjuh, M. Bumbasirevic, A. Lesic and H. Heinle (2008). A role of ion channels in the endothelium-independent relaxation of rat mesenteric artery induced by resveratrol. J Pharmacol Sci 108:124-130.

Gouriou, Y., P. Bijlenga and N. Demaurex (2013). Mitochondrial Ca2+ uptake from plasma membrane Cav3.2 protein channels contributes to ischemic toxicity in PC12 cells. J Biol Chem 288:12459-12468.

Grynkiewicz, G., M. Poenie and R. Y. Tsien (1985). A new generation of Ca2+ indicators with greatly improved fluorescence properties. J Biol Chem 260:3440-3450.

Heintz, N. H., Y. M. Janssen-Heininger and B. T. Mossman (2010). Asbestos, lung cancers, and mesotheliomas: from molecular approaches to targeting tumor survival pathways. Am J Respir Cell Mol Biol 42:133-139.

Huang, L., B. M. Keyser, T. M. Tagmose, J. B. Hansen, J. T. Taylor, H. Zhuang, M. Zhang, D. S. Ragsdale and M. Li (2004). NNC 55-0396 [(1S,2S)-2-(2-(N-[(3-benzimidazol-2-yl)propyl]-N-methylamino)ethyl)-6-fluoro-1,2, 3,4-tetrahydro-1-isopropyl-2-naphtyl cyclopropanecarboxylate dihydrochloride]: a new selective inhibitor of T-type calcium channels. J Pharmacol Exp Ther 309:193-199.

Jakab, M., S. Lach, Z. Bacova, C. Langeluddecke, V. Strbak, S. Schmidt, E. Iglseder, M. Paulmichl, J. Geibel and M. Ritter (2008). Resveratrol inhibits electrical activity and insulin release from insulinoma cells by block of voltage-gated Ca+ channels and swelling-dependent Cl- currents. Cell Physiol Biochem 22:567-578.

Kampa, M., A. P. Nifli, G. Notas and E. Castanas (2007). Polyphenols and cancer cell growth. Rev Physiol Biochem Pharmacol 159:79-113.

Ke, Y., R. R. Reddel, B. I. Gerwin, H. K. Reddel, A. N. Somers, M. G. McMenamin, M. A. LaVeck, R. A. Stahel, J. F. Lechner and C. C. Harris (1989). Establishment of a human in vitro mesothelial cell model system for investigating mechanisms of asbestos-induced mesothelioma. Am J Pathol 134:979-991.

Kopp, R. F., C. A. Leech and M. W. Roe (2013). Resveratrol Interferes with Fura-2 Intracellular Calcium Measurements. J Fluoresc.

Kundu, J. K. and Y. J. Surh (2008). Cancer chemopreventive and therapeutic potential of resveratrol: mechanistic perspectives. Cancer Lett 269:243-261.

Lacinova, L., N. Klugbauer and F. Hofmann (2000). Low voltage activated calcium channels: from genes to function. Gen Physiol Biophys 19:121-136.

Lang, F. and C. Stournaras (2014). Ion channels in cancer: future perspectives and clinical potential. Philos Trans R Soc Lond B Biol Sci 369:20130108.

Li, W., S. L. Zhang, N. Wang, B. B. Zhang and M. Li (2011). Blockade of T-type Ca(2+) channels inhibits human ovarian cancer cell proliferation. Cancer Invest 29:339-346.

Loughlin, K. R. (2014). Calcium channel blockers and prostate cancer. Urol Oncol 32:537-538.

Ma, X., X. Tian, X. Huang, F. Yan and D. Qiao (2007). Resveratrol-induced mitochondrial dysfunction and apoptosis are associated with Ca2+ and mCICR-mediated MPT activation in HepG2 cells. Mol Cell Biochem 302:99-109.

Marchetti, C., C. Amico and C. Usai (1995). Functional characterization of the effect of nimodipine on the calcium current in rat cerebellar granule cells. J Neurophysiol 73:1169-1180.

Marchetti, C., I. Baranowska-Bosiacka and P. Gavazzo (2014). Multiple effects of copper on NMDA receptor currents. Brain Res 1542:20-31.

Marchetti, C. and P. Gavazzo (2012). Nickel modulation of voltage- and ligand-gated ionic channels in neurons Metal Ions in Stroke J. H. Z. Yang V Li, Springer:783-803.

Martinez, J. and J. J. Moreno (2000). Effect of resveratrol, a natural polyphenolic compound, on reactive oxygen species and prostaglandin production. Biochem Pharmacol 59:865-870.

Mazzolini, M., S. Traverso and C. Marchetti (2001). Multiple pathways of Pb(2+) permeation in rat cerebellar granule neurones. J Neurochem 79:407-416.

McCalley, A. E., S. Kaja, A. J. Payne and P. Koulen (2014). Resveratrol and calcium signaling: molecular mechanisms and clinical relevance. Molecules 19:7327-7340.

Monteith, G. R., F. M. Davis and S. J. Roberts-Thomson (2012). Calcium channels and pumps in cancer: changes and consequences. J Biol Chem 287:31666-31673.

Munaron, L., S. Antoniotti, A. Fiorio Pla and D. Lovisolo (2004). Blocking Ca2+entry: a way to control cell proliferation. Curr Med Chem 11:1533-1543.

Okubo, K., T. Takahashi, F. Sekiguchi, D. Kanaoka, M. Matsunami, T. Ohkubo, J. Yamazaki, N. Fukushima, S. Yoshida and A. Kawabata (2011). Inhibition of T-type calcium channels and hydrogen sulfide-forming enzyme reverses paclitaxel-evoked neuropathic hyperalgesia in rats. Neuroscience 188:148-156.

Park, E. K., K. Takahashi, T. Hoshuyama, T. J. Cheng, V. Delgermaa, G. V. Le and T. Sorahan (2011). Global magnitude of reported and unreported mesothelioma. Environ Health Perspect 119:514-518.

Pass, H. I., N. Vogelzang, S. Hahn and M. Carbone (2004). Malignant pleural mesothelioma. Curr Probl Cancer 28:93-174.

Patel, K. R., V. A. Brown, D. J. Jones, R. G. Britton, D. Hemingway, A. S. Miller, K. P. West, T. D. Booth, M. Perloff, J. A. Crowell, D. E. Brenner, W. P. Steward, A. J. Gescher and K. Brown (2010). Clinical pharmacology of resveratrol and its metabolites in colorectal cancer patients. Cancer Res 70:7392-7399.

Paudel, R. C., S. Kiviluoto, J. B. Parys and G. Bultynck (2014). Resveratrol is not compatible with a Fura-2-based assay for measuring intracellular Ca(2)(+) signaling. Biochem Biophys Res Commun 450:1626-1630.

Petrovski, G., N. Gurusamy and D. K. Das (2011). Resveratrol in cardiovascular health and disease. Ann N Y Acad Sci 1215:22-33.

Polycarpou, E., L. B. Meira, S. Carrington, E. Tyrrell, H. Modjtahedi and M. A. Carew (2013). Resveratrol 3-O-D-glucuronide and resveratrol 4'-O-D-glucuronide inhibit colon cancer cell growth: evidence for a role of A3 adenosine receptors, cyclin D1 depletion, and G1 cell cycle arrest. Mol Nutr Food Res 57:1708-1717.

Ranzato, E., S. Biffo and B. Burlando (2011). Selective ascorbate toxicity in malignant mesothelioma: a redox Trojan mechanism. Am J Respir Cell Mol Biol 44:108-117.

Ranzato, E., V. Magnelli, S. Martinotti, Z. Waheed, S. M. Cain, T. P. Snutch, C. Marchetti and B. Burlando (2014). Epigallocatechin-3-gallate elicits Ca2+ spike in MCF-7 breast cancer cells: essential role of Cav3.2 channels. Cell Calcium 56:285-295.

Ranzato, E., S. Martinotti, V. Magnelli, B. Murer, S. Biffo, L. Mutti and B. Burlando (2012). Epigallocatechin-3-gallate induces mesothelioma cell death via H2 O2 -dependent T-type Ca2+ channel opening. J Cell Mol Med 16:2667-2678.

Roe, O. D. and G. M. Stella (2015). Malignant pleural mesothelioma: history, controversy and future of a manmade epidemic. Eur Respir Rev 24:115-131.

Sareen, D., S. R. Darjatmoko, D. M. Albert and A. S. Polans (2007). Mitochondria, calcium, and calpain are key mediators of resveratrol-induced apoptosis in breast cancer. Mol Pharmacol 72:1466-1475.

Stayner, L., L. S. Welch and R. Lemen (2013). The worldwide pandemic of asbestos-related diseases. Annu Rev Public Health 34:205-216.

Su, H. C., L. M. Hung and J. K. Chen (2006). Resveratrol, a red wine antioxidant, possesses an insulin-like effect in streptozotocin-induced diabetic rats. Am J Physiol Endocrinol Metab 290:E1339-1346.

Taylor, J. T., L. Huang, J. E. Pottle, K. Liu, Y. Yang, X. Zeng, B. M. Keyser, K. C. Agrawal, J. B. Hansen and M. Li (2008). Selective blockade of T-type Ca2+ channels suppresses human breast cancer cell proliferation. Cancer Lett 267:116-124.

Taylor, J. T., X. B. Zeng, J. E. Pottle, K. Lee, A. R. Wang, S. G. Yi, J. A. Scruggs, S. S. Sikka and M. Li (2008). Calcium signaling and T-type calcium channels in cancer cell cycling. World J Gastroenterol 14:4984-4991.

Trapp, V., B. Parmakhtiar, V. Papazian, L. Willmott and J. P. Fruehauf (2010). Anti-angiogenic effects of resveratrol mediated by decreased VEGF and increased TSP1 expression in melanoma-endothelial cell co-culture. Angiogenesis 13:305-315.

Uchino, T., S. Isomoto, T. Noguchi and K. Ono (2013). Window current through the T-type Ca2+ channel triggers the mechanism for cellular apoptosis via mitochondrial pathways. Heart Vessels 28:658-666.

Volta, V., E. Ranzato, S. Martinotti, S. Gallo, M. V. Russo, L. Mutti, S. Biffo and B. Burlando (2013). Preclinical demonstration of synergistic Active Nutrients/Drug (AND) combination as a potential treatment for malignant pleural mesothelioma. PLoS One 8:e58051.

Wang, T. T., N. W. Schoene, Y. S. Kim, C. S. Mizuno and A. M. Rimando (2010). Differential effects of resveratrol and its naturally occurring methylether analogs on cell cycle and apoptosis in human androgen-responsive LNCaP cancer cells. Mol Nutr Food Res 54:335-344.

Zhang, Y., X. Jiang, T. P. Snutch and J. Tao (2013). Modulation of low-voltage-activated T-type Ca(2)(+) channels. Biochim Biophys Acta 1828:1550-1559.

Figure legends

Fig. 1 –Resveratrol (Res) fluorescence does not hinder Fura-2 measurements of internal Ca^{2+} elevation at pharmacologically relevant doses.

(A) Concentration-dependent curve of Res intrinsic fluorescence measured in cell-free solution with Ex 340 nm and Em 510 nm (bandwidth 20 nm). Fluorescent values (F, relative arbitrary units) were normalized to the value in the absence of Res (F_0). The dose-response curve displayed EC_{50} = 122 μM.

(B) Time-course of 510 nm fluorescence (in relative fluorescent units, RFU) recorded following 340 and 380 nm Ex in Fura-2-loaded REN cells exposed to 100 and 400 μM Res (B1), to 10 μM Res (B2), and to 1 μM thapsigargin in Ca^{2+}-free solution (B3). The lower graphs represent the time course of the ratio F340/F380, in each case. The higher doses of Res caused an increase of fluorescence with both 340 and 380 nm excitations; the ratio, F340/F380, increased steeply as soon as Res was applied (B1). In contrast, the lower dose of Res (B2), as well as thapsigargin (B3), caused a fluorescence rise with 340 nm excitation and a decrease with 380 nm excitation, indicating a specific response of the Ca^{2+} sensitive dye, as also revealed by the ratio time course. (C) Intracellular Ca^{2+} peaks following stimulation with 1, 3, 10 μM Res in Fura-2-loaded REN cells. Treatments are marked by bars under the traces. $[Ca^{2+}]_i$ was calculated from the parameter values obtained at the end of each experiment by incubation of the cells in 10μM ionomycin in Ca^{2+}-free and standard Ca^{2+} solutions. (D) Stimulation with 10 μM Res did not elicit Ca^{2+} rise in Fura2-loaded REN cells when Ca^{2+} was removed from the bath (0 Ca), but the response was restored when Ca^{2+} was added again. This observation indicates that the effect of Res is dependent on external Ca^{2+}.

Fig. 2 - Resveratrol driven elevation of intracellular Ca^{2+} in Ren cells is dependent on the activity of T-type Ca^{2+} channels.

(A) Immunofluorescence imaging of REN cell monolayer labelled with primary antibody anti-Cav3.2, followed by Alexa fluor 594-secondary antibody (red; left picture), and without primary antibody (right picture). In both cases, FITC-phalloidin counterstain (green) is present. Red staining reveals the distribution of Cav3.2 protein channels (left), suggesting channel clustering in the plasma membrane. Cells hybridized only with secondary antibody show negligible red fluorescence (right). (B) Treatments with 30 μM Ni^{2+} or (C) with 5 μM NNC 55-0396 (marked by bars under the traces) reversibly reduce the internal Ca^{2+} elevation induced by 10 μM Res in Fura-2-loaded REN cells. (D) Summary of the above effects in different (n=4) experiments. * indicates $p<0.05$ with respect to control.

Fig. 3 – Cav3.2 silencing reduces Res-induced Ca^{2+} peaks.

(A) Western immunoblot analysis of cell lysates showing expression of Cav3.2 protein in REN cells and Cav3.2 down-regulation by specific RNA interference (siRNA). REN cells were transfected or not (control) with negative control siRNA (scramble) or specific Cav3.2 siRNA and results were recorded after 48 hr. (B) Fluorescent measurement of internal Ca^{2+} peaks following Res application to REN cells 48h after transfection with scramble or specific Cav3.2 siRNA. (C) Summary of the results in 5-9 different experiments. * = $p<0.05$ with respect to scramble.

Fig. 4. The effect of Res on intracellular Ca^{2+} is more pronounced in REN cells than in normal mesothelium MeT5A cells.

(A) Comparison of Ca^{2+} elevations following stimulation with increasing doses (1, 3, 5, 10 μM) of Res in Fura-2-loaded REN cells (left) and normal mesothelium Met5A cells (right). (B) Dose dependence of $[Ca^{2+}]_i$ variations induced by Res in MPM REN cells and normal mesothelium MeT-5A cells. Data are means±sem of peak values normalized as $\Delta[Ca^{2+}]/basal[Ca^{2+}]$. Experimental points were approximated by the function:

$$\Delta[Ca^{2+}]/basal[Ca^{2+}] = A/(1+(EC_{50}/x)^n)$$

where x is Res concentration. The best fit yielded $A = (\Delta[Ca^{2+}]/basal[Ca^{2+}])_{max} = 3$ for both cell types, EC_{50} = 2.7 μM, n= 1.7, for MPM REN cells, and EC_{50} = 4.9 μM, n = 3.5, for Met5A cells.

(C). Growth curves obtained by calcein-AM cell density assay for REN (left) and MeT-5A (right) cells, incubated with 0, 3, and 10 μM Res for 1-7 days. Data are means±sd (n=16) of cell densities, normalized to the initial and maximum value in control (0 Res) condition. * = $p<0.05$ with respect to control.

Figures

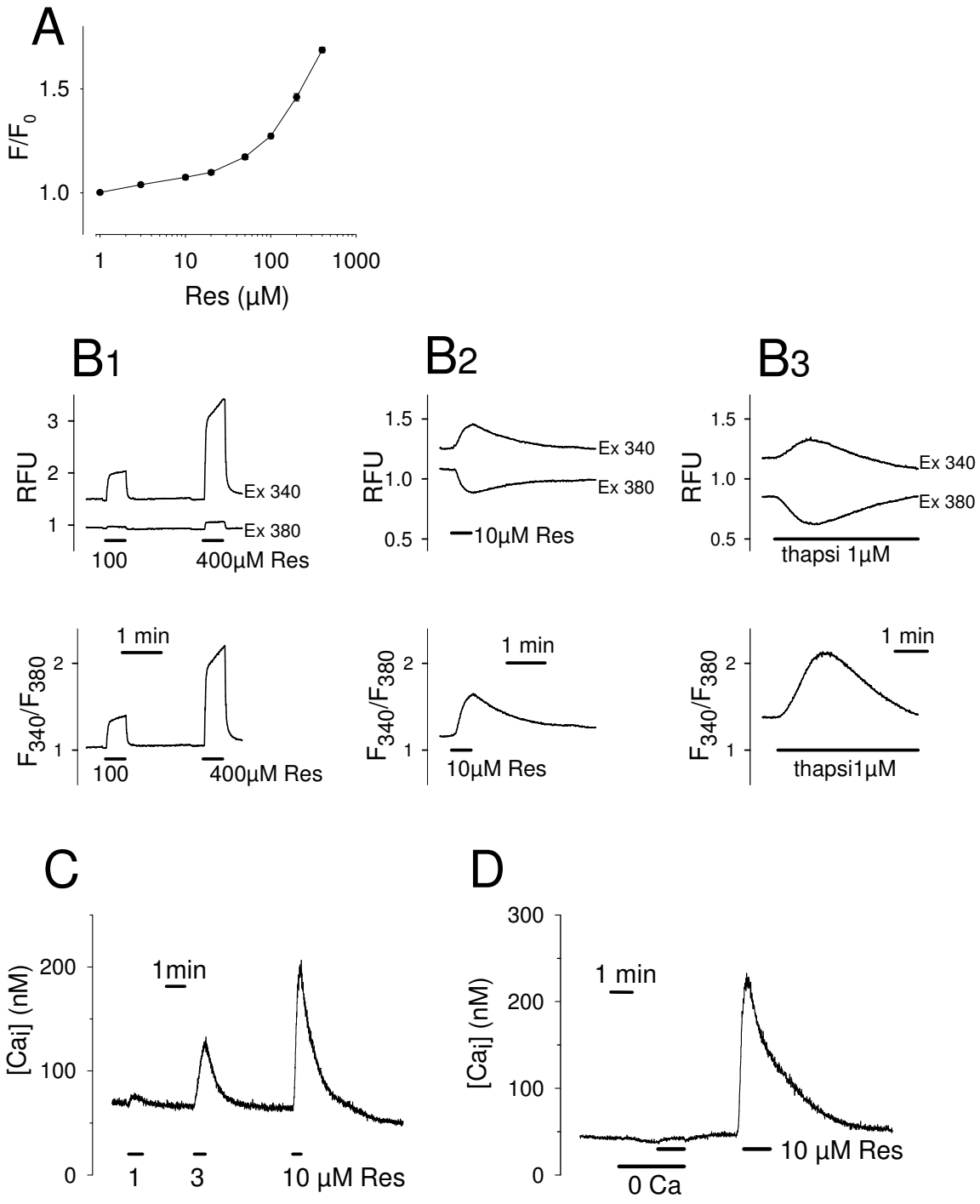

Figure 1.

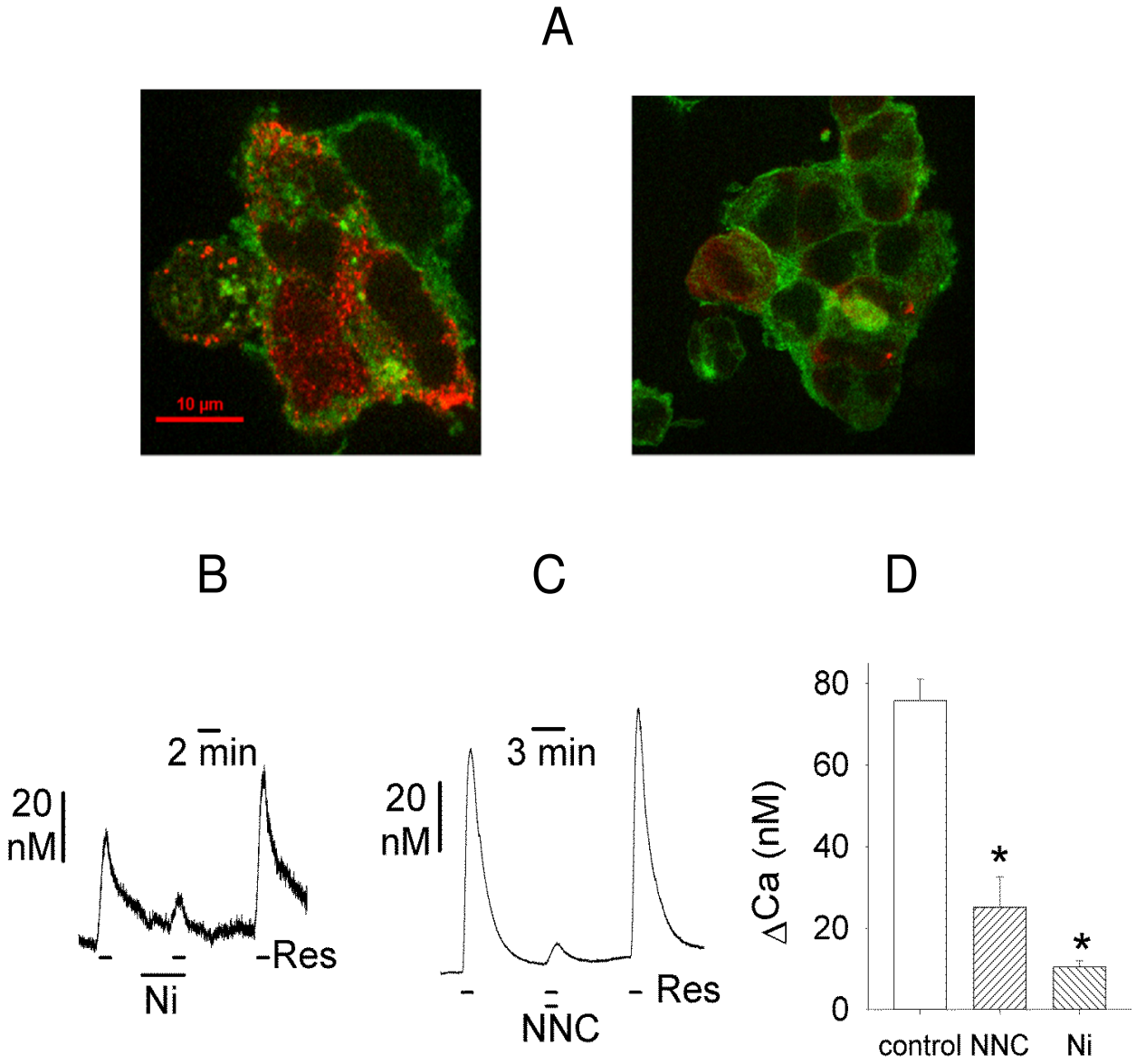
A
10 µm
B
2 min
20
nM
Ni
Res
C
3 min
20
nM
NNC
Res
D
80
60
40
20
0
ΔCa (nM)
*
*
control
NNC
Ni

Figure 2.

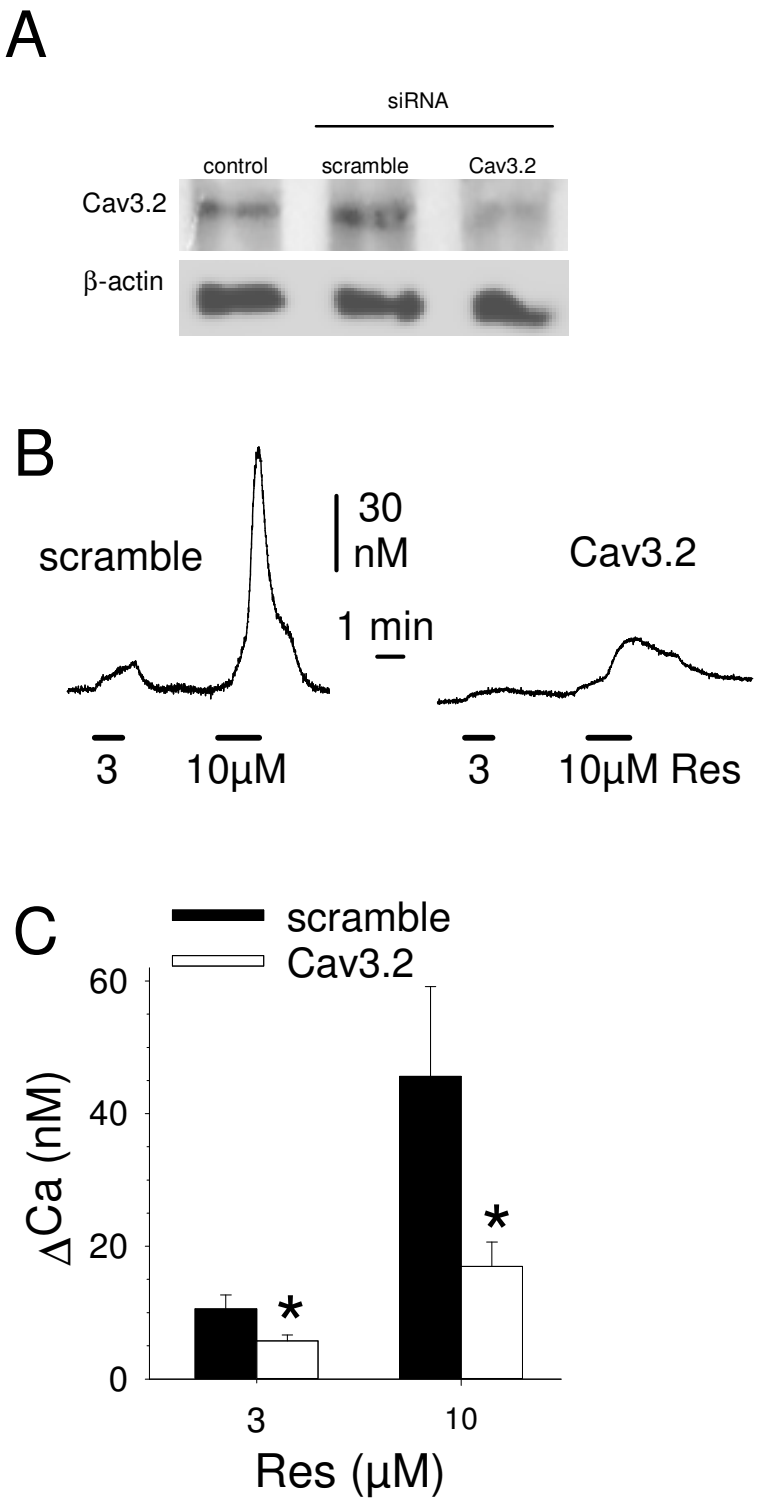
A
siRNA
control
scramble
Cav3.2
Cav3.2
β-actin
B
scramble
30
nM
1 min
Cav3.2
3
10μM
3
10μM Res
C
scramble
Cav3.2
60
40
20
0
ΔCa (nM)
*
*
3
10
Res (μM)

Figure 3.

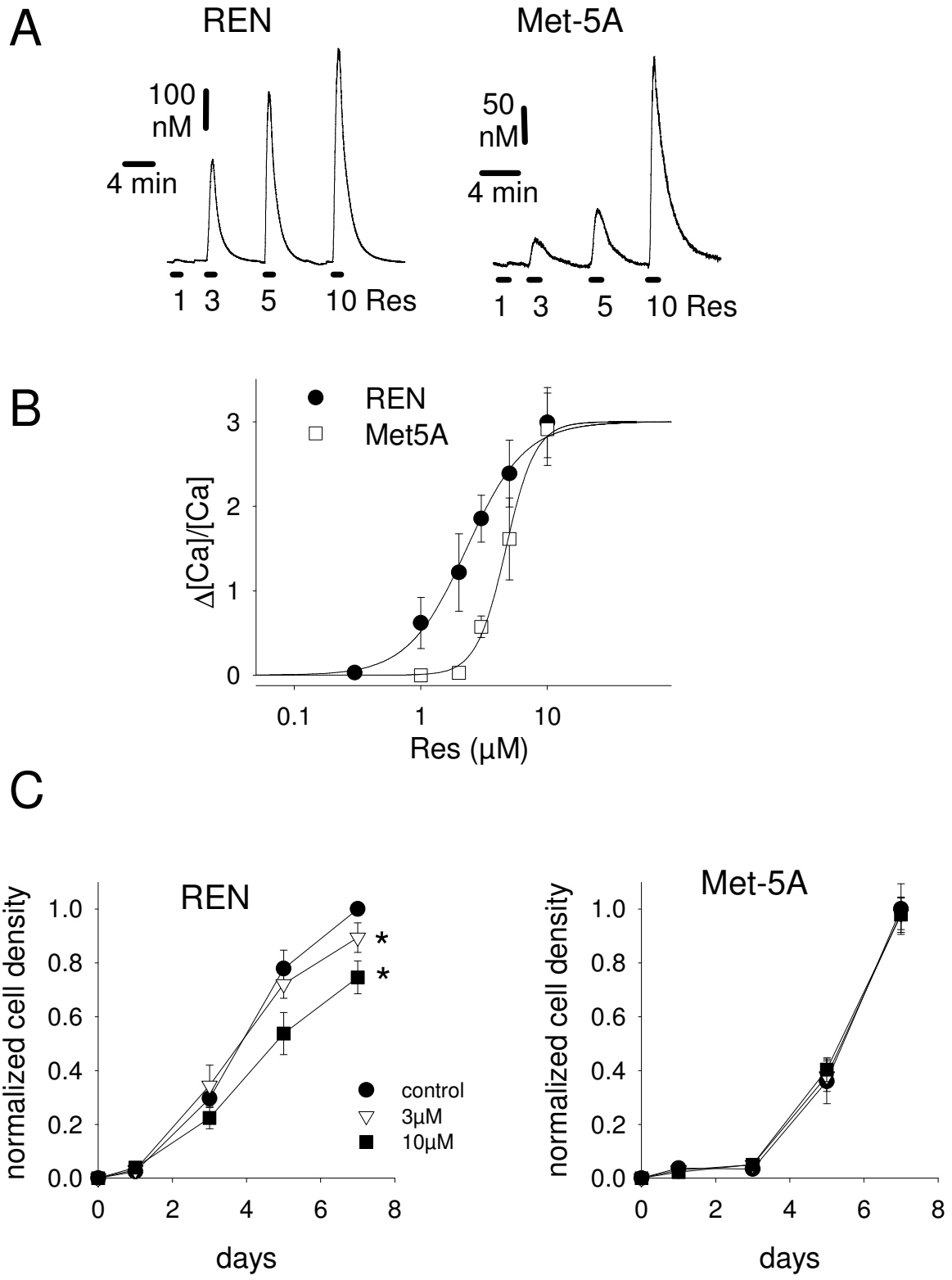
A
REN
Met-5A
100 nM
4 min
1 3 5 10 Res
50 nM
4 min
1 3 5 10 Res
B
REN
Met5A
Δ[Ca]/[Ca]
Res (μM)
C
REN
Met-5A
normalized cell density
control
3μM
10μM
days

Figure 4.

Conclusions

MPM is an aggressive cancer, with a poor prognosis and an increasing incidence as a result of widespread exposure to asbestos. Despite the implementation of various therapeutic approaches, the response rates to treatment are generally very low and the need to improve therapies is urgent. Surgery and radiotherapy have a limited role in highly selected patients and systemic therapy is the only potential treatment option for the majority of patients. Among alternative remedies for cancer treatment, there is a growing interest in the anticancer action of natural substances.

In this study we have highlighted a novel mechanism of action for oleuropein, and its metabolite hydroxytyrosol.

We have developed a method for obtaining olive leaf extract enriched in oleuropein, involving raw extraction, extract partitioning, and chromatographic separation.

Treatments with oleuropein-enriched, leaf extract fraction, and its major component oleuropein induce $[Ca^{2+}]_i$ rises in mesothelioma REN cells followed by a prompt recovery of the baseline level upon washout. These data indicate that the observed $[Ca^{2+}]_i$ spikes are not due to cell membrane injury but rather depend on the influx of Ca^{2+} through membrane Ca^{2+} channels. Removal of Ca^{2+} from the external solution almost inhibits oleuropein effect and the use of the T-type Ca^{2+} channel inhibitor NNC-55-0396 reversibly reduces the Ca^{2+} spike suggesting at least a partial involvement of T-type Ca^{2+} channels. Hydroxytyrosol is more powerful than oleuropein in inducing Ca^{2+} spikes. Similar to the oleuropein fraction, increasing doses of standard oleuropein induce dose-dependent $[Ca^{2+}]_i$ spikes but the cytotoxic effect of the oleuropein fraction is slightly, but not significantly, stronger than that of standard oleuropein. This kind of effect suggests a possible use of the oleuropein fraction from olive leaves in the treatment of mesothelioma (156).

In this study we have also evaluated the pharmacological potentials of the grapes stilbene resveratrol.

The effect of Res on MPM REN cells was studied by means of microspectrophotometry microscopy after cell loading with the fluorescent probe fura-2. Resveratrol shows autofluorescence that may affect Ca^{2+} measurements but this intrinsic aspect of Res does not hinder Fura-2 measurements of $[Ca^{2+}]_i$ at pharmacological doses.

Cells transiently exposed to 1, 3, or 10μM Res show increasing peaks of $[Ca^{2+}]_i$. No effect is visible in Ca^{2+}-free medium, while the $[Ca^{2+}]_i$ peak is reduced by non-selective (Ni^{2+}) and highly selective (NNC 55-0396) T-type Ca^{2+} channel blockers. Dose-dependent curves of Res-induced $[Ca^{2+}]_i$ peaks show a rightward shift for normal MeT-5A mesothelial cells (EC50 = 4.9 μM) with respect to MPM REN cells (EC50 = 2.7 μM), indicating higher sensitivity of tumor cells to Res. Accordingly, incubation with 3 or 10μM Res for 7 days resulted in cell growth inhibition for REN cells but not for mesothelial cells. The effect shows selectivity towards MPM cells, suggesting its possible use in the clinical treatment of mesothelioma malignancies. The complex of data indicates that Res induces a Ca^{2+} influx that is possibly mediated by T-type Ca^{2+}channels and in particular the Cav3.2 isoform. Specific expression of Cav3.2 Ca^{2+} channels in REN cells was revealed by immunofluorescence coupled to confocal microscopy, suggesting a clustering of these channels in the plasma membrane. Cav3.2 gene silencing by siRNA abolishes the expression of Cav3.2 channel and reduces the effect of resveratrol on Ca^{2+} (157).

The complex of data shows that various polyphenols, such as oleuropein, hydroxythyrosol and resveratrol, are able to induce non-physiological Ca^{2+} dynamics in mesothelioma cells, involving T-type Ca^{2+} channels. Data also show that such a disturbance affect MPM cell growth rates, possibly interfering with tumor development, and suggesting T-type Ca^{2+} channels as possible therapeutic targets. Also, the effect occurs at low pharmacological concentrations, possibly inducing limited side effects. Therefore, these polyphenols are possible candidates for the development of low-toxicity chemotherapies to be used as synergistic agents in combination with more cytotoxic conventional antitumor drugs (158).

In conclusion, the results of the present study are consistent with the increasing interest for natural compounds with antitumor properties, suggesting a promising future for this kind of approach in MPM therapy, as well as in other kinds of poor-prognosis cancer.

References

156. Marchetti C, Clericuzio M, Borghesi B, Cornara L, Ribulla S, Gosetti F, Marengo E, Burlando B. *Oleuropein-enriched olive leaf extract affects calcium dynamics and impairs viability of malignant mesothelioma cells.* Evidence-Based Complementary and Alternative Medicine 2015: 908493.

157. Marchetti C, Ribulla S, Magnelli V, Patrone M, Burlando B. 2016. *Resveratrol induces intracellular Ca2+ rise via T-type Ca2+ channels in a mesothelioma cell line*. Life Sciences (in press).

158. Block K.I, Gyllenhaal C, Lowe L, Amedei A, Amin A.R, Amin A, et al. *Designing a broad-spectrum integrative approach for cancer prevention and treatment.* Semin Cancer Biol. 2015, 35 Suppl:S276-304.

Acknowledgements

Alla fine del mio percorso accademico desidero ringraziare i miei tutor di Dottorato, il Professor Bruno Burlando, per la sua professionalità ed i preziosi insegnamenti ed il Professor Mauro Patrone, sempre presente e disponibile.
Ringrazio la Dott.ssa Carla Marchetti del CNR di Genova, con la quale ho collaborato in questi anni di Dottorato, per avermi affiancata sempre con molta pazienza e per avermi dedicato molto del suo tempo.
Un "grazie" sincero ai colleghi del DiSIT, in particolare a Sara e Stefano, per i loro consigli e per aver condiviso con me i momenti belli e quelli più difficili di questi anni.
Grazie di cuore alle amiche di sempre ed al mio fidanzato per i continui incoraggiamenti.
Infine, il ringraziamento più grande va i miei genitori, al mio papà per aver sempre avuto fiducia nelle mie capacità ed alla mia mamma, è a lei che devo tutta la mia tenacia.